

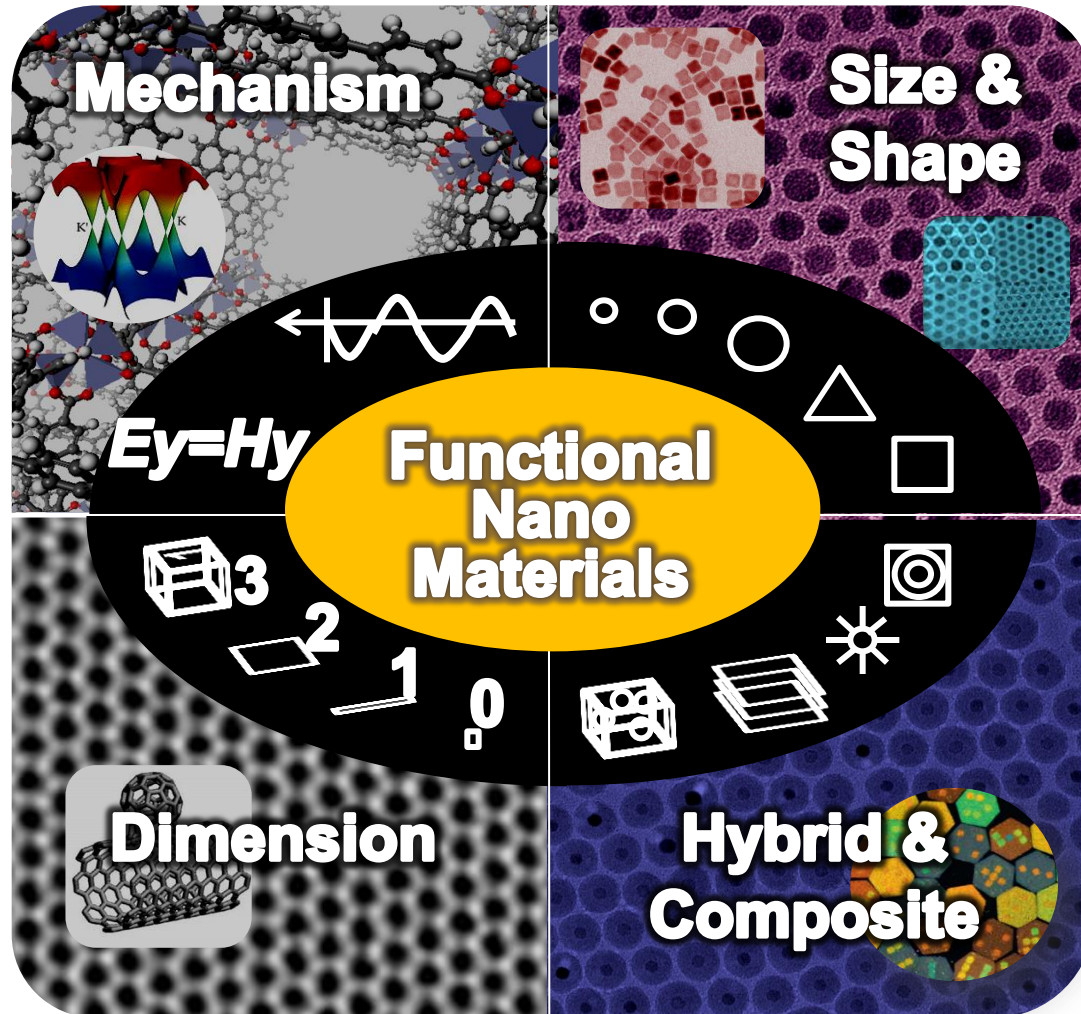
BIOMEDICAL APPLICATIONS OF UNIFORM-SIZED NANOPARTICLES

Taeghwan HYEON (현택환; 玄澤煥)

Center for Nanoparticle Research, Institute for Basic Science (IBS),
and School of Chemical and Biological Engineering,
Seoul National University (SNU), Seoul 151-742, Korea

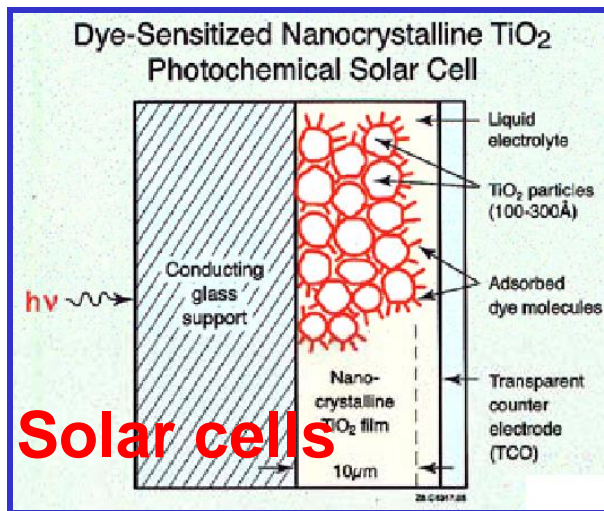
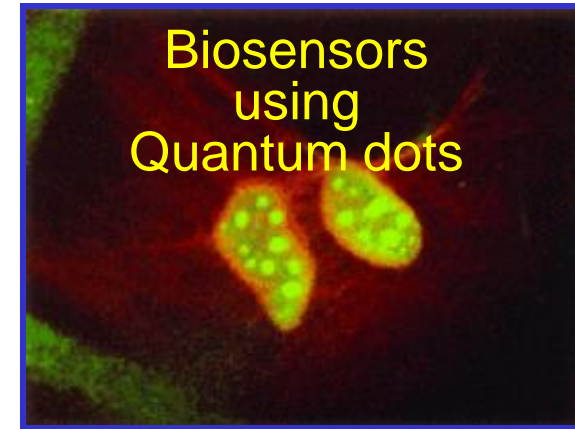
Part I.

Chemical Synthesis of Uniform-sized Iron Oxide Nanocrystals

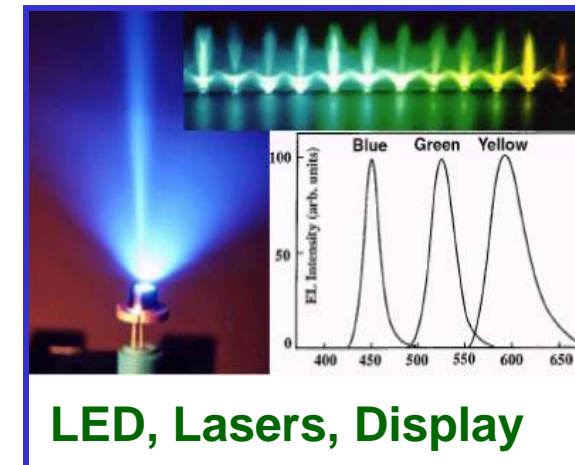
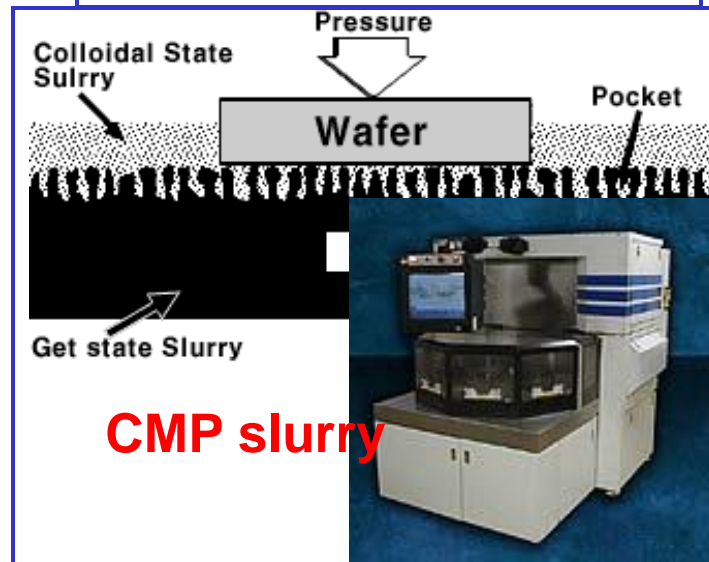


Why Nanocrystals are Important?

Like Alphabets, Nanocrystals are Key Base Materials for the implementation of Nanotechnology.



Solar cells



Why is Size Uniformity of Nanoparticles Important?

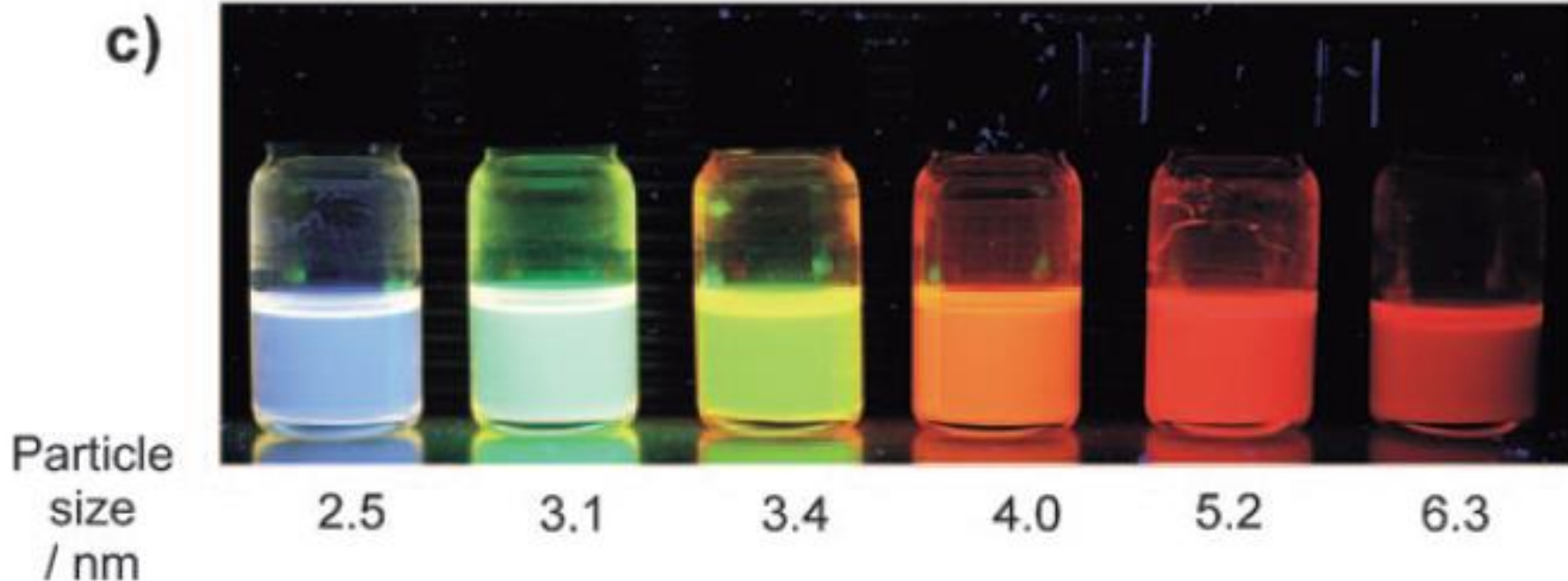
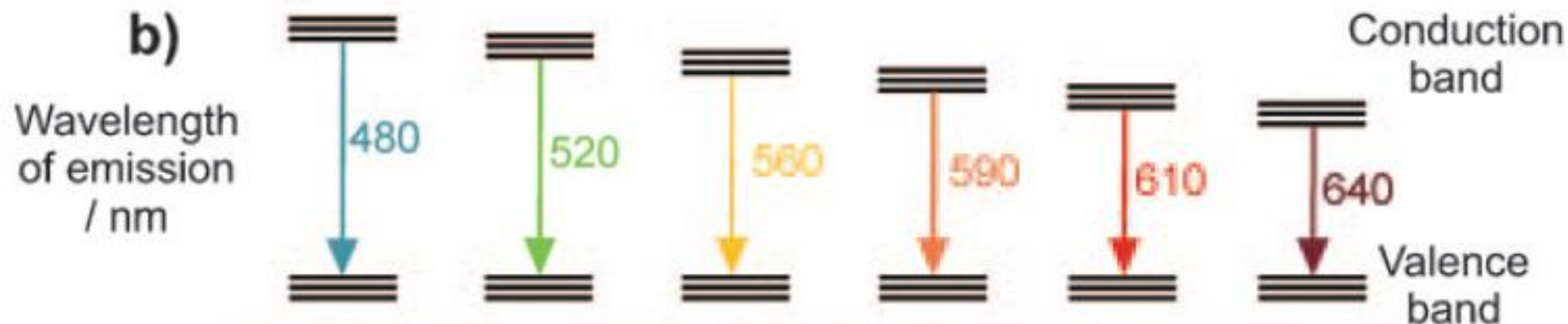
- Physical properties of nanoparticles are directly dependent on the particle size.

- For various applications, uniform-sized nanoparticles are critical.

J. Park *et al.* *Angew. Chem. Int. Ed. (Invited Review)* **2007**, 46, 4630.

S. Kwon and T. Hyeon, *Acc. Chem. Res.* **2008**, 41, 1696.

CdSe semiconductor Quantum Dots



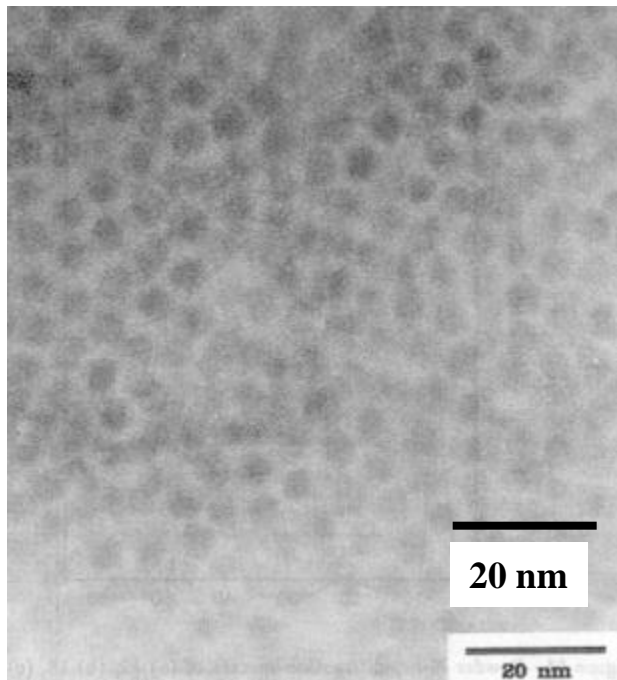
H. Goesmann, C. Feldmann, *Angew. Chem., Int. Ed.* **2010**, 49, 1362-1395.

D. V. Talapin, J.-S. Lee, M. V. Kovalenko, E. V. Shevchenko, *Chem. Rev.* **2010**, 110, 389.

Synthesis of Monodisperse Nanocrystals Using Hot-injection methods

MIT

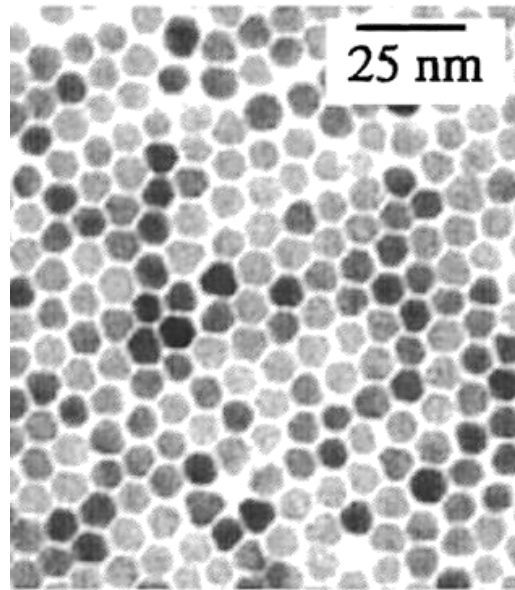
5.1 nm CdSe



Murray, Norris and Bawendi,
J. Am. Chem. Soc. **1993**, 115, 8706

UC-Berkeley

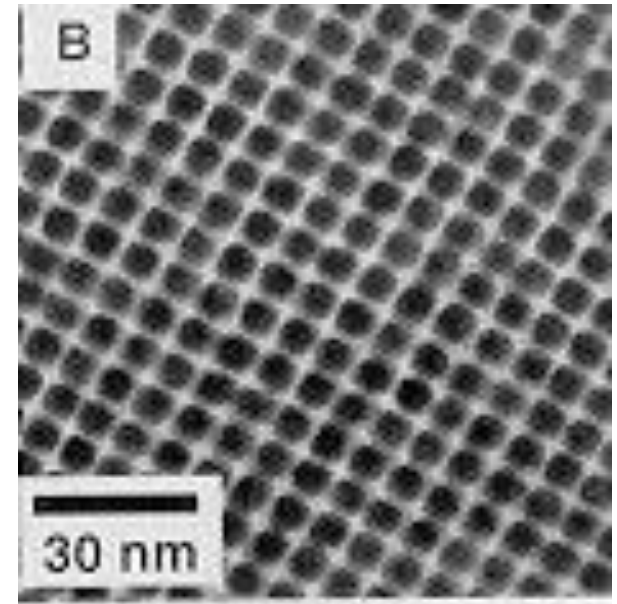
8.5 nm CdSe



Peng and Alivisatos,
J. Am. Chem. Soc. **1998**, 120, 5343

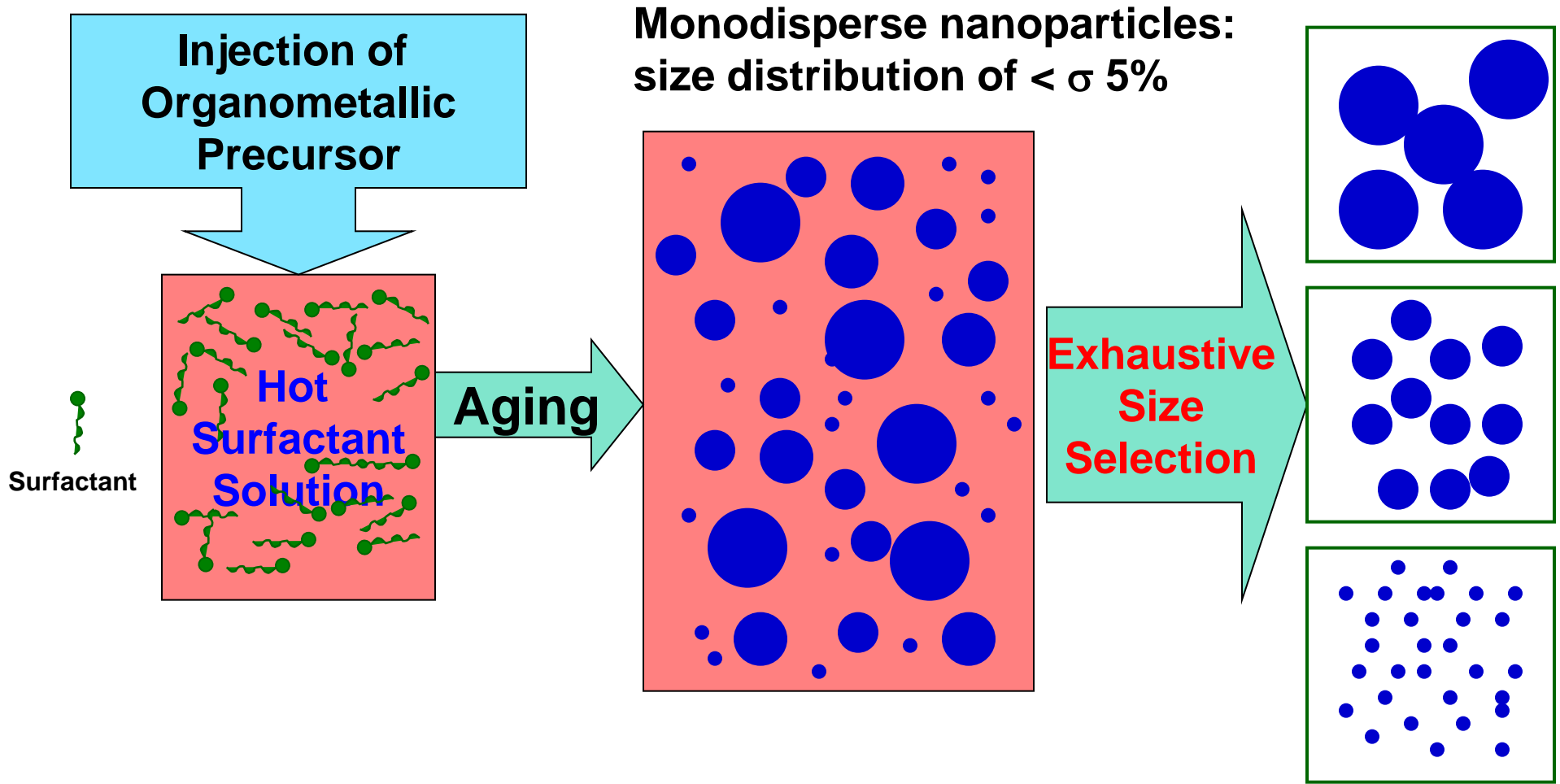
IBM Watson

5 nm Fe-Pt alloy



Sun and Murray,
Science **2000**, 287, 1989.

Conventional Synthesis of Monodisperse Nanocrystals



Heat-up Process:
Direct Synthesis of
Monodisperse 11 nm Magnetite Nanocrystals
Without Size Sorting Process

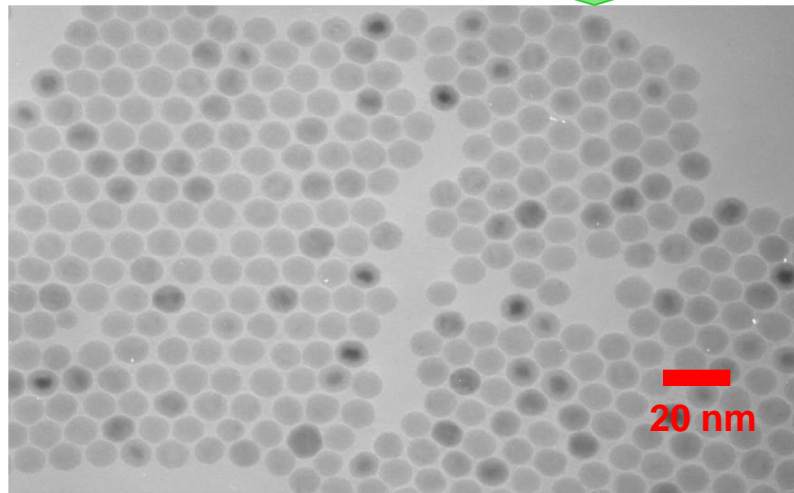
0.2 μm



T. Hyeon *et al.* *J. Am. Chem. Soc.* 2001, 123, 12798

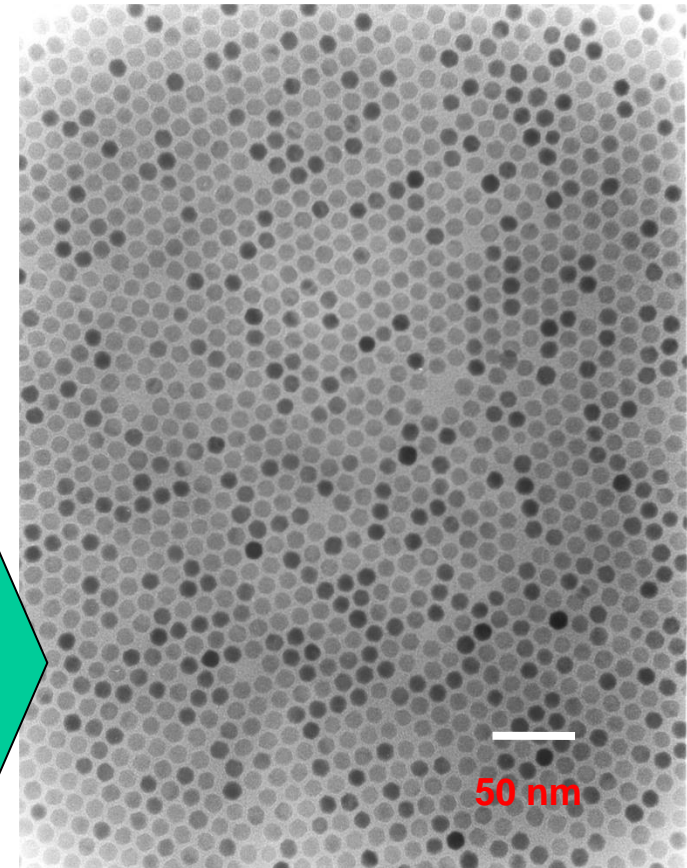
Heat-up Process to produce Uniform Fe_3O_4 Nanocrystals by slowing heating Fe-oleate complex to 320 °C

Slowly heating Fe-oleate complex
from R.T. to 320 °C
followed by Aging for ~ 10 min



11 nm Fe nanoparticles

Controlled
Mild chemical
Oxidation
Using Me_3NO

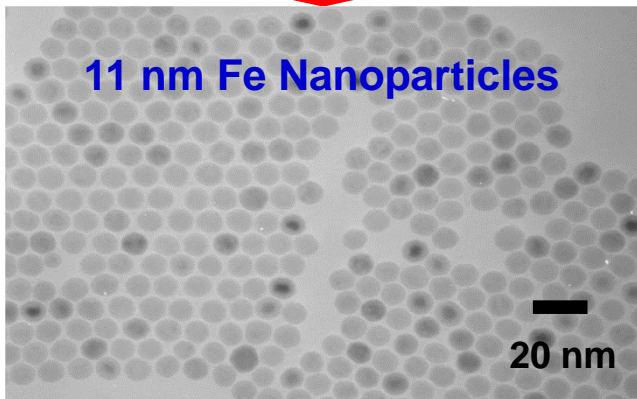


11 nm Iron oxide
Nanocrystals

**Main problem: expensive & toxic precursor
 $\text{Fe}(\text{CO})_5$ (\$ 2000 USD/Kg)**

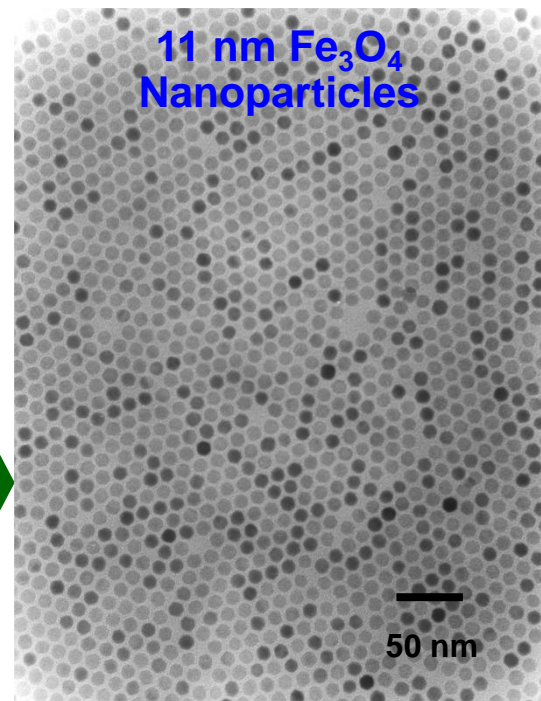
**Synthesis of
Fe-Oleate complex from
the reaction of $\text{Fe}(\text{CO})_5$ & Oleic acid**

**Thermolysis of
Fe-oleate complex**



T. Hyeon *et al.* *J. Am. Chem. Soc.*
2001, 123, 12798

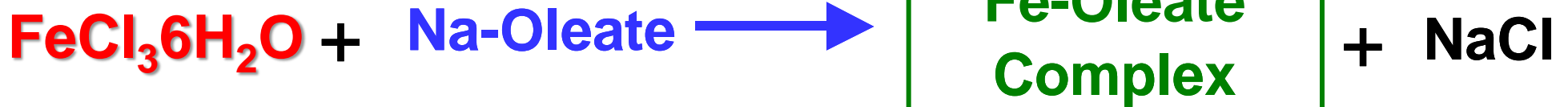
**Controlled
Oxidation**



40 gram of Monodisperse Magnetite Nanocrystals are produced using $\text{FeCl}_3 \cdot 6\text{H}_2\text{O}$

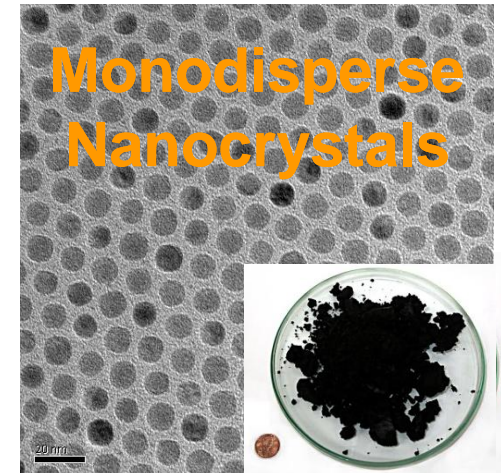


Now UNIST



**Fe-Oleate
Complex**

**Heating from RT to B.P.
Followed by Aging**

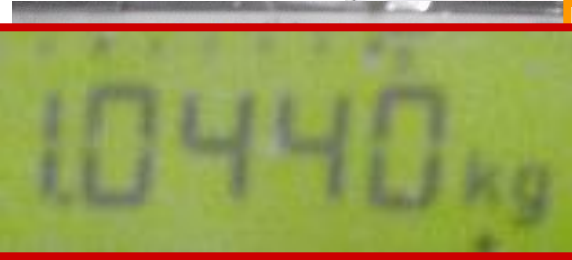


> 1 kg of 11 nm Fe₃O₄ Nanocrystals



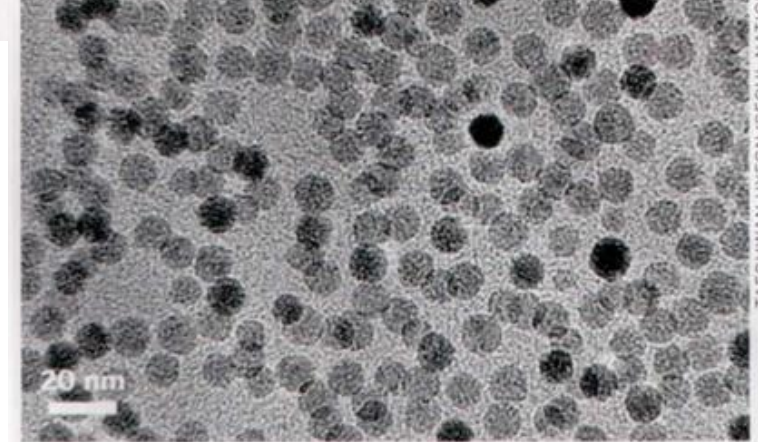
Chem. & Eng. News, August 24, 2009
SCIENCE & TECHNOLOGY CONCENTRATES

<http://pubs.acs.org/cen/news/87/i34/8734news10.html>



NANOCRYSTALS BY THE KILOGRAM

Kilogram-scale batches of uniform-sized nanocrystals can be prepared via a simple synthesis procedure, according to researchers in South Korea. The availability of a low-cost method for making bulk quantities of monodisperse (single-sized) nanocrystals may speed up development of nanotechnology applications. Several methods for preparing monodisperse nanocrystals have already been reported, but typically those methods yield gram quantities of product and require size-sorting steps. Taeghwan Hyeon, a professor of chemical engineering at Seoul National University, reported that his research group, in collaboration with Wan-Jae Myeong and coworkers at Hanwha



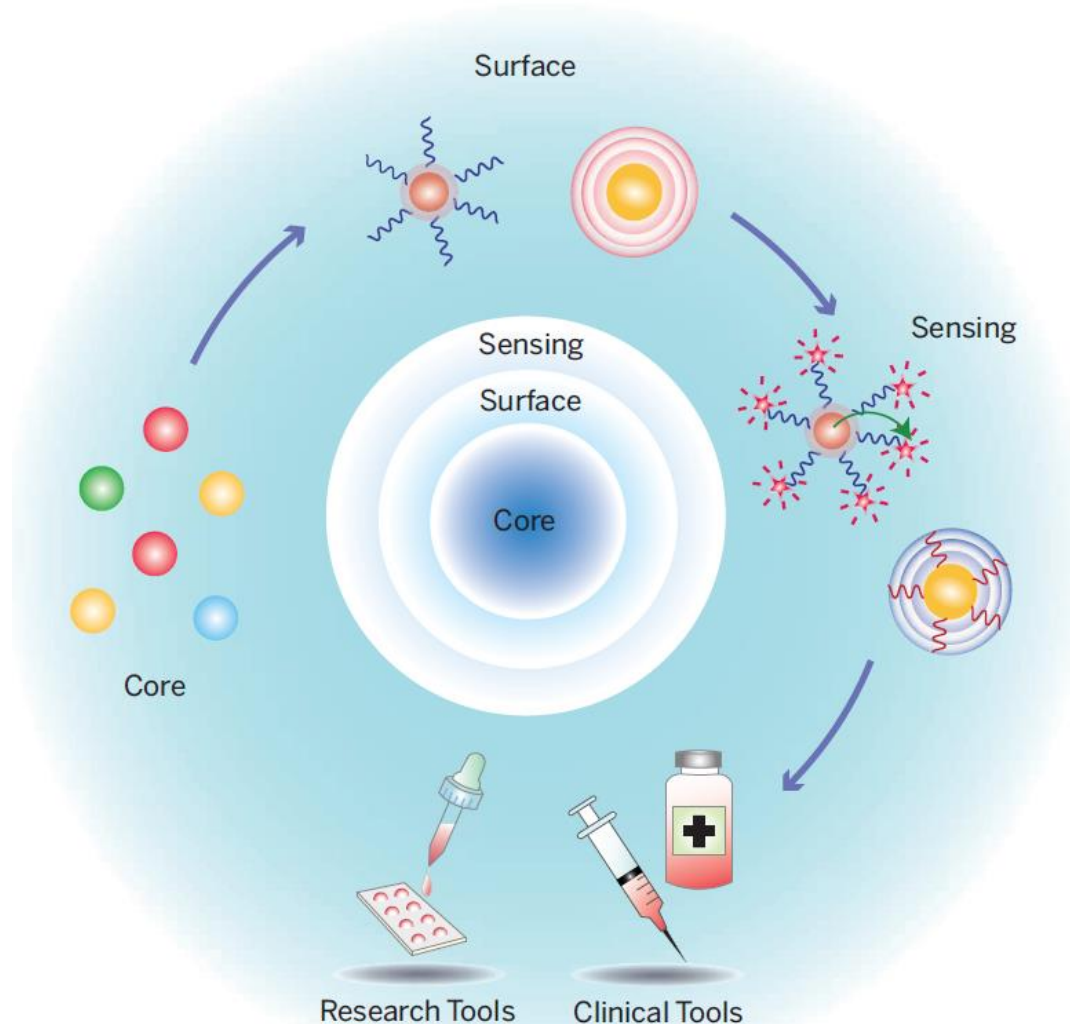
TEM analysis shows that these Fe₃O₄ (magnetite) crystals, which were made via a kilogram-scale preparation method, are highly uniform in size and shape.

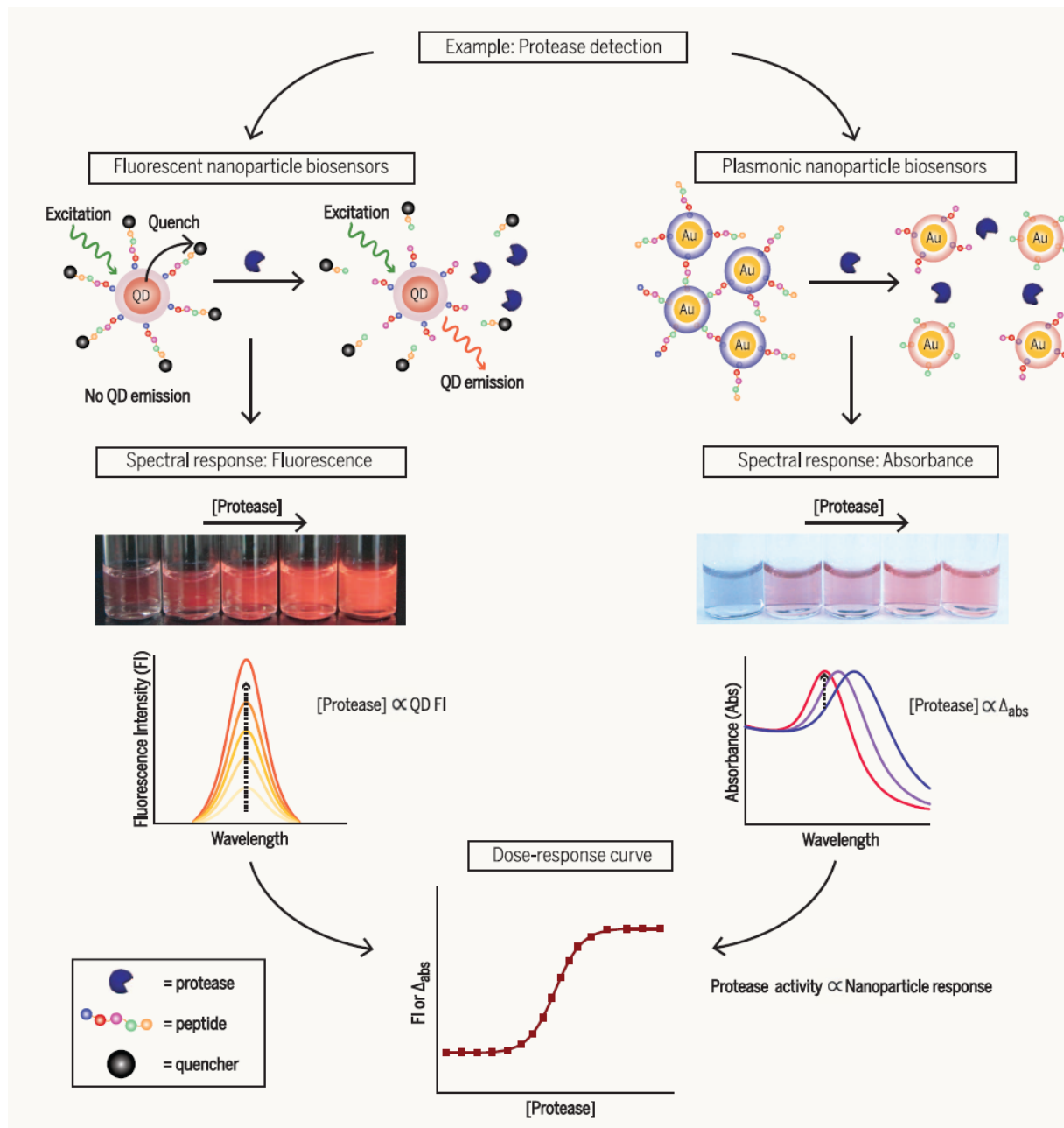
Chemical, also in Seoul, have synthesized kilogram-scale batches of uniformly sized 11-nm-diameter magnetite (Fe₃O₄) crystals via a procedure they developed. The method, which takes less than seven hours to complete and does not require size-

- Hanwha Chemicals Co.**
- Pilot Plant of 100ℓ reactor**
- kg/batch for < 7 hour**

sorting steps. All for making a surfactant with hydrated iron chloride, an inexpensive reagent, and then heating the complex to form a highly dispersible magnetite. Scaling the synthesis even further may be particularly useful for applications in data storage, medical imaging, and the locally directed drug delivery. —MJ

Colloidal nanoparticles as advanced biological sensors, Philip D. Howes, Rona Chandrawati, Molly M. Stevens* P. D. Howes *et al.*, *Science* **346**, 53 (2014)

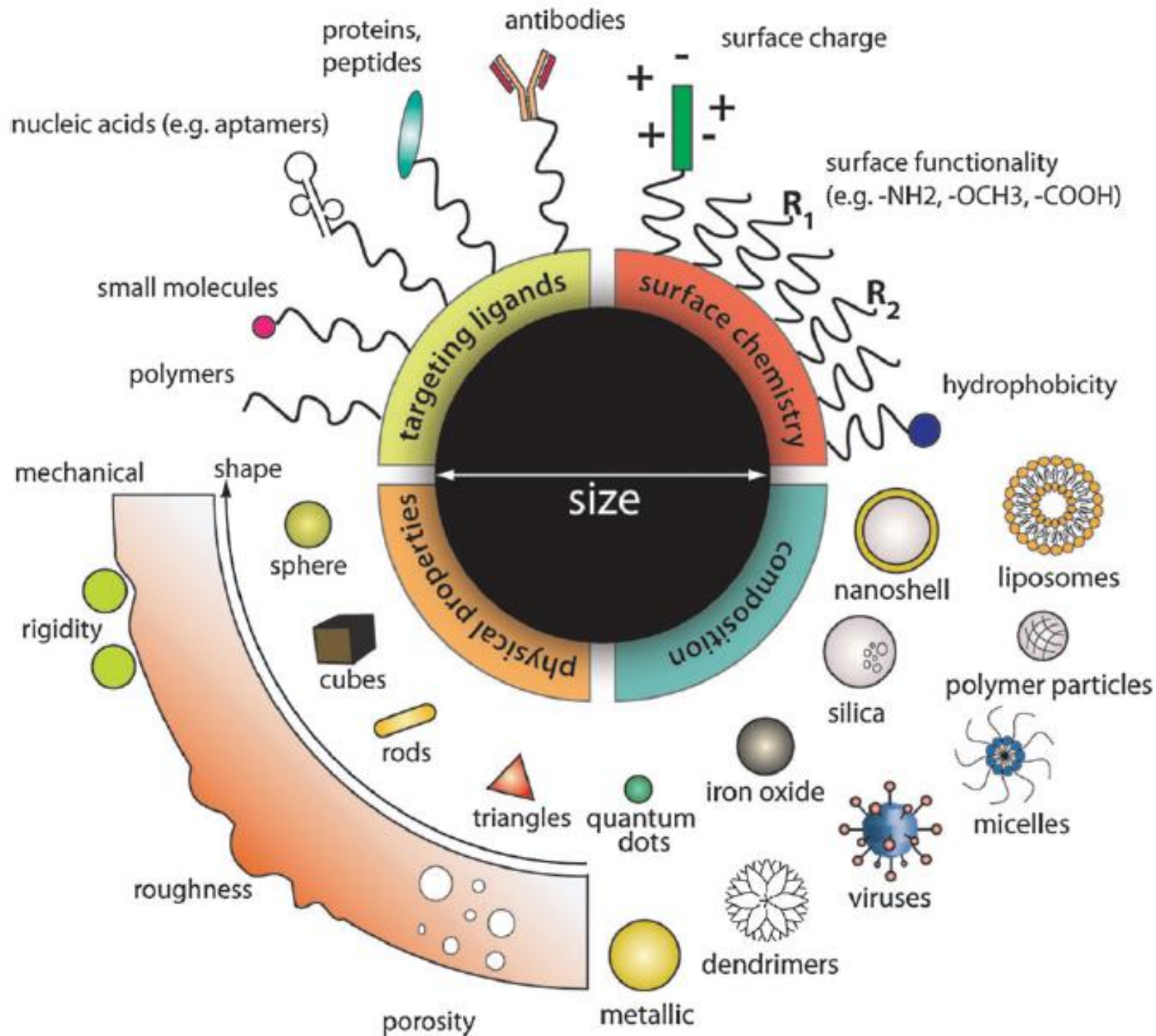




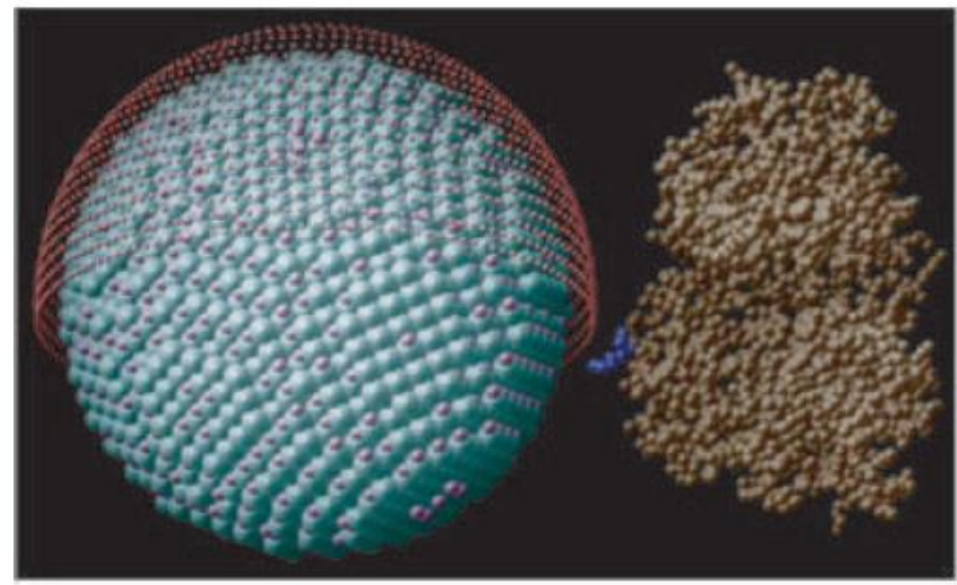
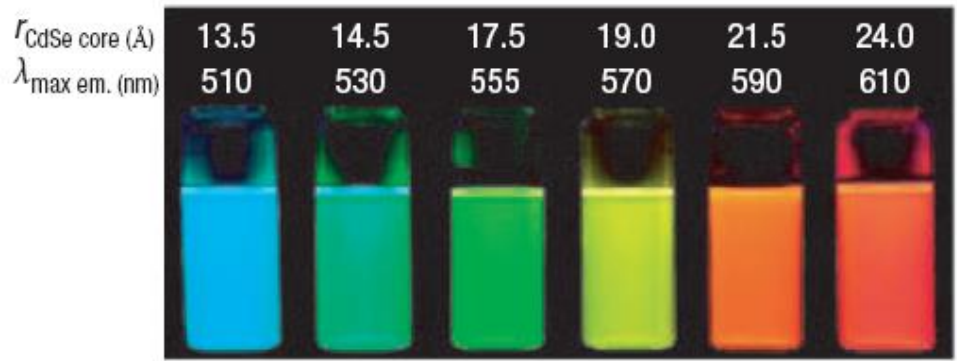
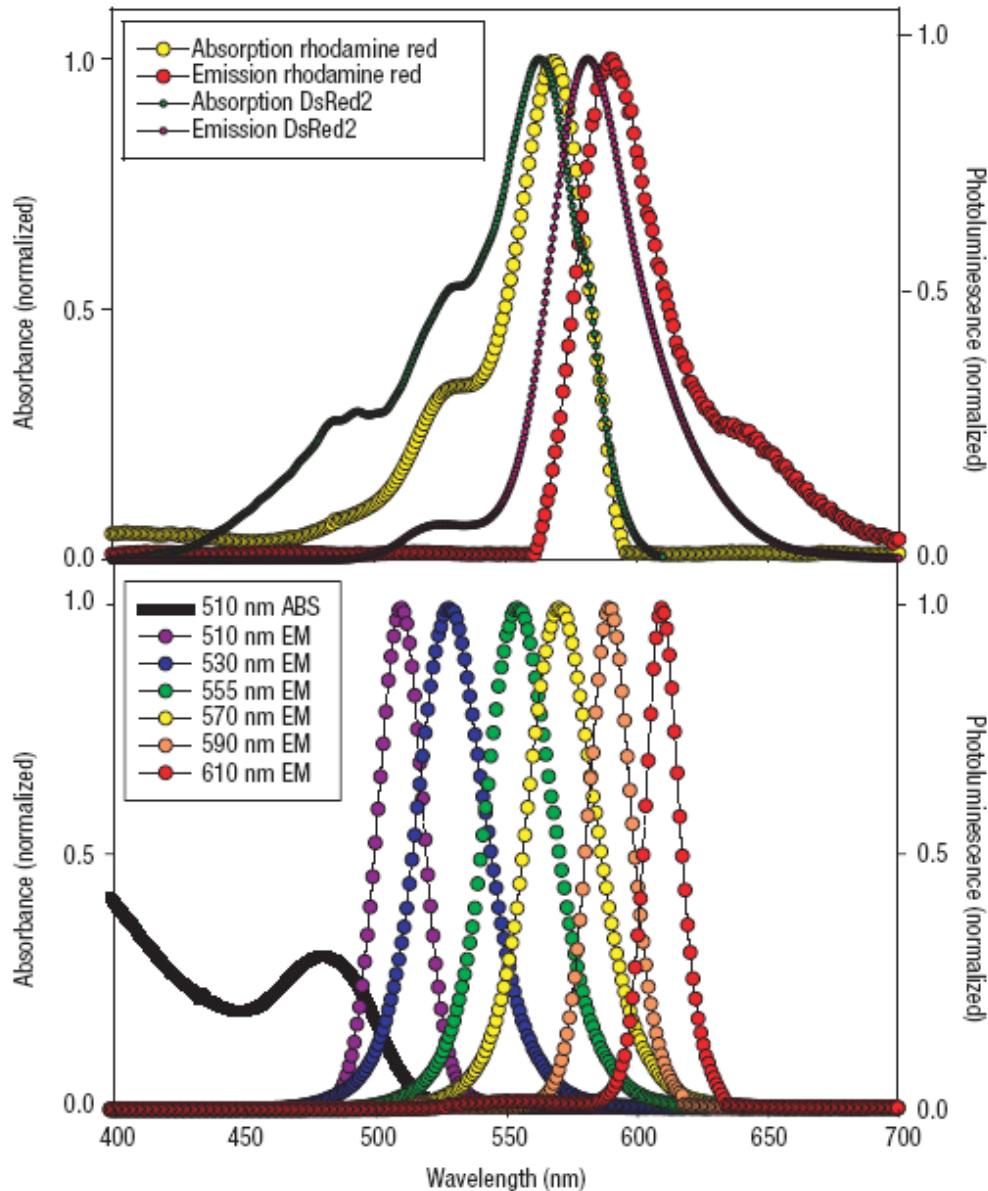
Quantum dot bioconjugates for imaging, labelling and sensing

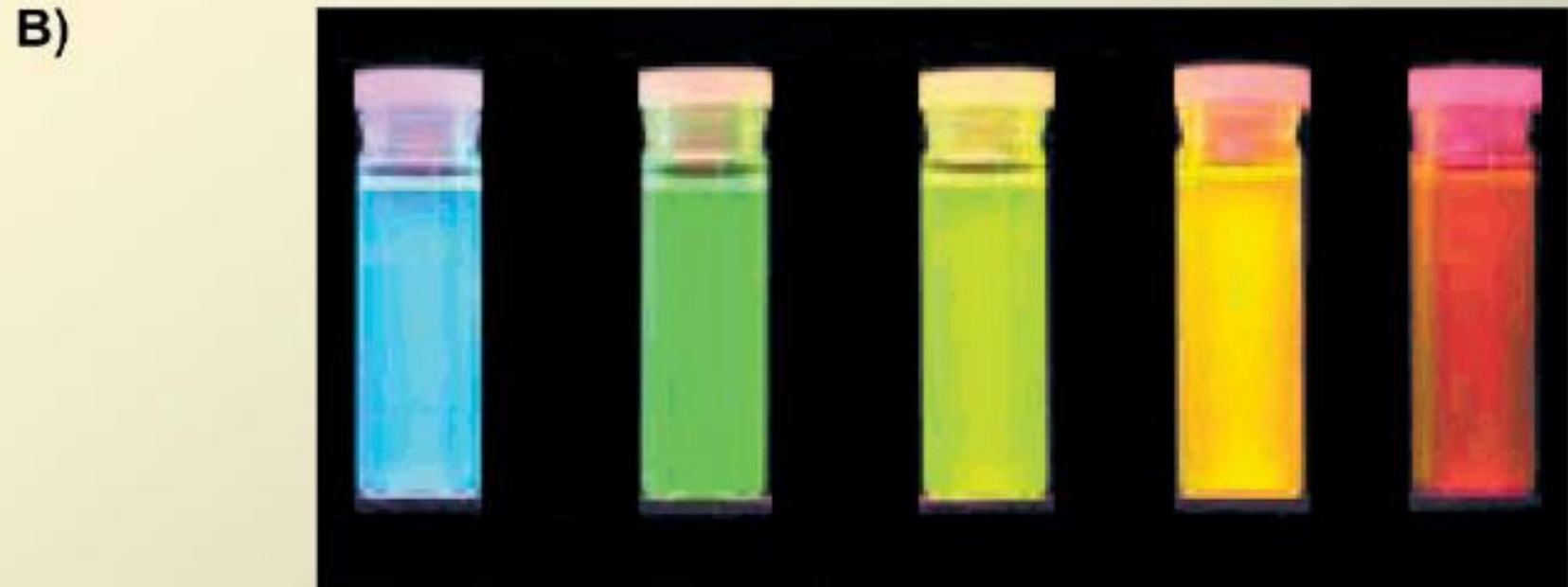
H. Mattoussi, *Nature Mater.* **2005**, 4, 435.

- Applications in cellular labelling, deep-tissue imaging, assay labelling and as efficient fluorescence resonance energy transfer donors.
- High quantum yield, high molar extinction coefficients ($\sim 10\text{--}100\times$ that of organic dyes)
- Broad absorption with narrow, symmetric photoluminescence (PL) spectra (full-width at half-maximum $\sim 25\text{--}40$ nm) spanning the UV to near-infrared, large effective Stokes shifts
- High resistance to photobleaching
- Exceptional resistance to photo- and chemical degradation
- Size-tune fluorescent emission as a function of core size
- Broad excitation spectra, which allow excitation of mixed QD populations at a single wavelength far removed (>100 nm) from their respective emissions \rightarrow 'multiplexing' (simultaneous detection of multiple signals).



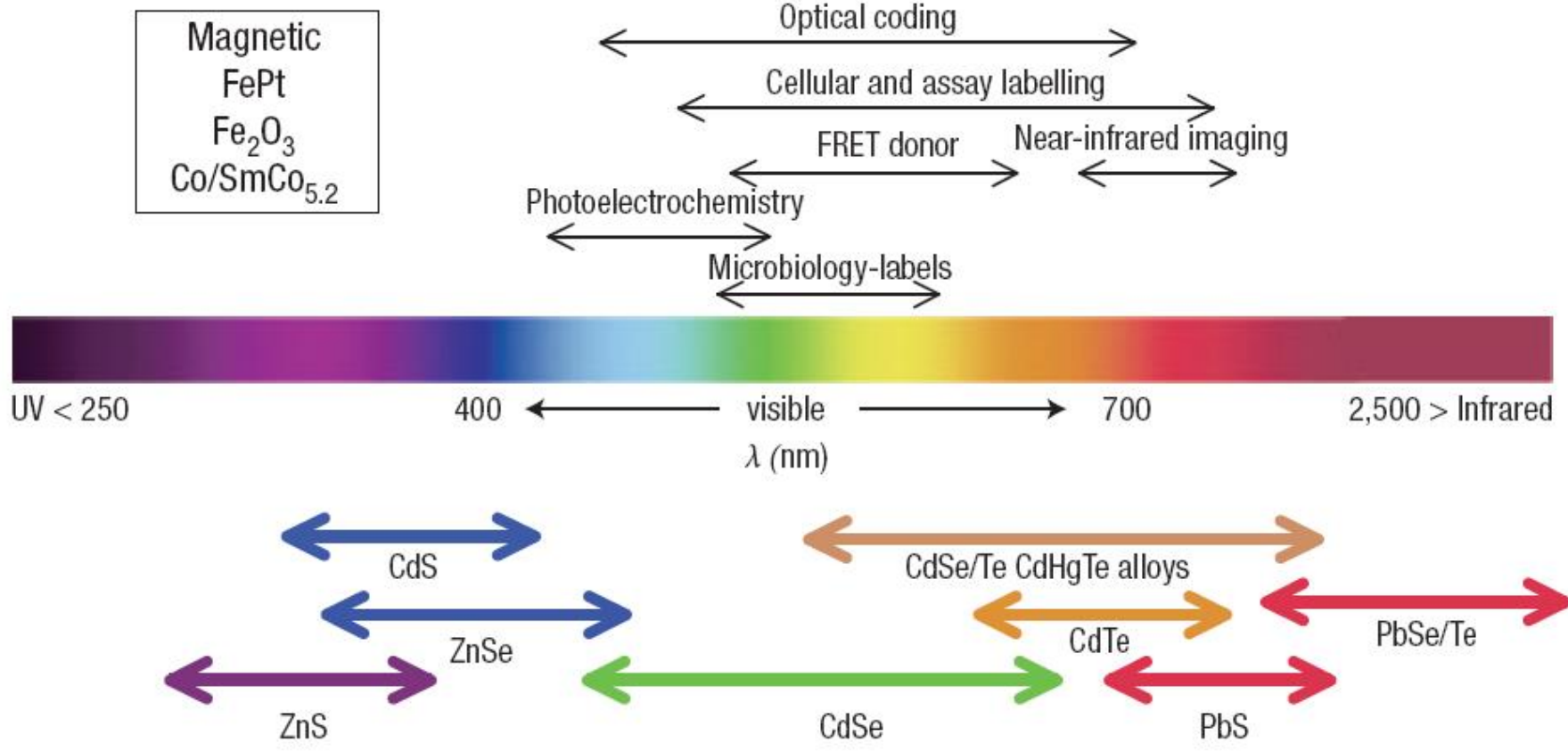
Comparison of rhodamine red/DsRed2 spectral properties to those of QDs highlighting how multiple narrow, symmetric QD emissions can be used in the same spectral window as that of an organic dye.





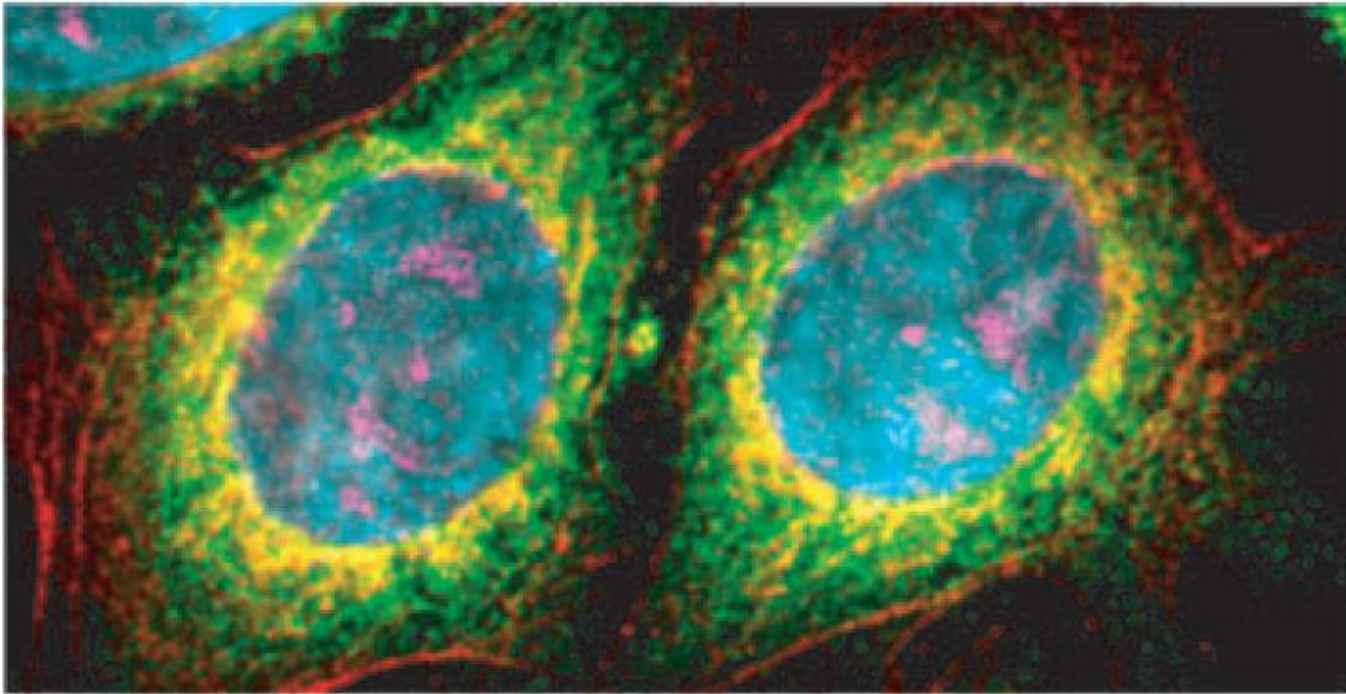
Representative QD core materials scaled as a function of their emission wavelength superimposed over the spectrum.

Representative areas of biological interest

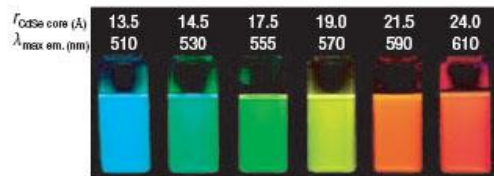
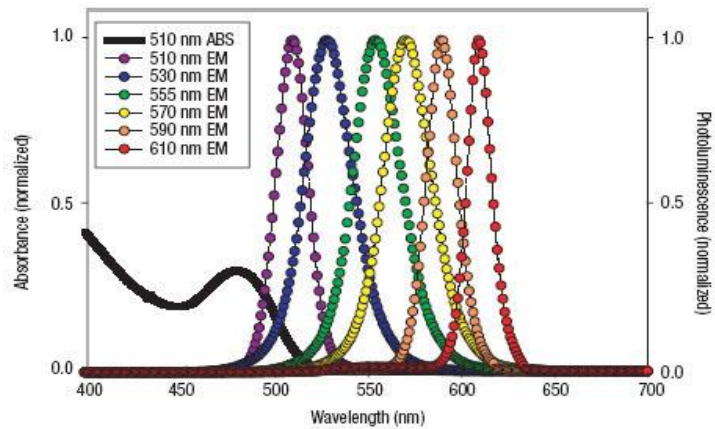


Pseudo-colored image depicting five-color QD staining of fixed human epithelial cells.

Cyan corresponds to 655-nm Qdots labelling the nucleus,
magenta 605-Qdots labelling Ki-67 protein,
orange 525-Qdots labelling mitochondria,
green 565-Qdots labelling microtubules
and red 705-Qdots labelling actin filaments.



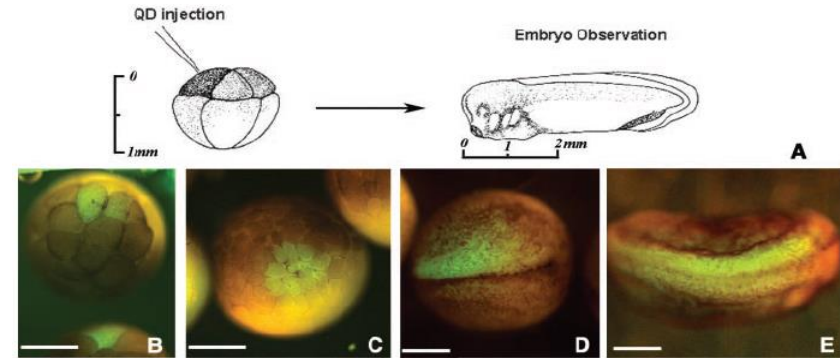
Fluorescent Bio-imaging using QDs



Medintz et. al. , *Nat. Mater.* **2005**, 4, 435.

Advantage

- Long term stability
- Various wavelength
- Narrow emission



Dubertret et. al., *Science* **2002**, 298, 1759.

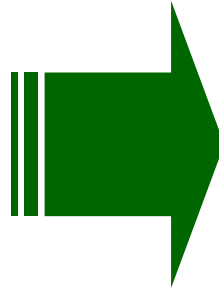
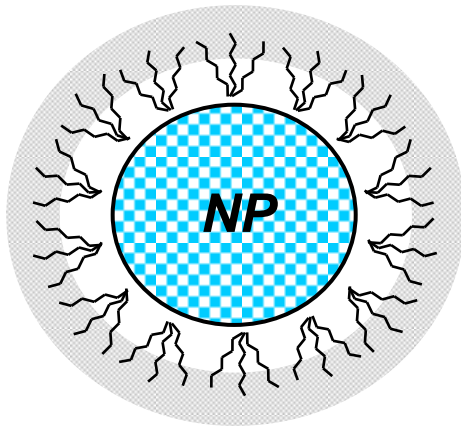
Differentiation of *Xenopus* embryos to cells

Limitation

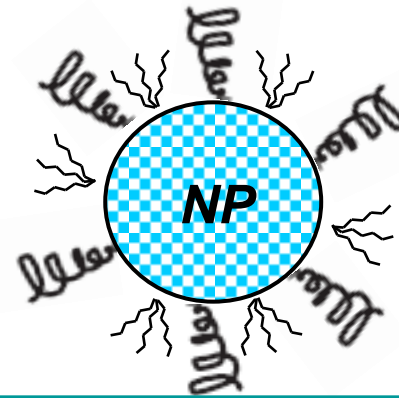
- Highly toxic cadmium
- Shallow penetration depth to living organ

Water-dispersible Nanoparticles

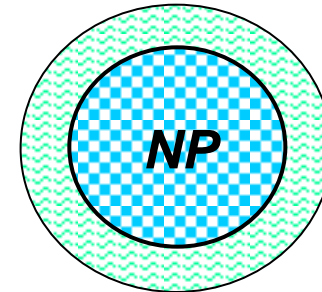
Hydrophobic shell



Ligand Exchange
with hydrophilic ligands



Encapsulation
with hydrophilic surface



Semiconductor Nanocrystals as Fluorescent Biological Labels

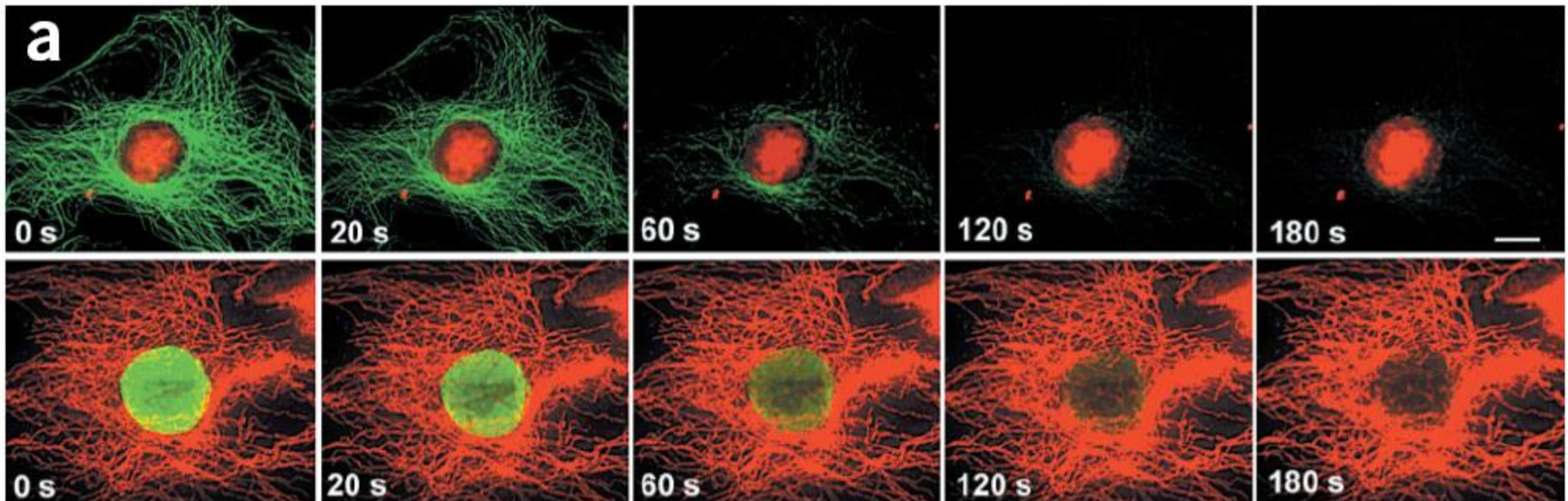
Shimon Weiss and A. Paul Alivisatos (U. California, Berkeley)

Science **1999**, 281, 2013.

The use of nanocrystals for biological detection.

A. Paul Alivisatos, *Nature Biotechnology* **2004**, 22, 47.

Demonstration of Photostability of QD's vs conventional dye



Near-infrared fluorescent type II quantum dots for sentinel lymph node mapping,

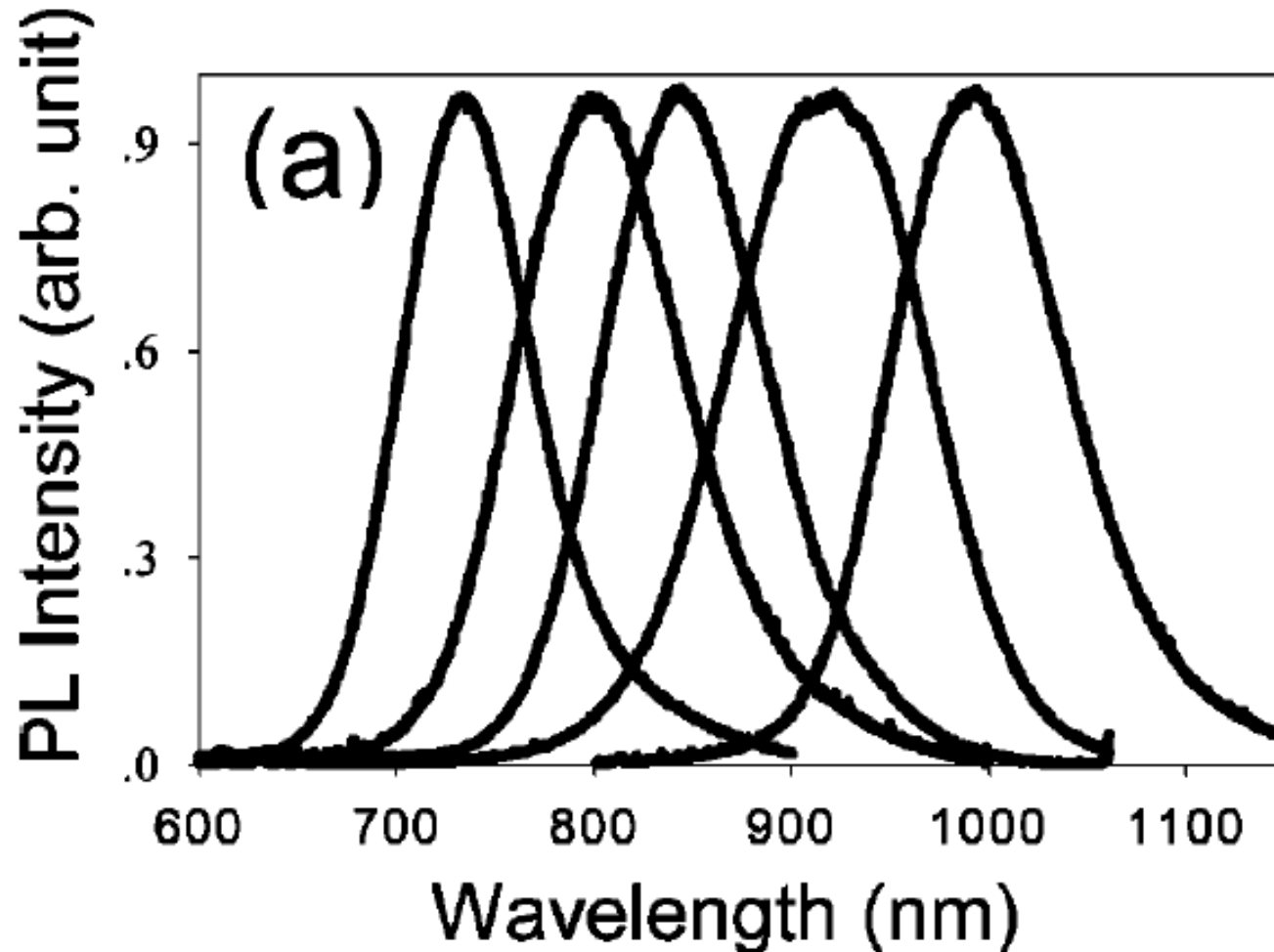
Sungjee Kim, Yong Taik Lim,, M. G. Bawendi, J. H. Frangioni,
Nature Biotechnology **2004**, 22, 93.

- Fluorescence emission of type II quantum dots can be tuned into the near infrared and that a polydentate phosphine coating renders them soluble, disperse and stable in serum.
- Type II NIR QDs with a hydrodynamic diameter of 15–20 nm, a maximal absorption cross-section, fluorescence at 840–860 nm
- NIR QD size of 16 nm = 440 kDa protein → critical diameter of 5 ~ 50 nm needed for retention of QDs in sentinel lymph node (SLN)

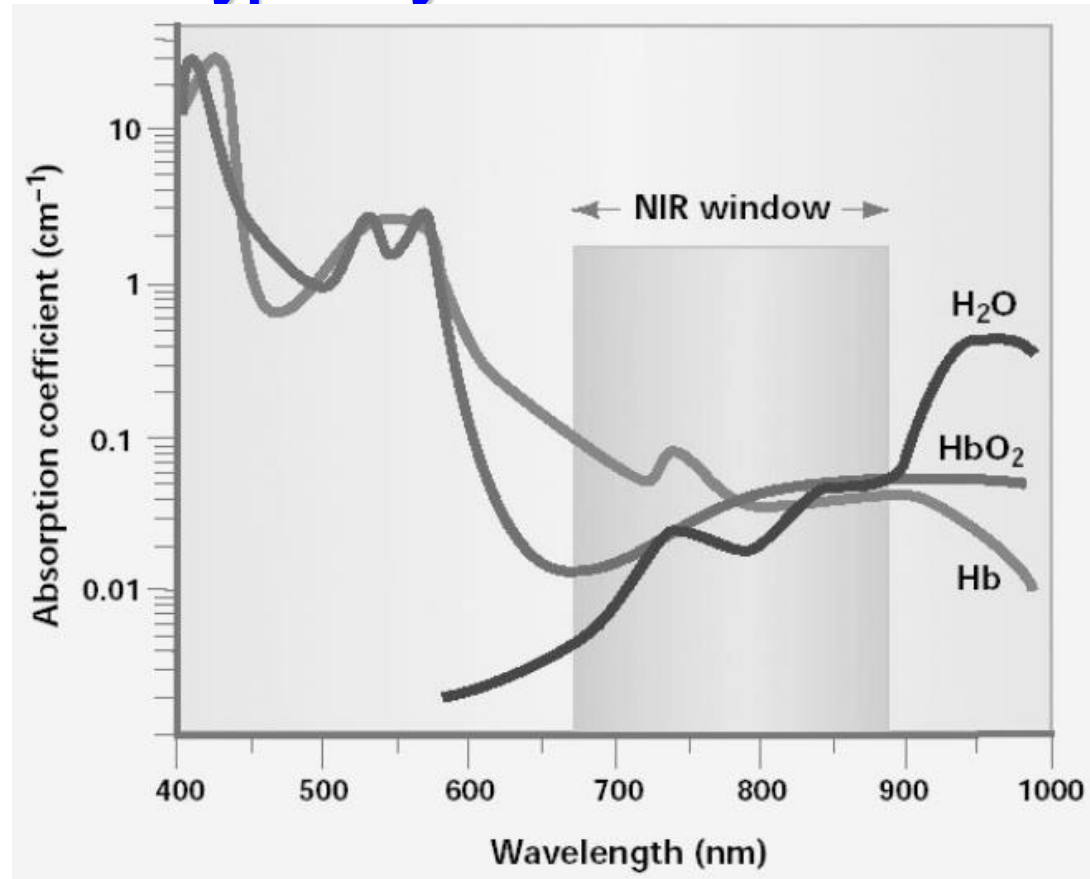
Sentinel lymph node:

First lymph node(s) reached by metastasizing cancer cells from a tumor.

- By changing the two variables of shell thickness and core size, the emission of type-II QDs can be easily and widely tuned.
- PL spectra from CdTe/CdSe QDs that range from 700 nm to over 1000 nm simply by changing the core size and shell thickness.



NIR emitting window is appealing for biological optical imaging because of the low tissue absorption and scattering effects. typically at 650–900 nm



R. Weissleder, *Nature Biotechnol.* **2001**, 19, 316.

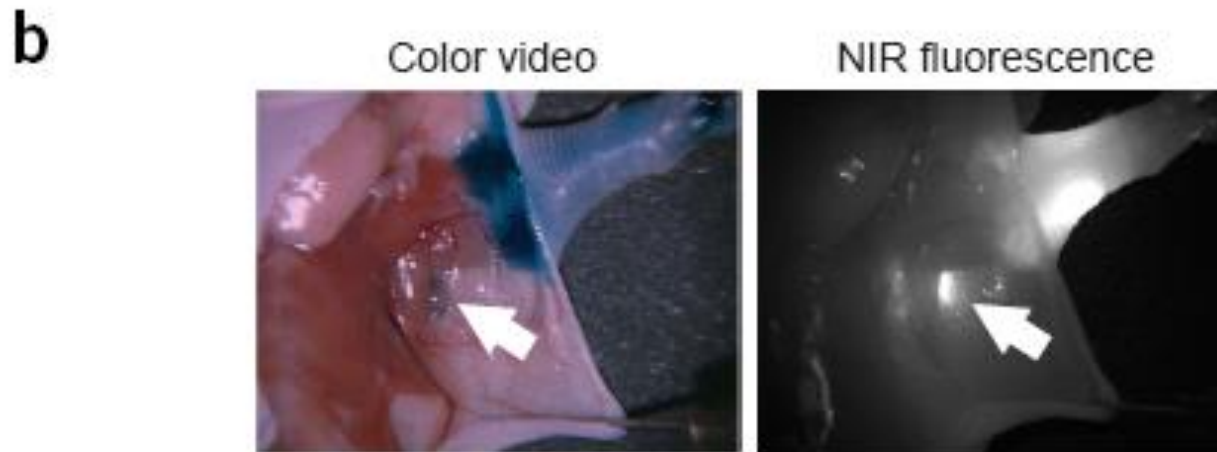
- Demonstrate that these quantum dots allow a **major cancer surgery, sentinel lymph node mapping, under complete image guidance.**
- Injection of only 400 pmol of near-infrared quantum dots permits **sentinel lymph nodes 1 cm deep** to be imaged easily in real time using excitation fluence rates of only 5 mW/cm².
- Localization of SLN → only 3 -4 min
- Image guidance using NIR QDs minimized size of incision to find node

Sentinel lymph node:

First lymph node(s) reached by metastasizing cancer cells from a tumor.

NIR QD sentinel lymph node mapping in the mouse

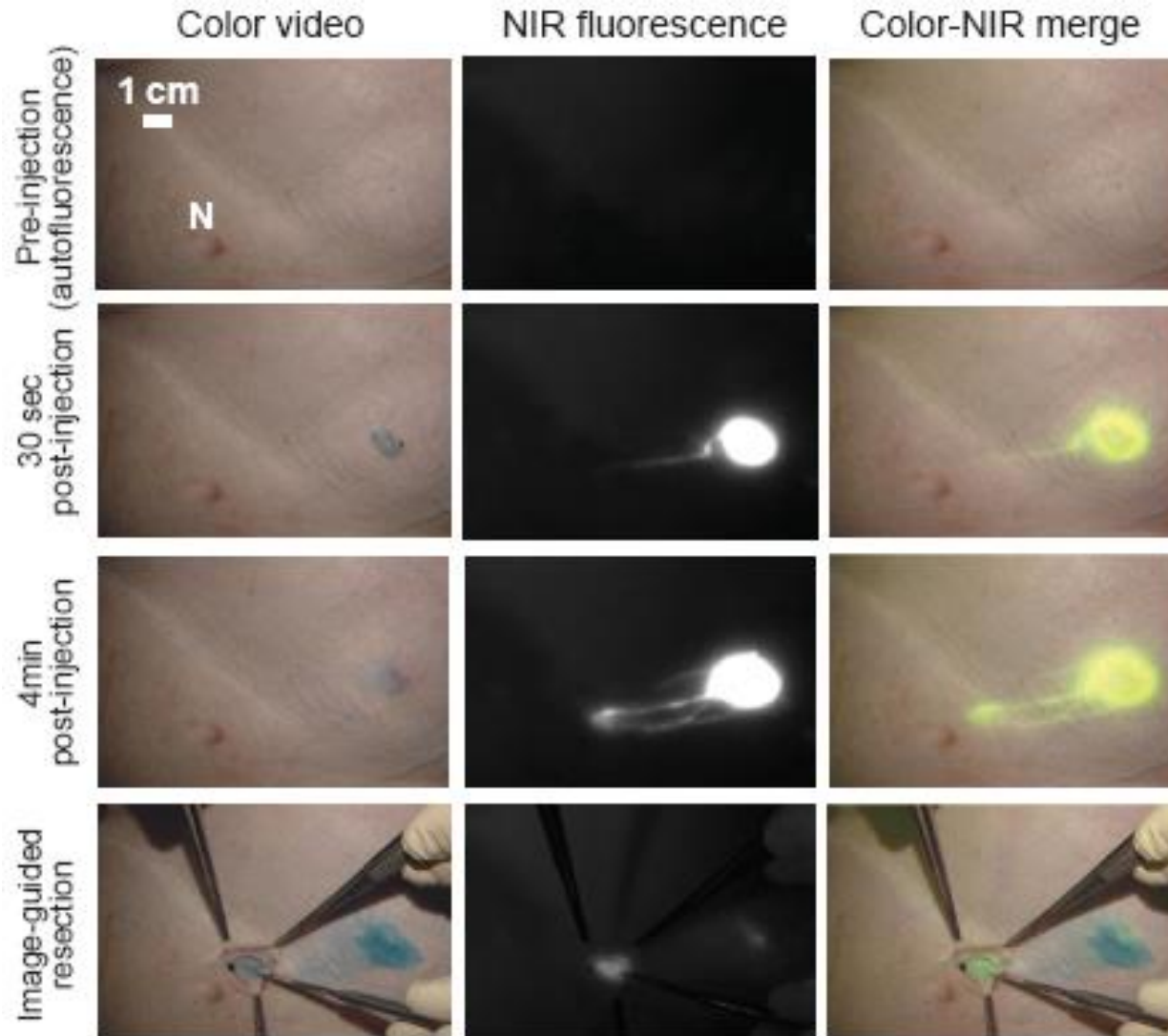
Images of mouse injected intradermally with 10 pmol of NIR QDs in the left paw.

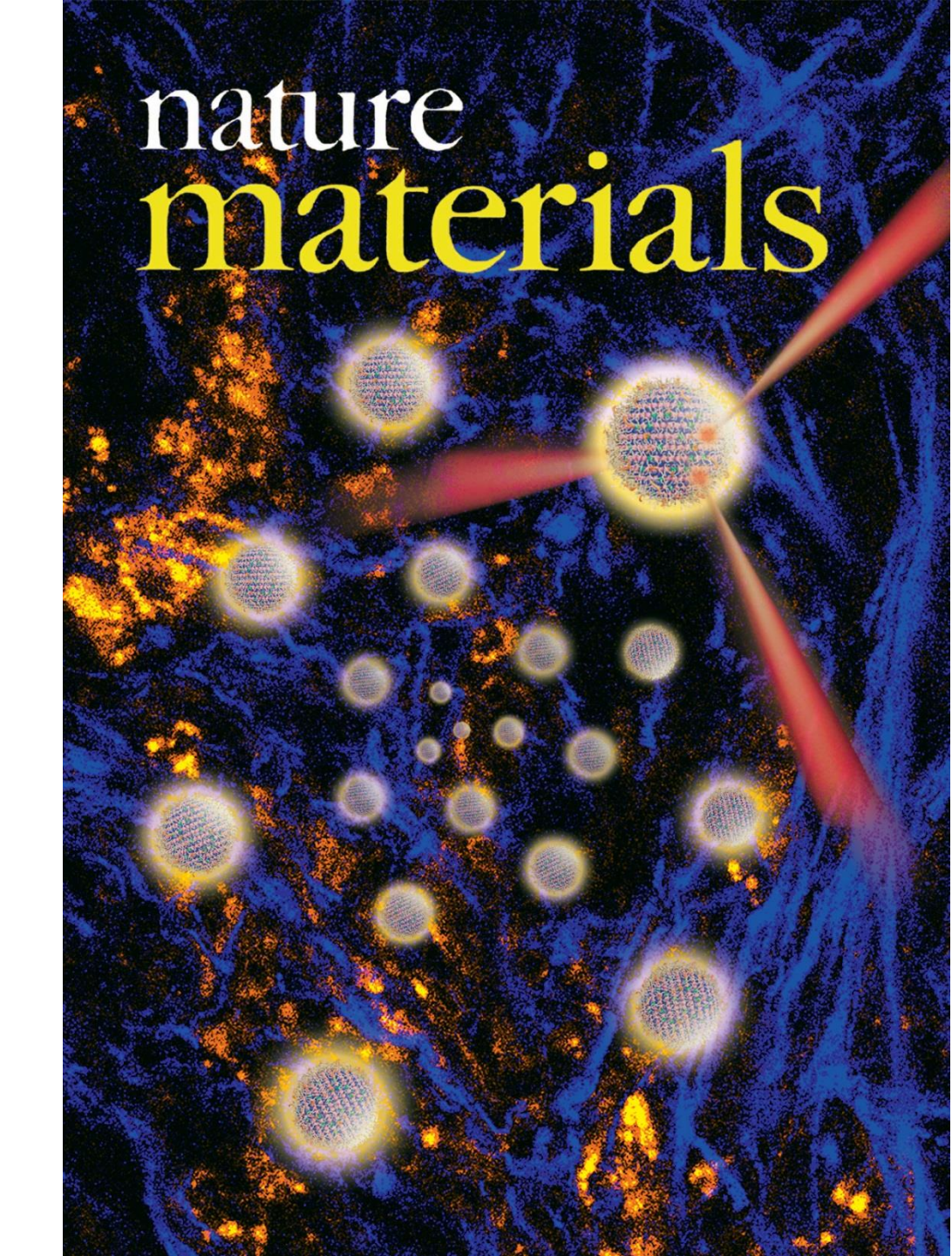


Sentinel lymph node:

First lymph node(s) reached by metastasizing cancer cells from a tumor.

Surgical field in a pig injected intradermally with 400 pmol of NIR QDs in the right groin.





nature
materials

**High-Resolution
Three-Photon
Biomedical Imaging
using Bright Doped
ZnS Nanocrystals**

J. Yu et al.,
Nature Mater. **2013**, 12, 359.

Toxicity Issue of Semiconductor Nanocrystals

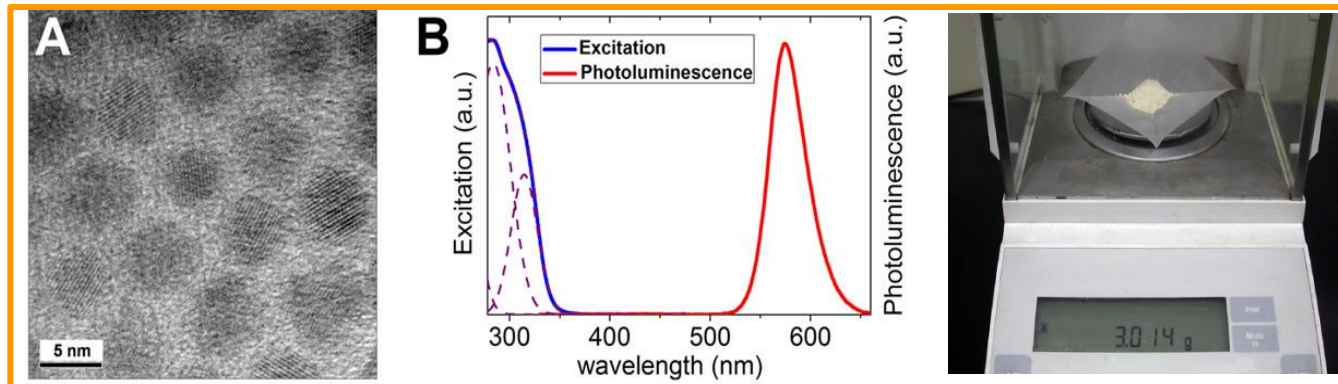
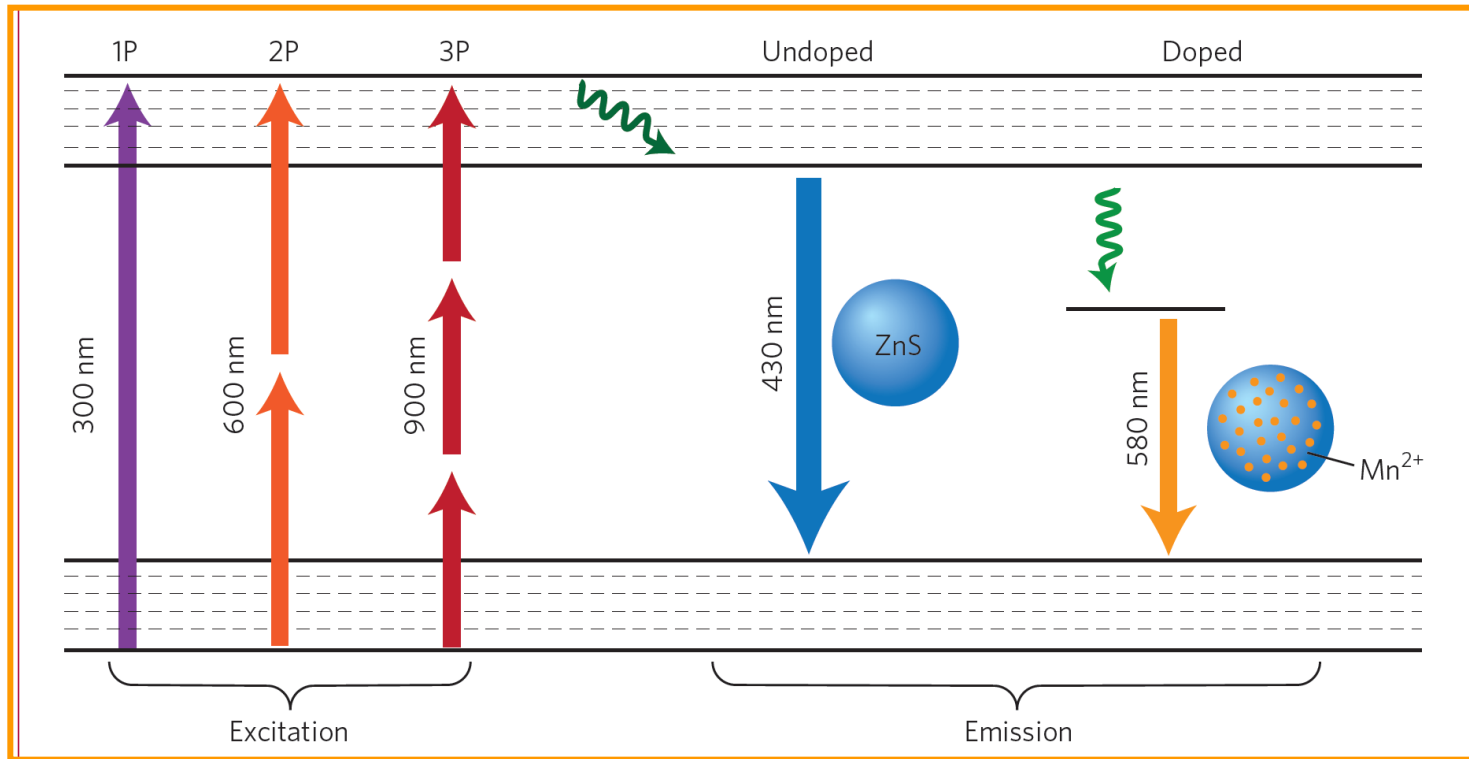
The in vivo accessible quantum dots are composed of toxic elements, and hardly degradable. Making smaller Q.D. < 6 nm requires more toxic element (Arsenic).

– Prof. Frangioni@MGH*Nat. Biotech.* Commentary 2011)

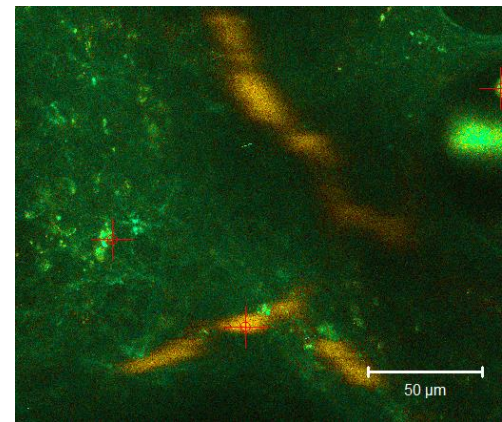
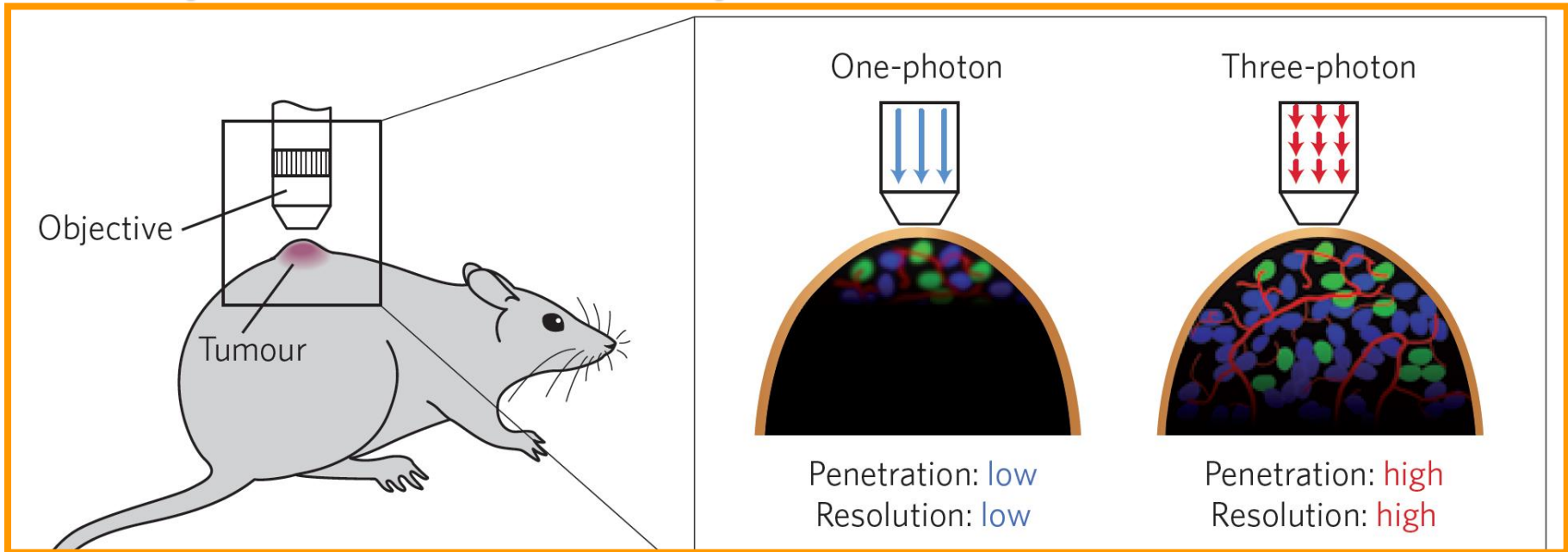
- Almost every fluorescence imaging semiconductor nanocrystal is composed of toxic elements (Cd, As, Se, etc.)
- **ZnS is a main-cover material to temporarily solve this problem.**

**CdSe/ZnS, CdTe/ZnS
InP/ZnS, InAs/ZnS**

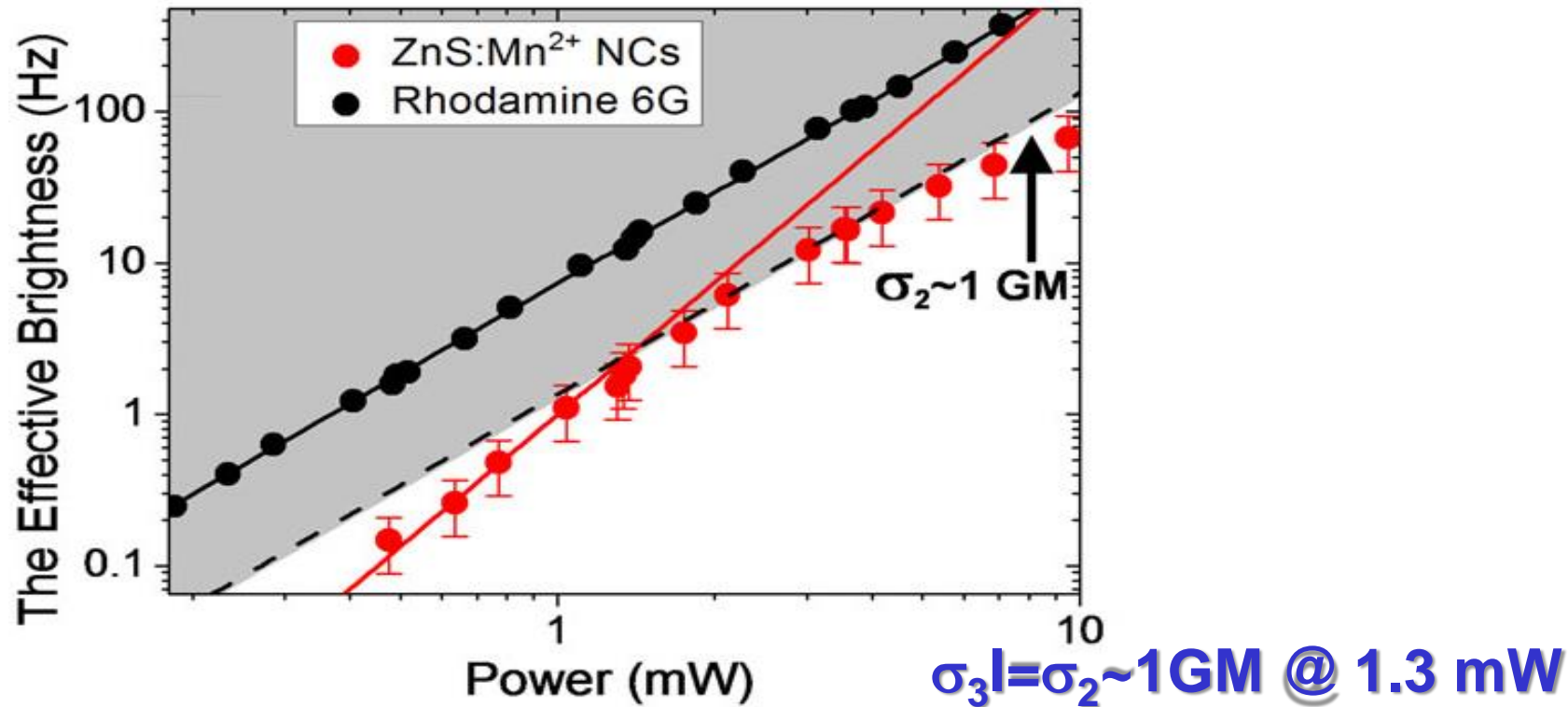
3-photon imaging using non-toxic & bright Mn²⁺-doped ZnS nanocrystals enables deeper tissue penetration *in vivo*.



3-photon fluorescence microscopy improves tissue penetration depth and resolution *in vivo*.

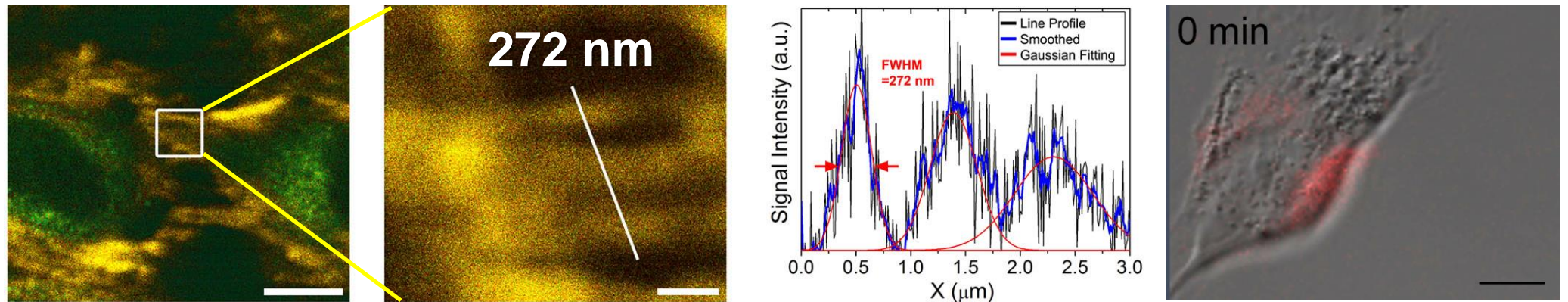


Fluorescence Correlation Spectroscopy



- The quantum mechanical probability of three-photon process is lower than that of one-photon and two-photon process.
(3PA~The 5th order nonlinear optical process!)
- Due to large 3PA cross section of ZnS:Mn NCs, the 3PL brightness reaches to the two-photon brightness of 1 GM at low power of 1.3 mW.

3PL High-Resolution Imaging of ZnS:Mn NCs

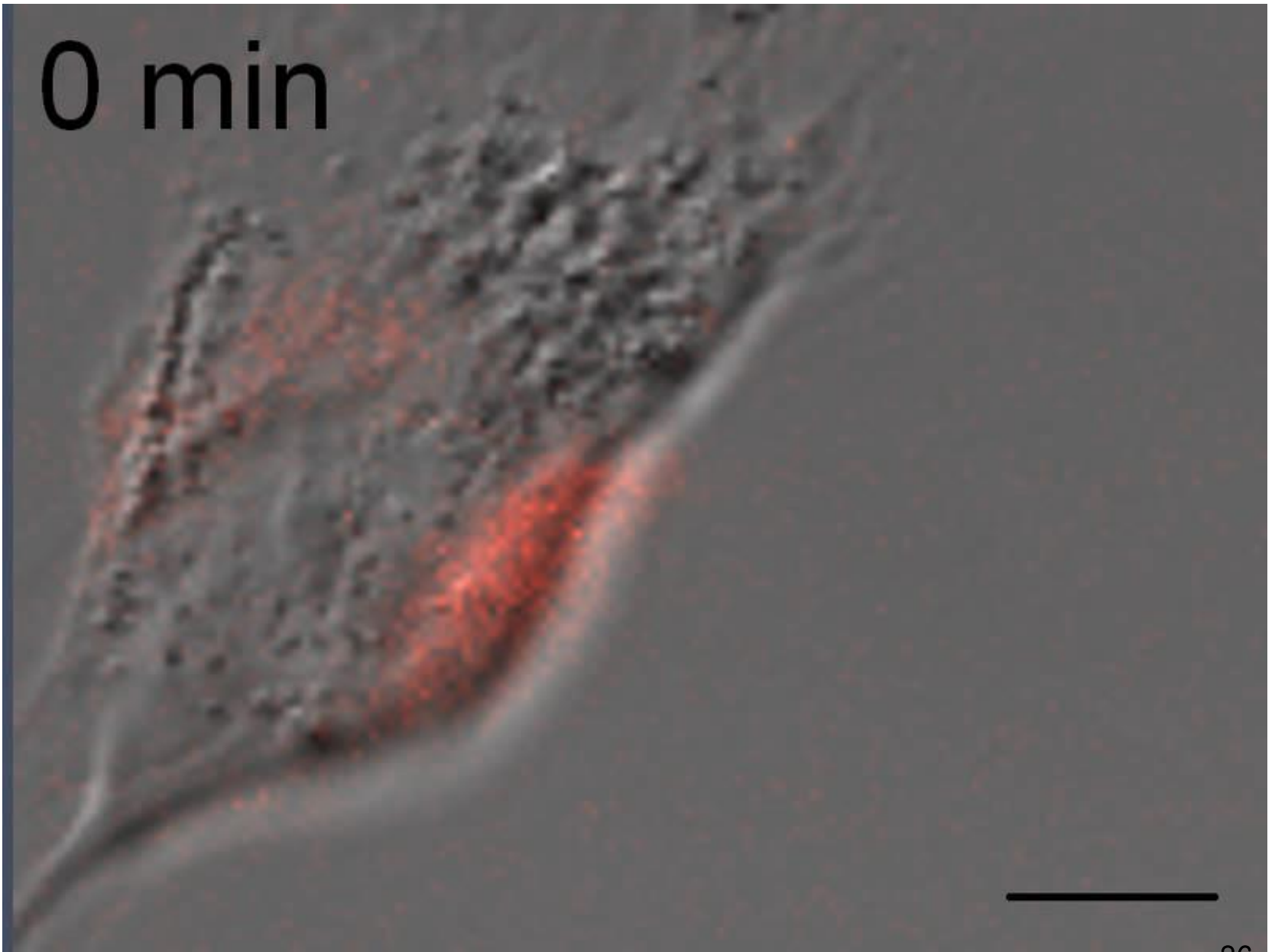


← **High-Resolution Imaging at non-saturation regime** → **Temporal Imaging @ low power (1mW)**

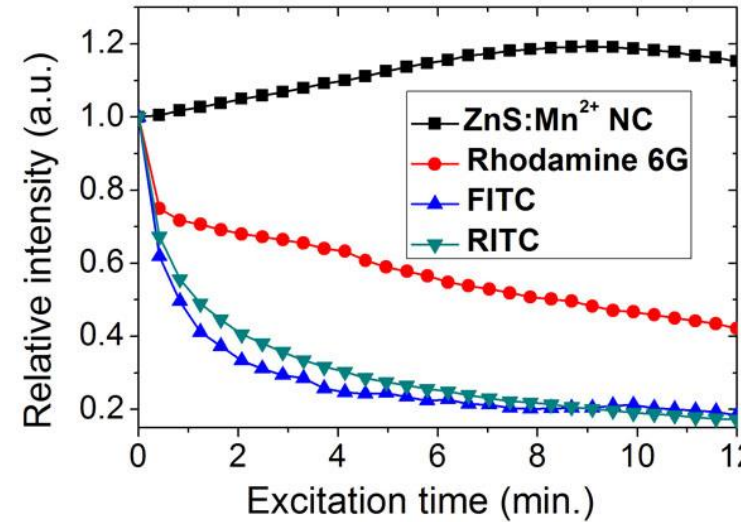
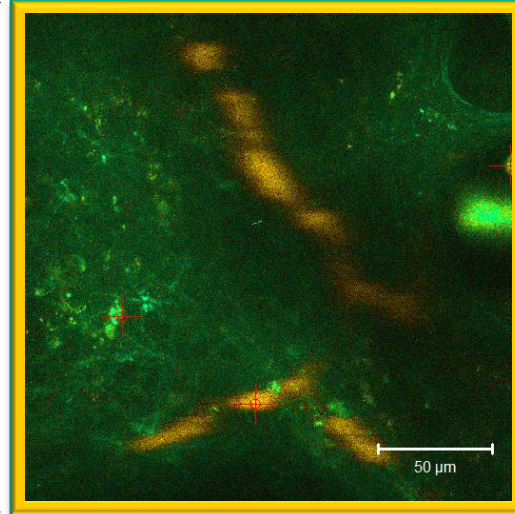
3PL of ZnS:Mn NCs enables **high-resolution imaging** approaching theoretical limit of 3PL Imaging (**272 nm** for 950 nm NIR excitation).

The ability of live cellular imaging for 10 hours demonstrates **no phototoxicity** at the imaging condition owing to **low power excitation of 0.5 mW**.

0 min



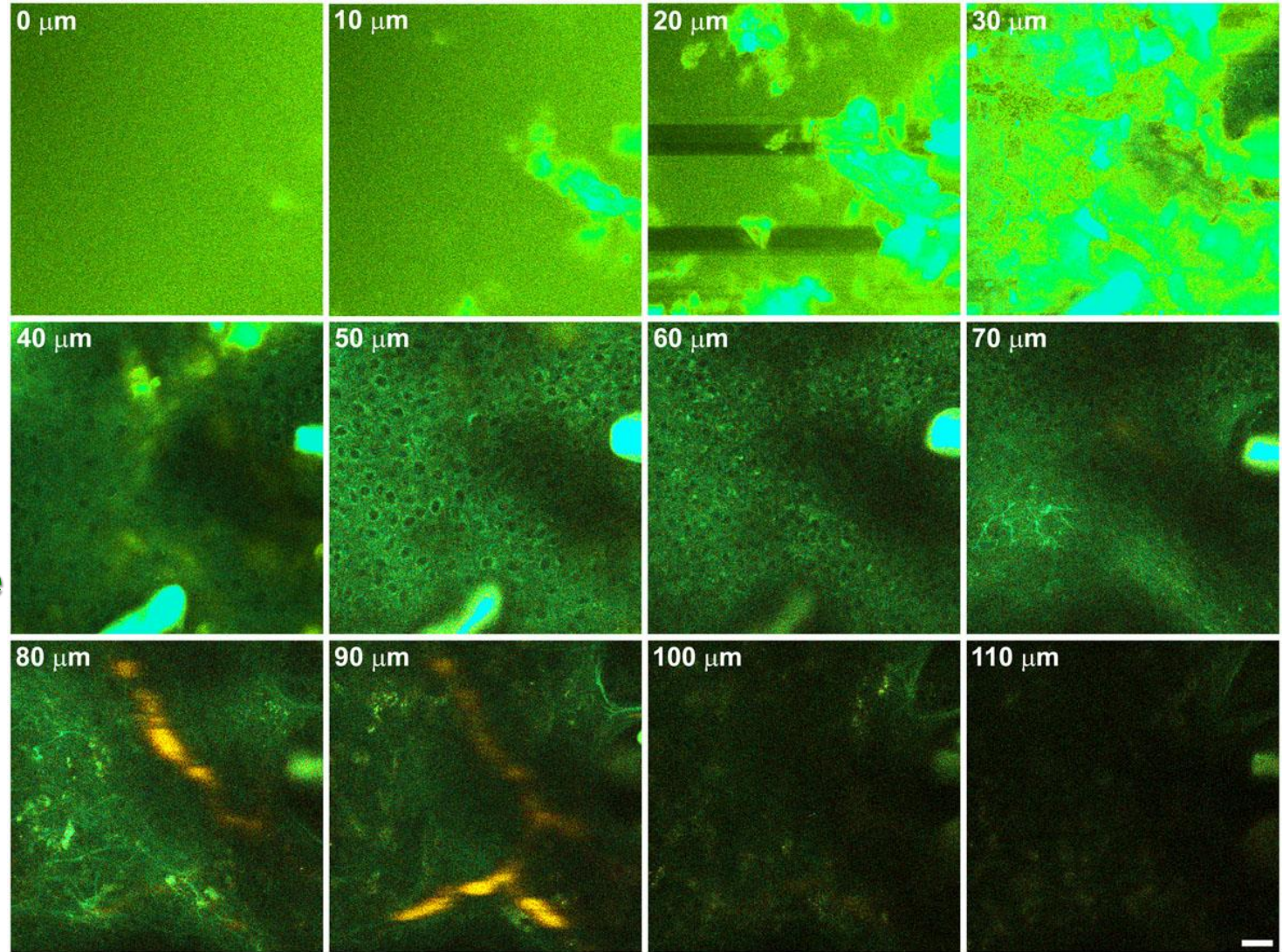
In Vivo 3PL Imaging of ZnS:Mn NC-RGD Conjugates



- High photostability of ZnS:Mn NCs enables *in vivo* 3PL imaging at high power (~10 mW).
- 3PL of RGD-conjugated ZnS:Mn NCs were visualized at the tumor vasculature due to the angiogenesis targeting.

Depth-projection of Tumor Vasculature

Background
autofluorescence



3PL of RGD-conjugated ZnS:Mn NCs can be imaged down to 100 μm even at the base of dermis (**Highly Scattering & Very Challenging**).

In Vivo 3PL Imaging of ZnS:Mn NC-targeting Tumor

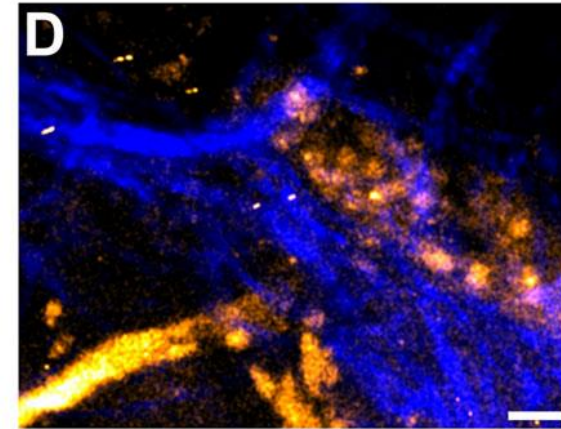
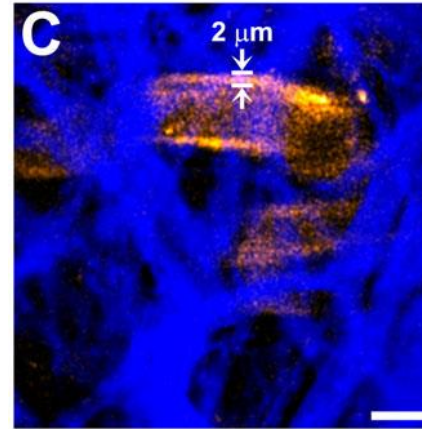
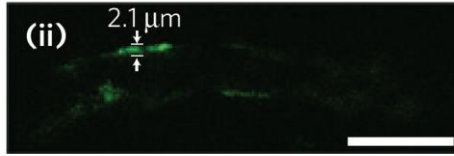
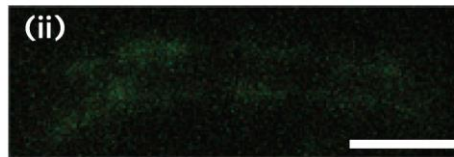
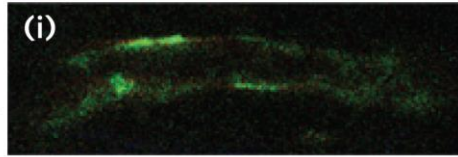
SHG from collagen fiber

Multiphoton imaging

One-photon imaging

ZnS:Mn NCs three-photon

FITC two-photon



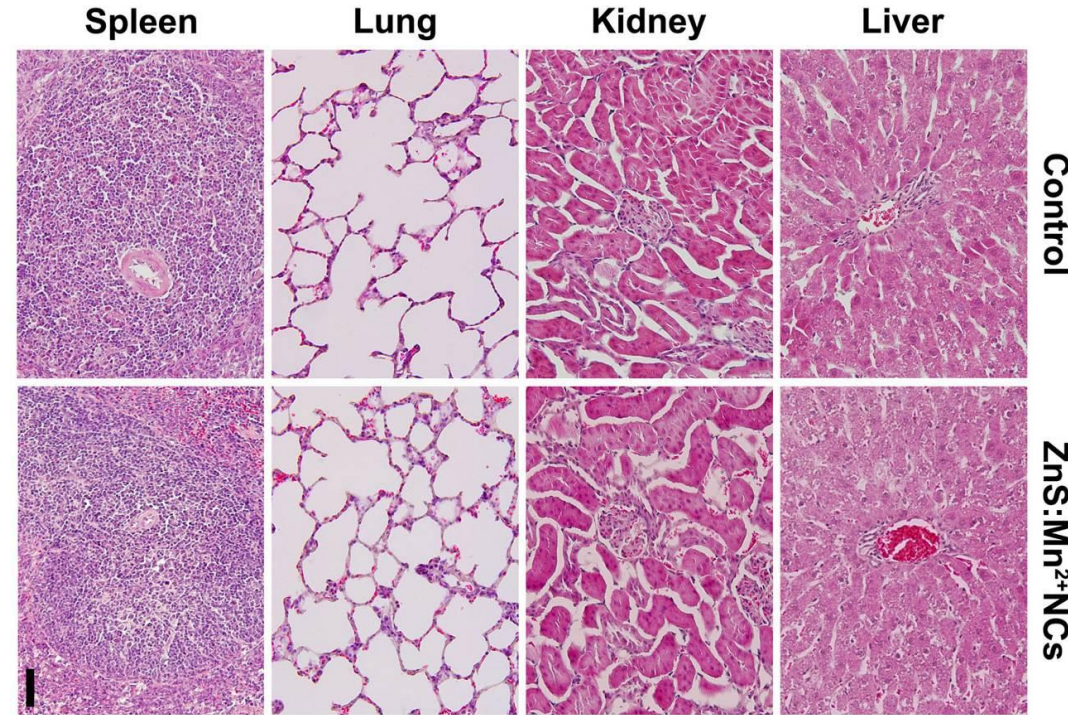
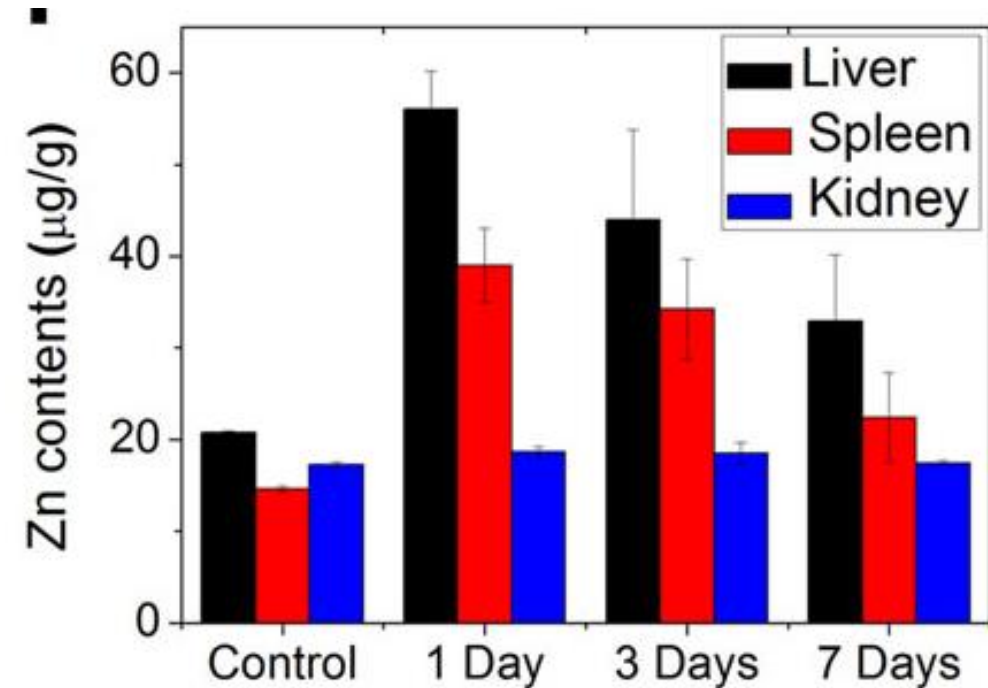
Endothelial Lining
(μm resolution)

Extravasation
(subcellular resolution)

- 3PL of ZnS:Mn NCs in tumor vasculature is **highly bright & spectrally distinguishable** from background fluorescence.

- 3PL Imaging of ZnS:Mn NCs-targeting Tumor at μm & **Subcellular Resolution.**

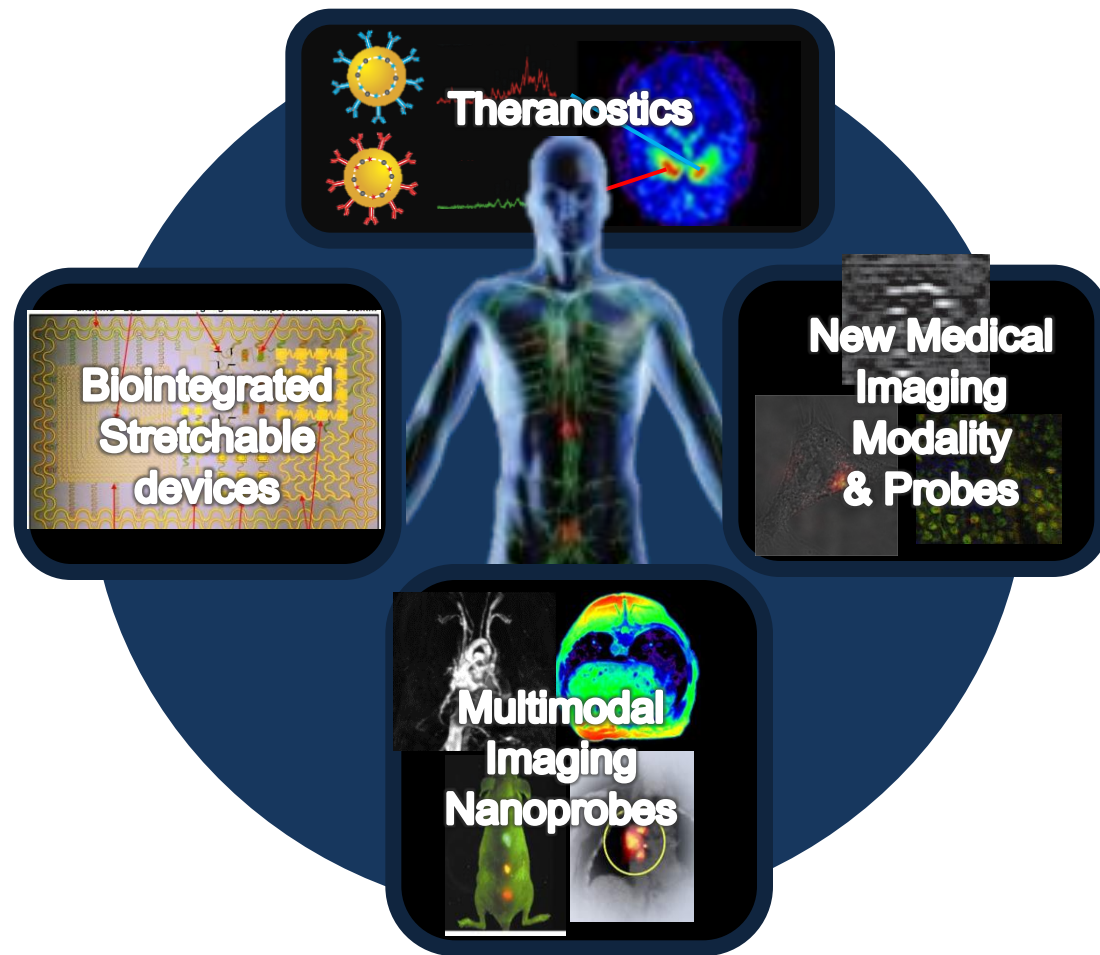
In Vivo Toxicity Examination of ZnS:Mn NCs



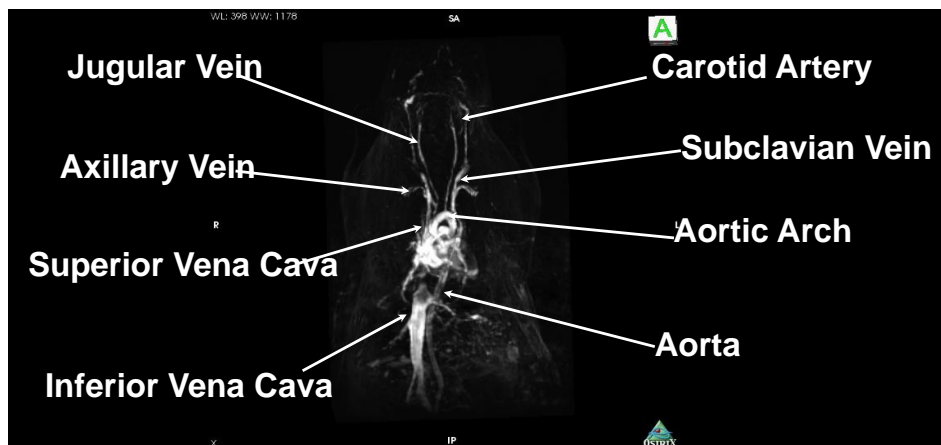
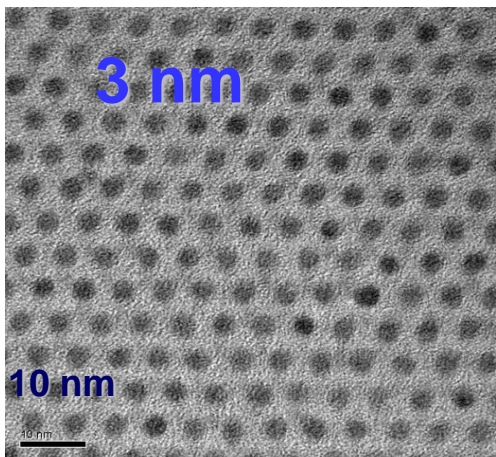
- The reticuloendothelial organs already contain non-negligible amounts of zinc ions ([Biocompatibility of ZnS nanocrystals](#)).
- The total amount of zinc ions is gradually decreased ([Clearance of ZnS nanocrystals](#)).
- The histological examination confirms no sign of in vivo toxicity ([Biocompatibility of ZnS nanocrystals](#)).

Part II.

Providing New Medical Diagnosis Tools and Therapeutic Methods using Nano



New non-toxic T1 MRI contrast agent using paramagnetic 3 nm Iron Oxide Nanoparticles

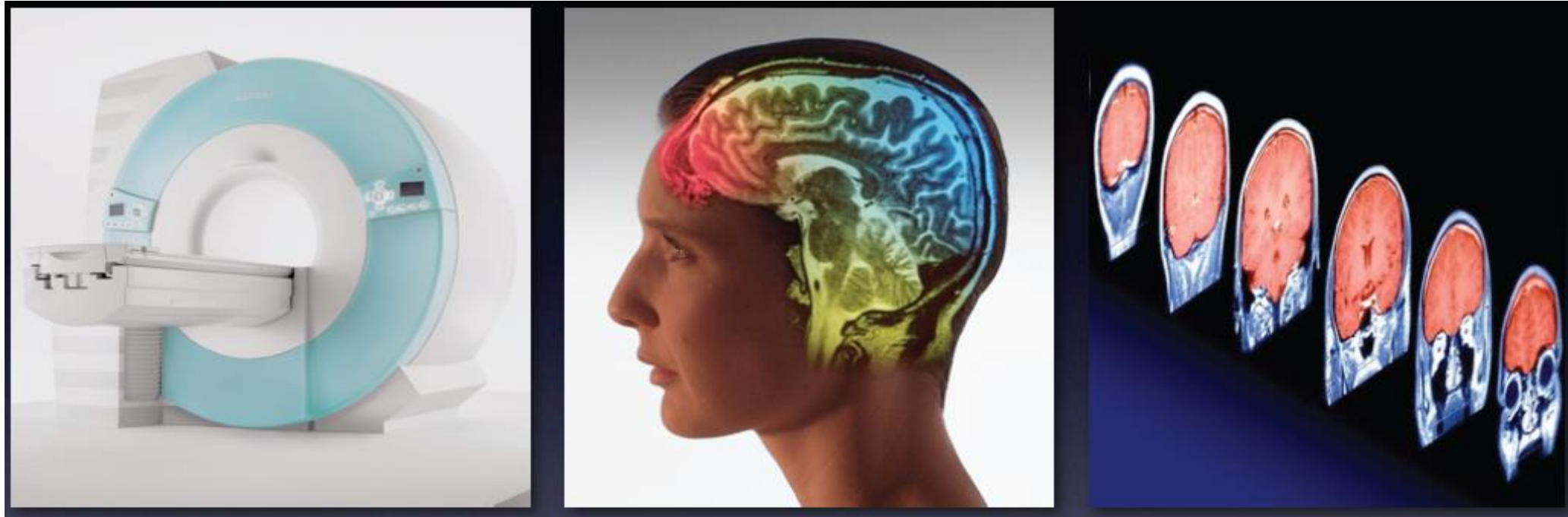


Nearly Paramagnetic

Was able to image blood vessel of $< 200 \mu\text{m}$

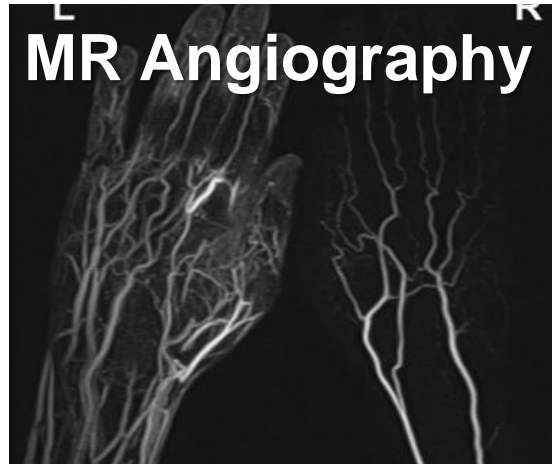
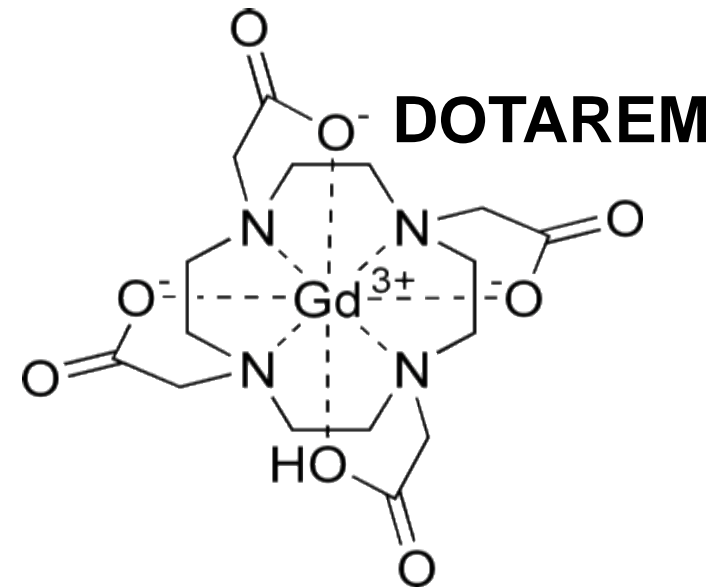
**In collaboration with Prof. Seung Hong Choi
at Radiology, Seoul National University Hospital**

Magnetic Resonance Imaging (MRI)



- Anatomical details in noninvasive & real-time
 - High resolution (vs. PET)
 - High sensitivity (vs. CT)
 - **Safer than PET&CT**

T1 MRI Contrast Agents using Paramagnetic Gd-complexes



Toxic Gd³⁺: Nephrogenic systemic fibrosis (NSF)

➔ New Non-toxic MRI contrast should be developed !



- Home
- Food
- Drugs
- Medical Devices
- Radiation-Emitting Products
- Vaccines, Blood & Biologics
- Animal & Veterinary
- Cosmetics
- Tobacco Products

Drugs

Home > Drugs > Drug Safety and Availability

Drug Safety and Availability

[Drug Alerts and Statements](#)

[Medication Guides](#)

[Drug Safety Communications](#)

[Drug Shortages](#)



[Postmarket Drug Safety Information for Patients and Providers](#)



[Information by Drug Class](#)

[Medication Errors](#)

[Drug Safety Podcasts](#)



[Safe Use Initiative](#)



FDA Drug Safety Communication: FDA evaluating the risk of brain deposits with repeated use of gadolinium-based contrast agents for magnetic resonance imaging (MRI)

[f SHARE](#)

[t TWEET](#)

[in LINKEDIN](#)

[p PIN IT](#)

[e EMAIL](#)

[p PRINT](#)

[7-27-2015]

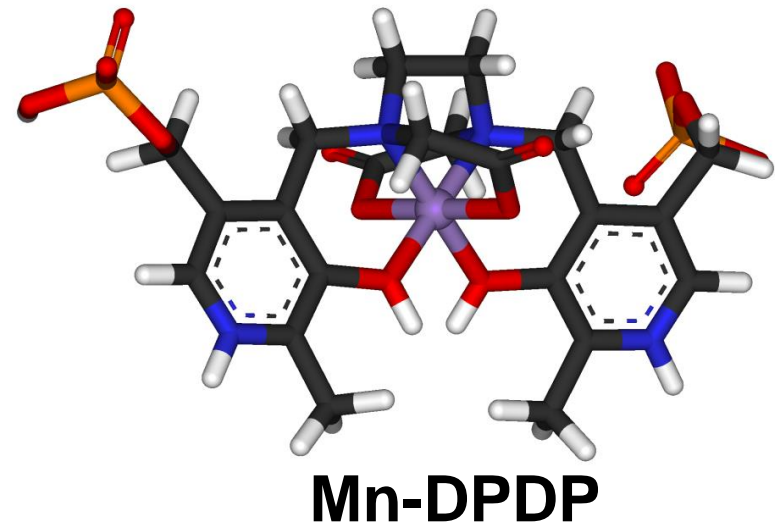
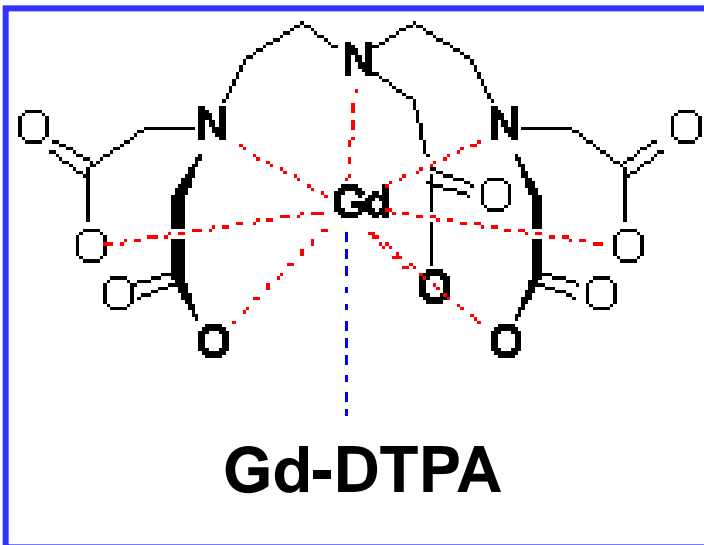
Safety Announcement



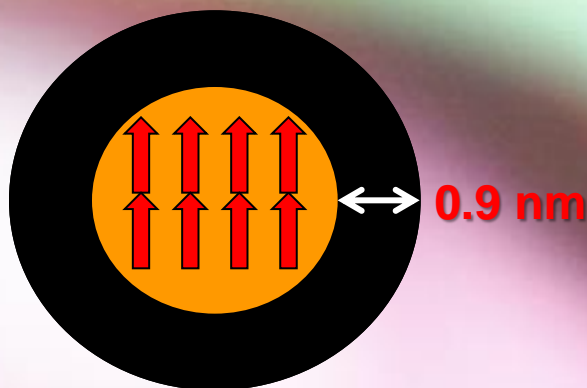
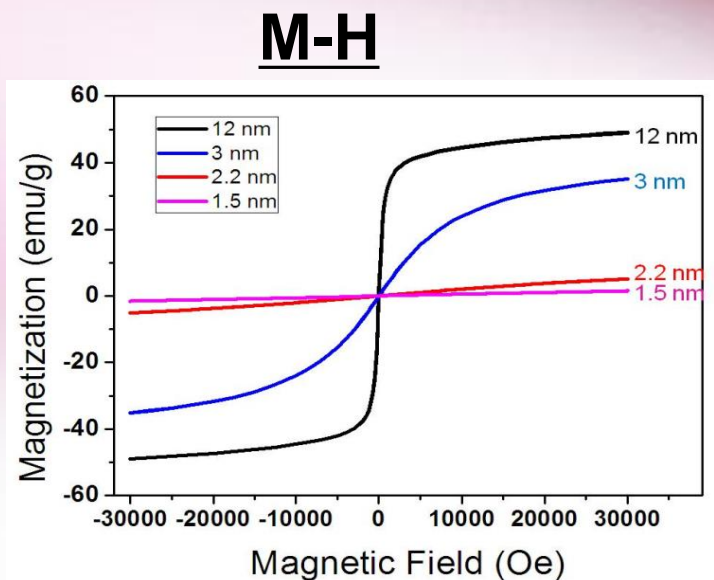
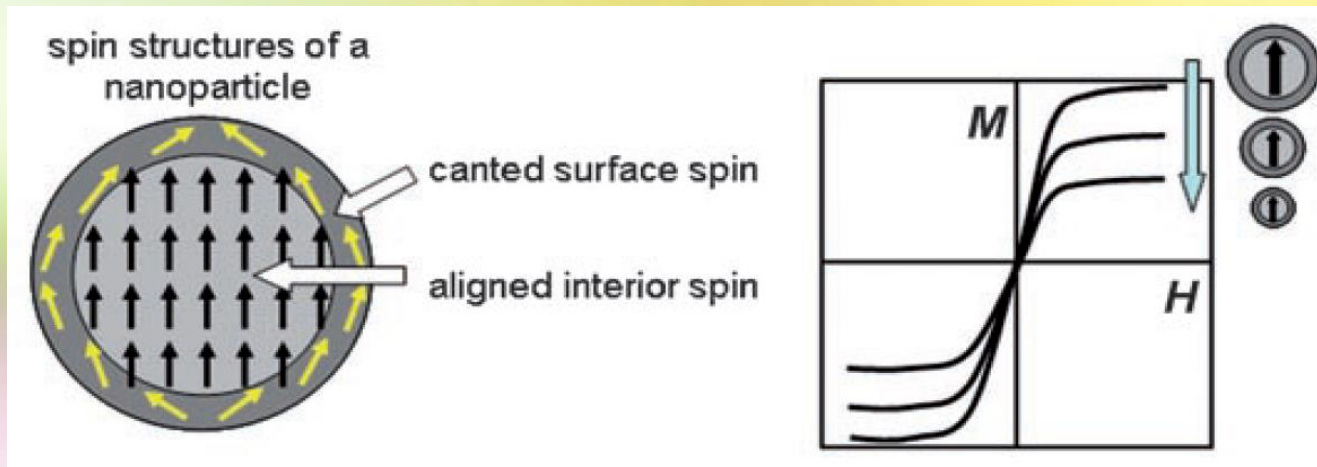
The U.S. Food and Drug Administration (FDA) is investigating the risk of brain deposits following repeated use of gadolinium-based contrast agents (GBCAs) for magnetic resonance imaging (MRI). MRIs help detect abnormalities of body organs, blood vessels, and other tissues. Recent publications in the medical literature have reported that deposits of GBCAs (See Table 1) remain in the brains of some patients who undergo four or more contrast MRI scans, long after the last administration.¹⁻²¹ It is unknown whether these gadolinium deposits are harmful or can lead to adverse health effects.

Paramagnetic T1 MRI contrast agents (Clinically used)

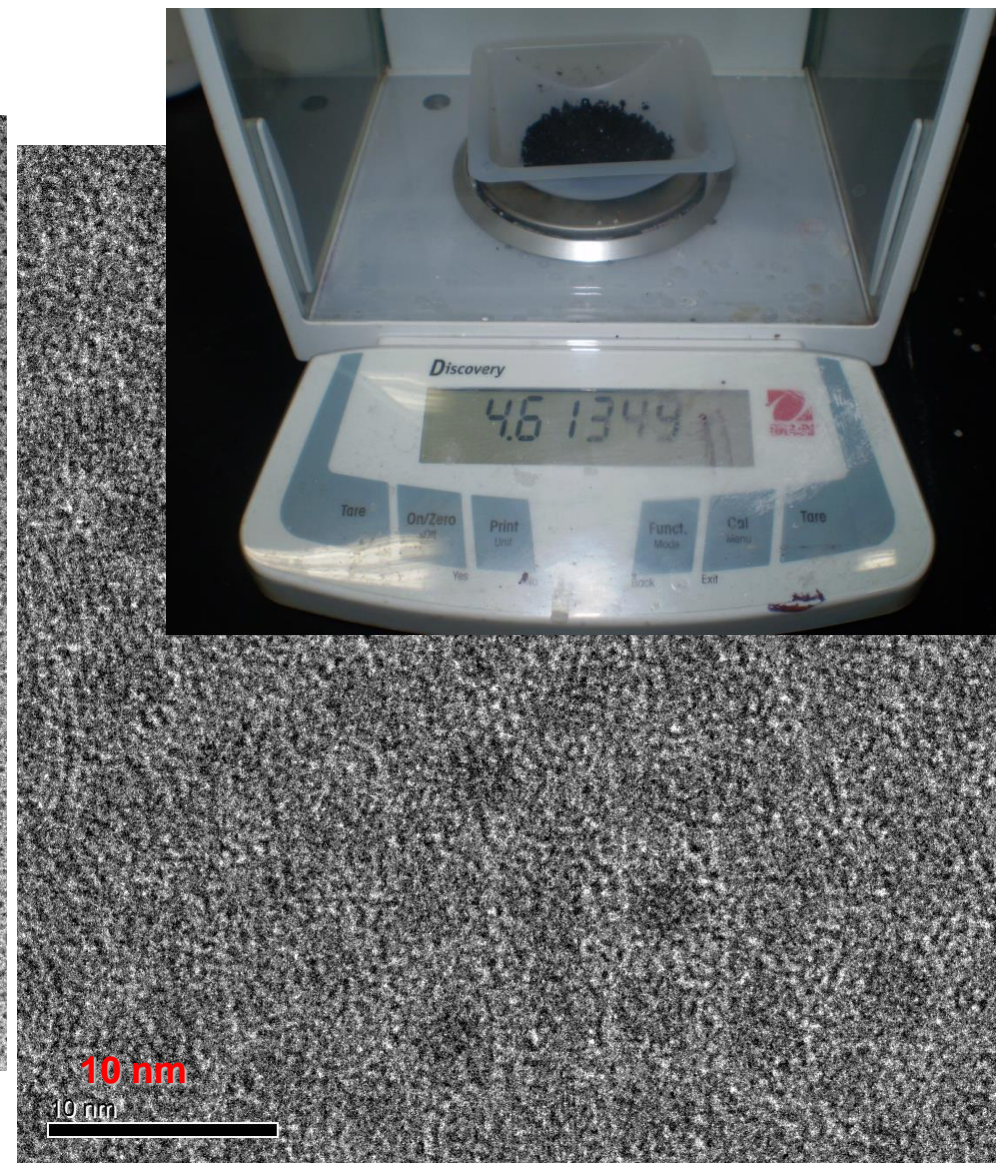
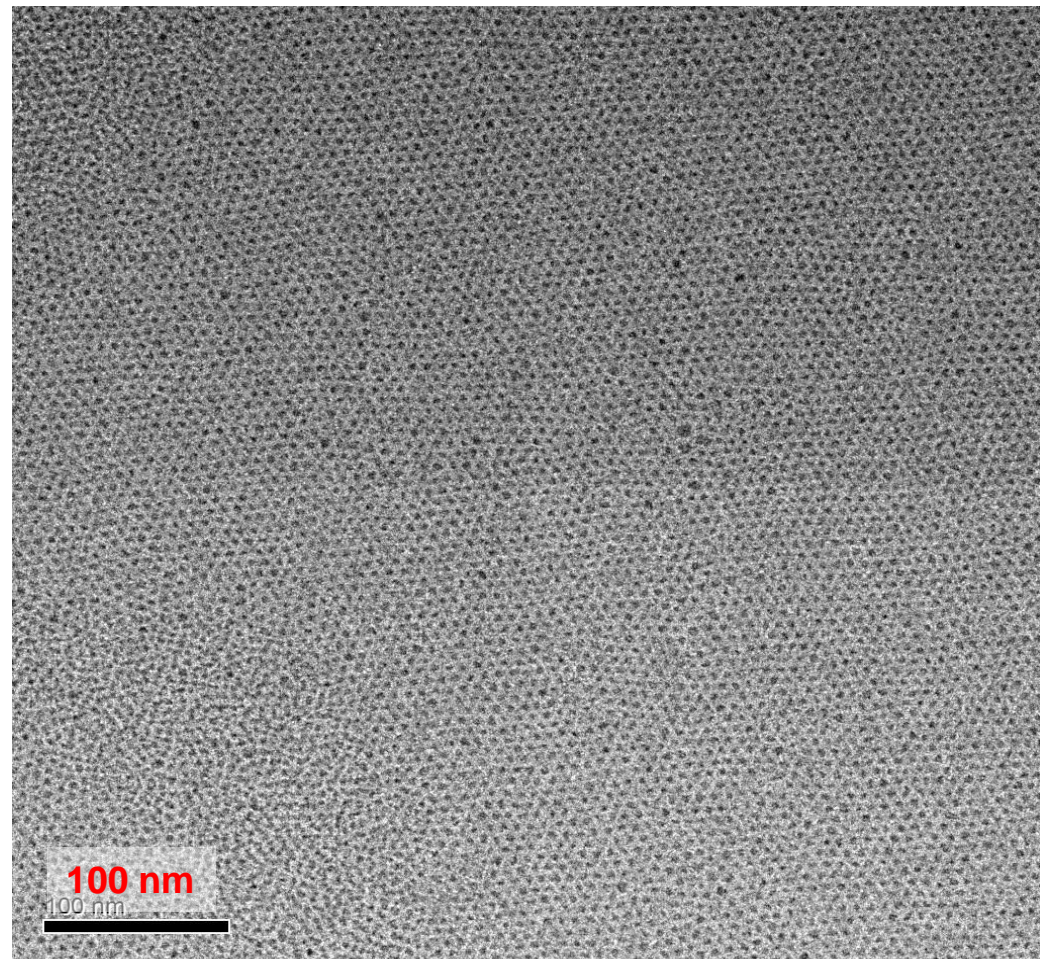
Ion		3d	4f	Magnetic moment (Bohr magneton)
Cr	3+	↑ ↑ ↑		3.8
Mn	2+	↑ ↑ ↑ ↑ ↑		5.9 (weak field)
Fe	3+	↑ ↑ ↑ ↑ ↑		5.9 (weak field)
Cu	2+	↑↓ ↑↓ ↑↓ ↑↓ ↑		1.7-2.2
Eu	3+		↑↓ ↑ ↑ ↑ ↑ ↑ ↑	(6.9)
Gd	3+		↑ ↑ ↑ ↑ ↑ ↑ ↑	7.9
Dy	3+		↑↓ ↑↓ ↑ ↑ ↑ ↑ ↑	(5.9)



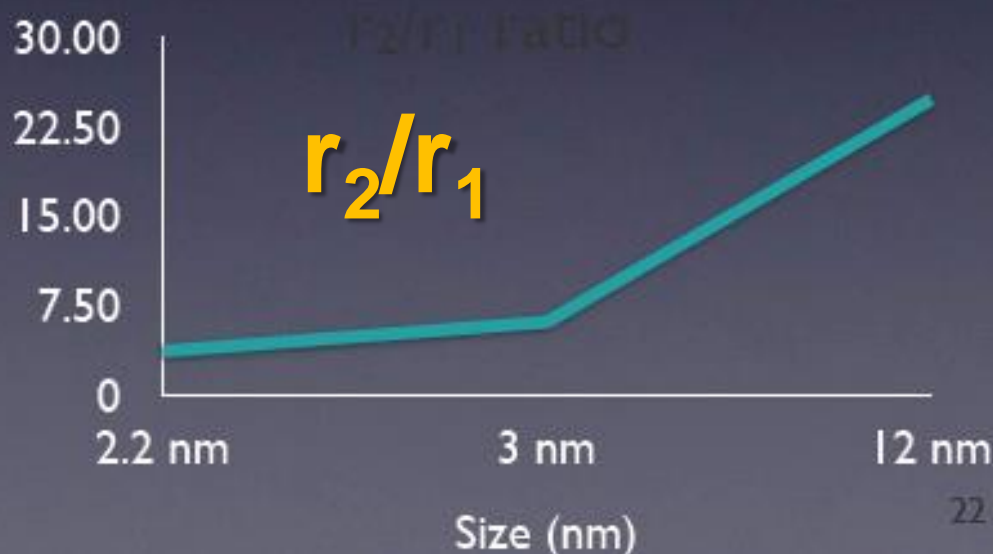
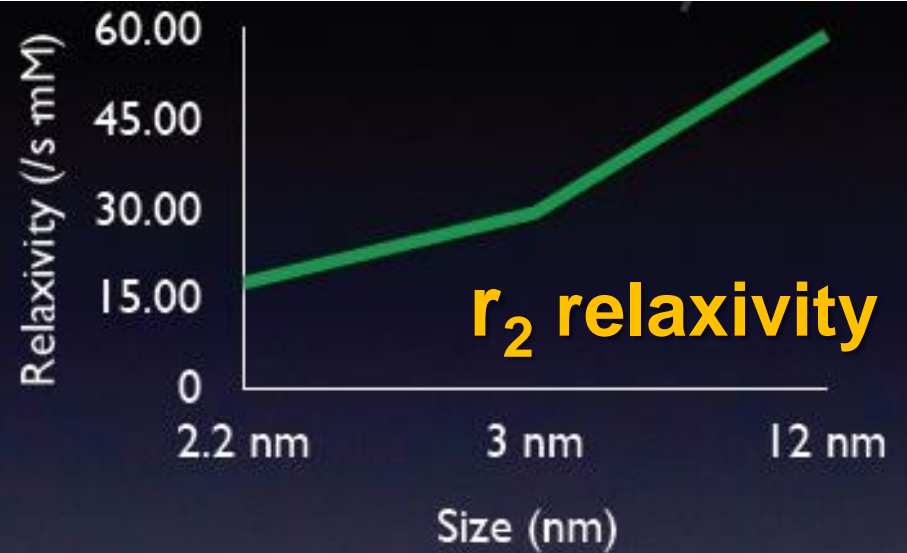
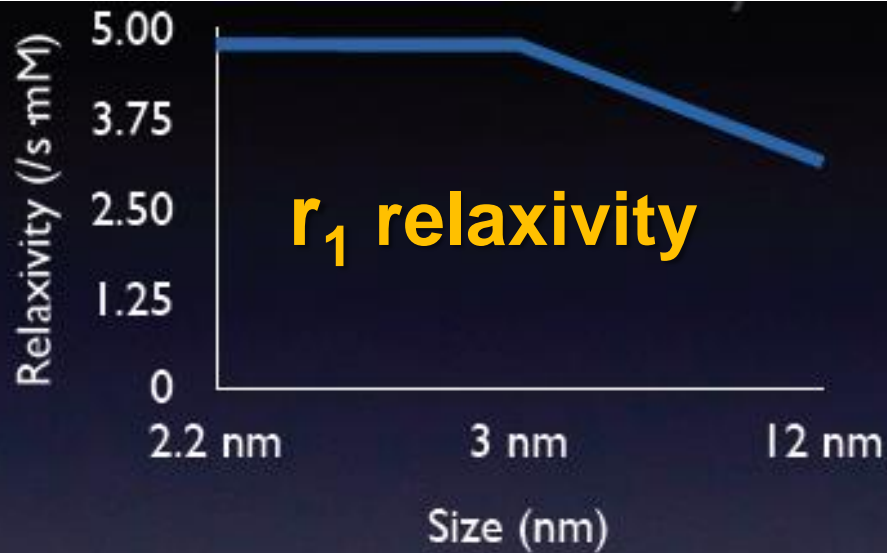
Spin Canting Effect



Gram-scale Synthesis of 3 nm-sized Iron oxide Nanocrystals



Relaxivity versus Size



**Small (< 3 nm)
Iron oxide nanoparticles**

High r_1 & Low r_2/r_1

Excellent T1 agent

In vivo MR blood pool Imaging



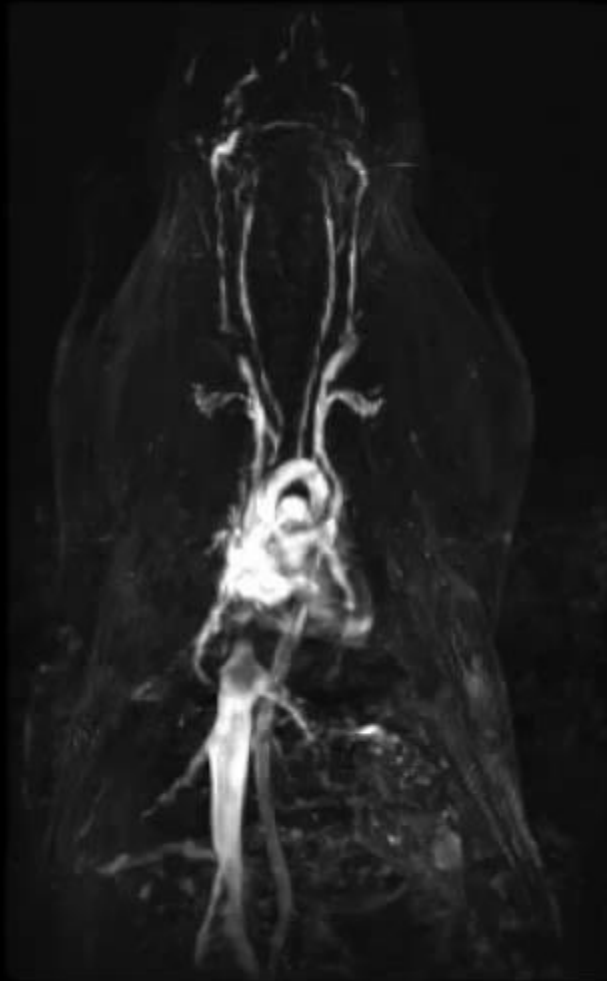
WL: 393 WW: 1168

S

A

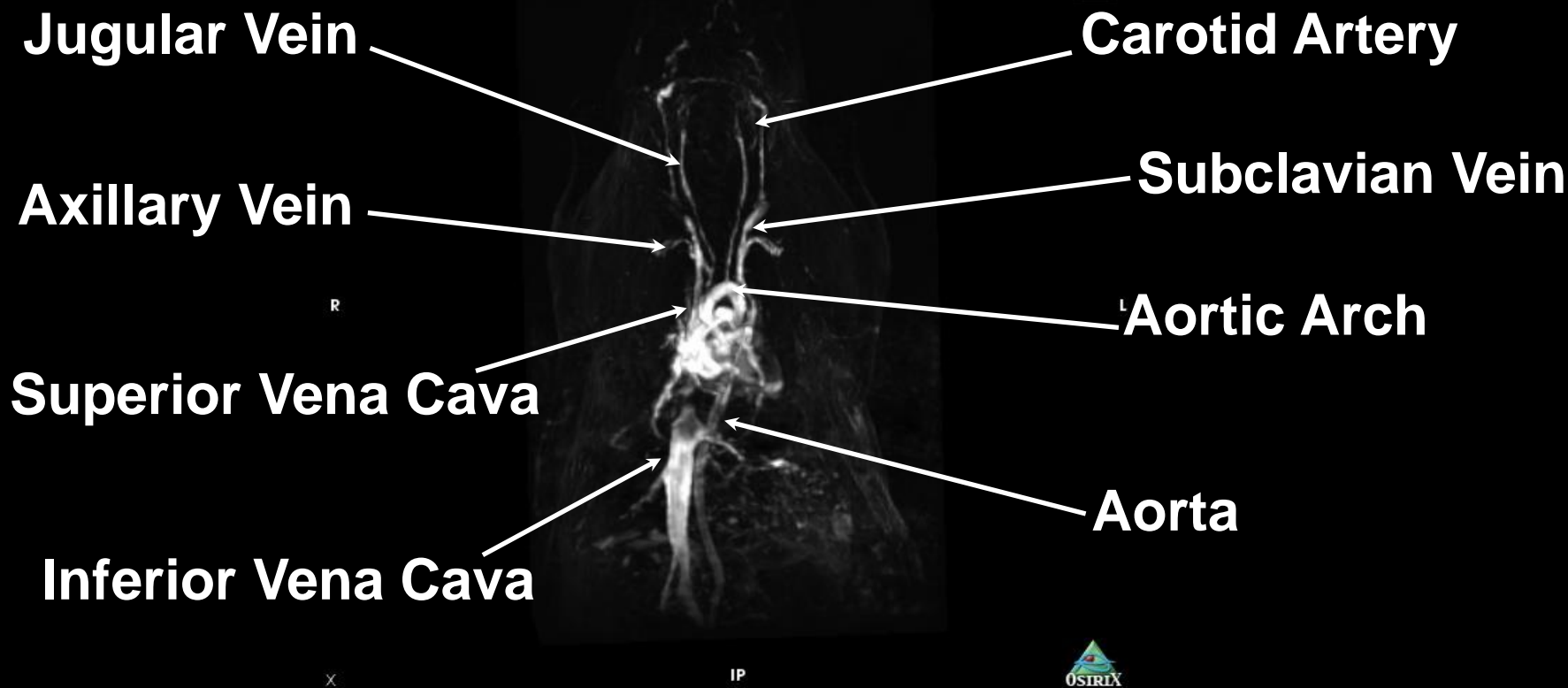
R

L



I



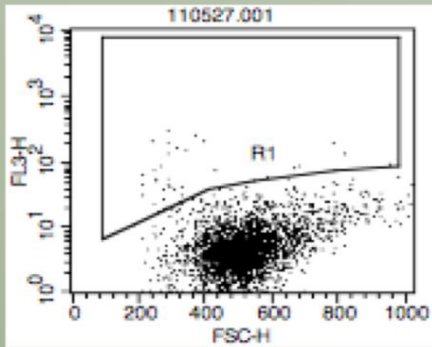


**was able to image blood vessels
of $< 200 \mu\text{m}$ (limit of MRI)**

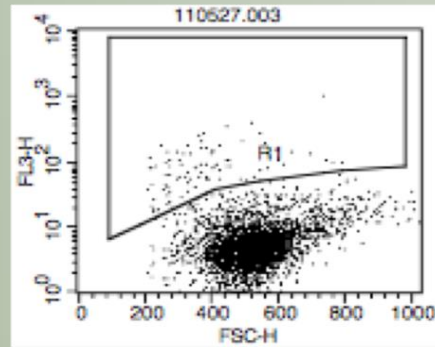
Toxicity Evaluation

7-AAD Assay

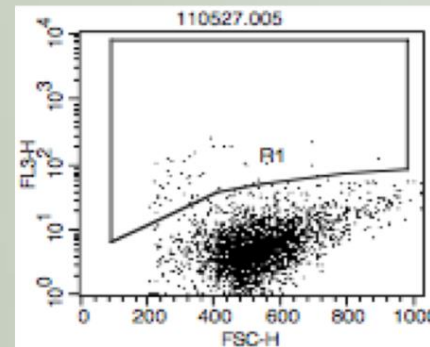
Control



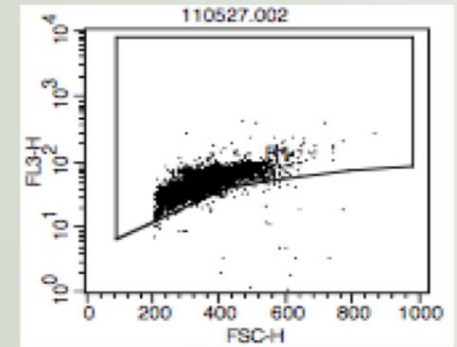
3 nm, 50 $\mu\text{g/mL}$



12 nm, 50 $\mu\text{g/mL}$

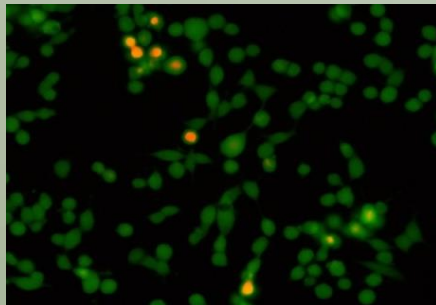


H₂O₂ treated

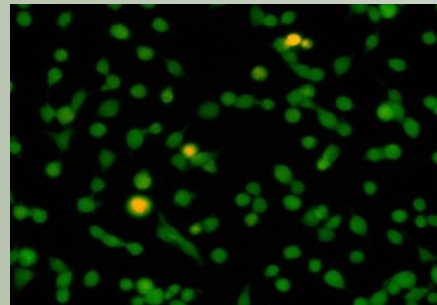


Calcein/PI Assay

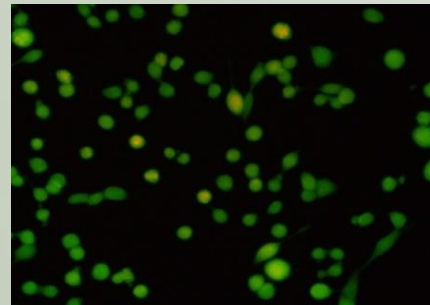
Control



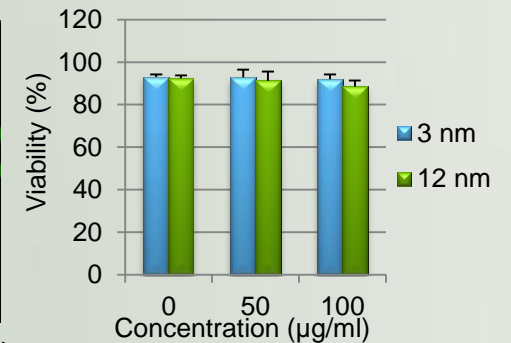
3 nm, 50 $\mu\text{g/ml}$



12 nm, 50 $\mu\text{g/ml}$



Red: Dead Cell; Green: Live Cell



Gold Nanoparticles

Marie-Christine Daniel and Didier Astruc*

Chem. Rev. **2004**, *104*, 293-346

Title: Gold nanoparticles: Assembly, supramolecular chemistry, quantum-size-related properties, and applications toward biology, catalysis, and nanotechnology

Author(s): Daniel MC, Astruc D

Source: CHEMICAL REVIEWS Volume: 104 Issue: 1 Pages: 293-346 Published: JAN 2004

Times Cited: **3,306**

Scanometric DNA Array Detection with Au Nanoparticle Probes

Detection of Cancer cells at very early stage.

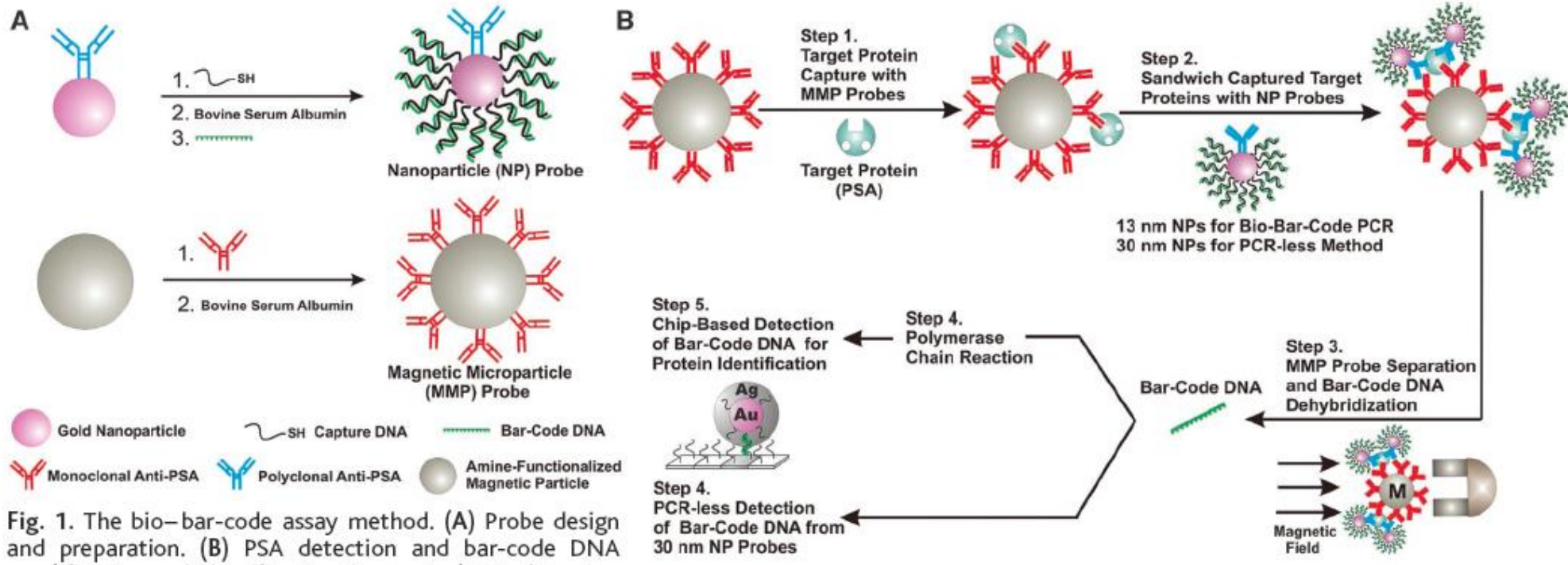
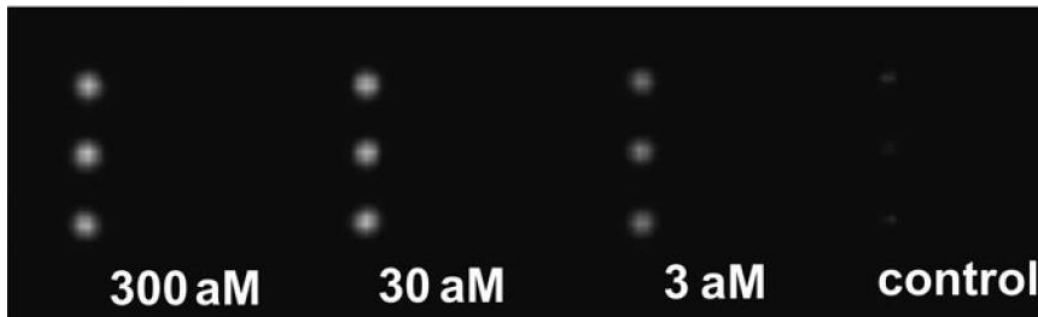


Fig. 1. The bio-bar-code assay method. (A) Probe design and preparation. (B) PSA detection and bar-code DNA

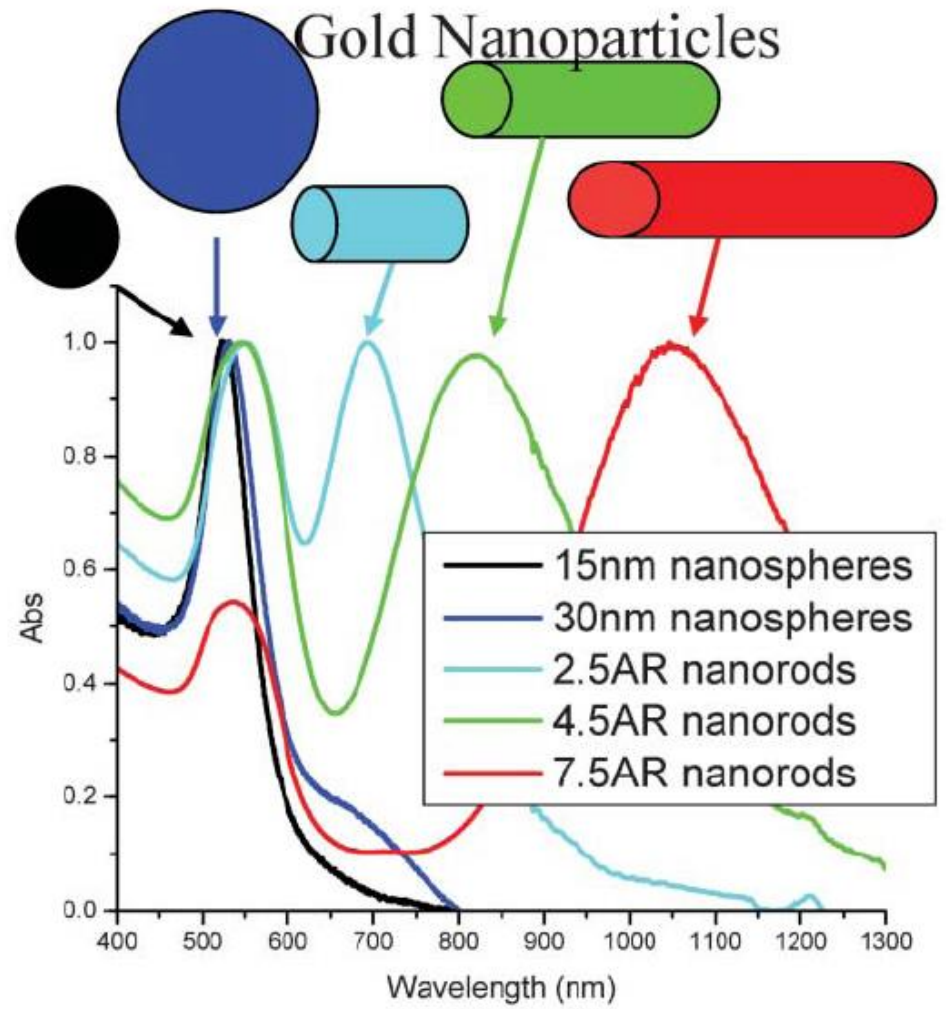
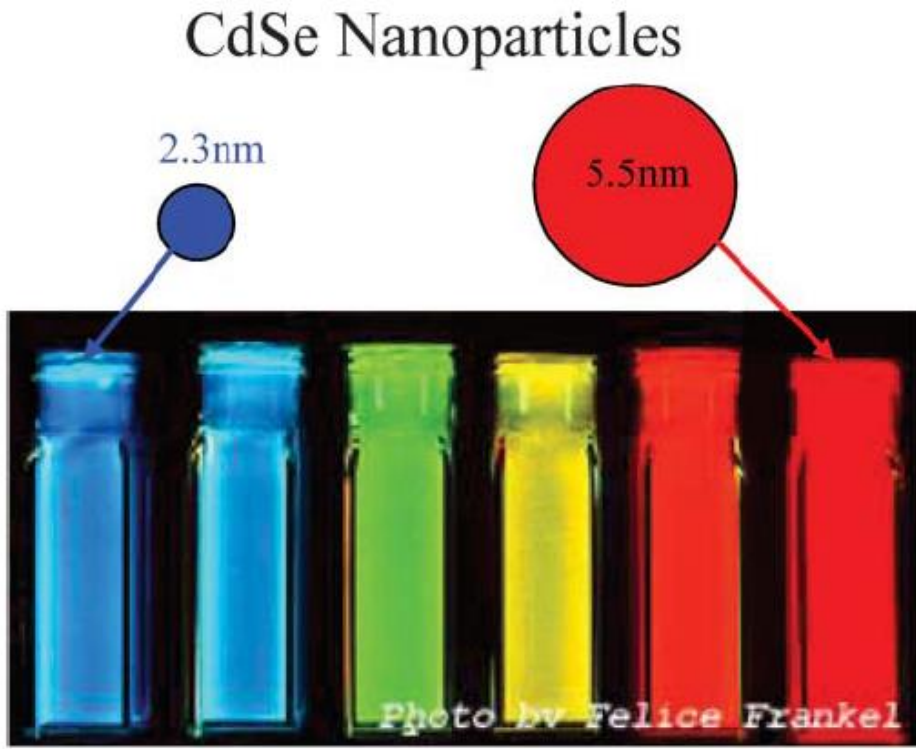


J.-M. Nam, C. S. Thaxton, C. A. Mirkin *Science* **2003**, 301, 1884.

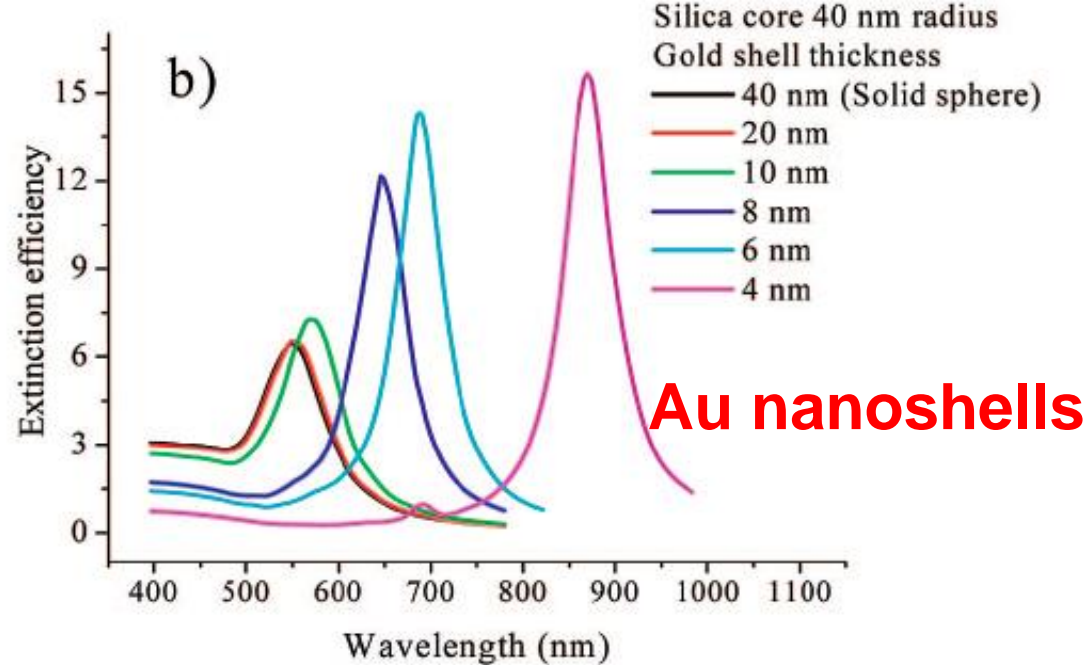
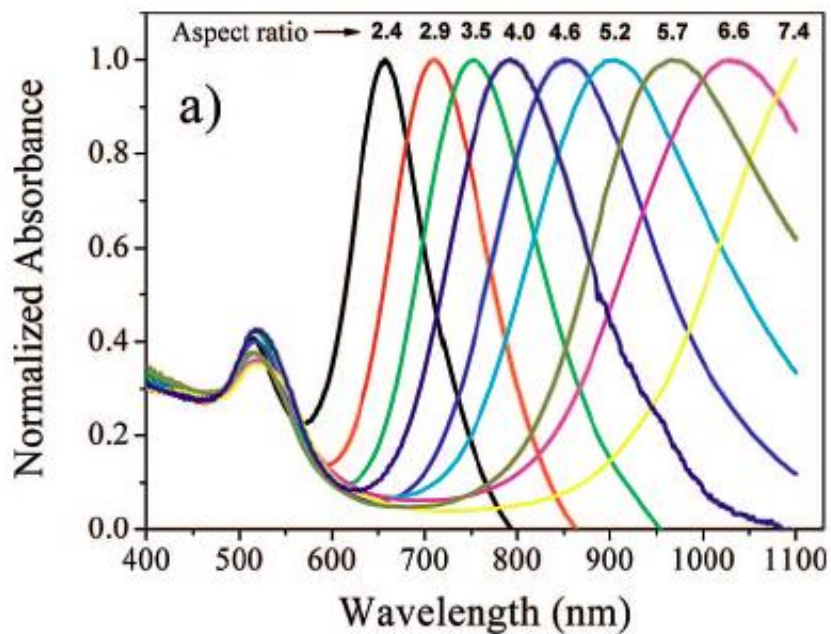
T. Andrew Taton, 1,2 Chad A. Mirkin, 1,2* Robert L. Letsinger 1* *Science* **2000**, 289, 1757.

QD's vs. Metal Nanoparticles

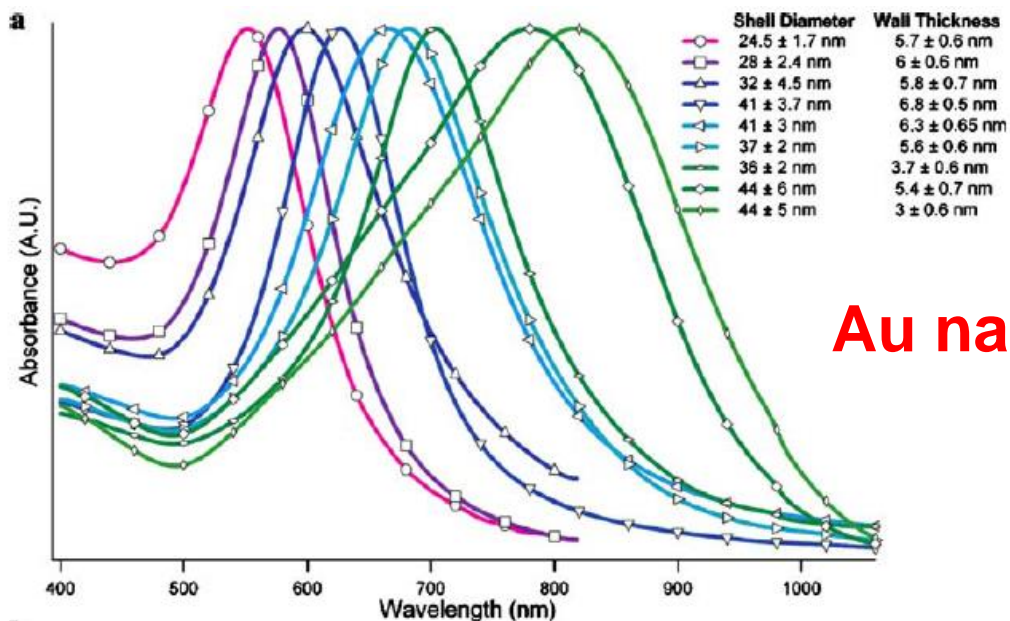
- This absorption does not derive from transitions between quantized energy states.
- Instead, in metal particles, collective modes of motion of the electron gas can be excited. They are referred to as **surface plasmons**.
- Freely mobile electrons are trapped in such metal boxes and show a characteristic collective oscillation frequency of the plasma resonance, giving rise to the so-called plasmon resonance band (PRB) observed near 530 nm in the 5-20-nm-diameter range.
- The **size dependence** of the plasmon frequency is **negligible**: No shift in Absorption maximum for colloidal gold nanocrystals in the range between 5 and 30 nm.



S. Eustis, M. A. El-Sayed, *Chem. Soc. Rev.* **2006**, 35, 209-217.



Au nanorods



Au nanoshells

Applications of Gold Nanoparticles

See references 506 – 517 of
Chem. Rev. **2004**, 104, 293-346.

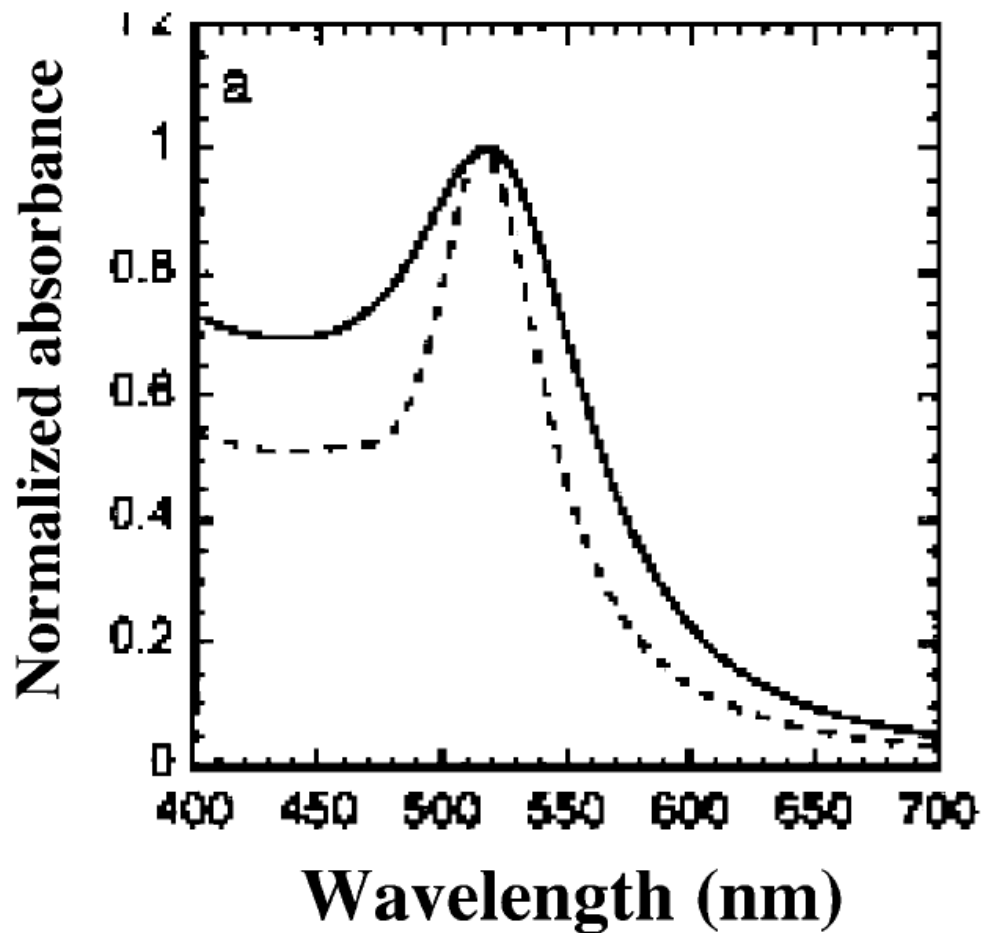
Surface Plasmon Band (SPB)

- Freely mobile electrons are trapped in such metal boxes and show a characteristic collective oscillation frequency of the plasma resonance, giving rise to the so-called plasmon resonance band (PRB) observed near 530 nm in the 5-20-nm-diameter range.
- The deep-red color of AuNP sols in water and glasses reflects the surface plasmon band (SPB), a broad absorption band in the visible region around 520 nm.
- The SPB is due to the **collective oscillations of the electron gas at the surface of nanoparticles** (6s electrons of the conduction band for AuNPs) that is correlated with the electromagnetic field of the incoming light, i.e., the excitation of the coherent oscillation of the conduction band.

Main characteristics of SPB

- (i) its position around 520 nm;
- (ii) its sharp decrease with decreasing core size for AuNPs with 1.4-3.2-nm core diameters due to the onset of quantum size effects that become important.
- (iii) SPB is absent for AuNPs with core diameter less than 2 nm, as well as for bulk gold.
- (iv) For AuNPs of mean diameter of 9, 15, 22, 48, and 99 nm, the SPB maximum λ_{\max} was observed at 517, 520, 521, 533, and 575 nm, respectively, in aqueous media.
- (v) The SPB maximum and bandwidth are also influenced by the **particle shape**, medium dielectric constant, and temperature.

Optical absorption spectra of 8.3 nm Au nanoparticles in water



Programmed Materials Synthesis with DNA

James J. Storhoff and Chad A. Mirkin*

Chem. Rev. **1999**, 99, 1849-1862

ORIGINAL PAPER:

DNA Based Method for Rationally Assembling Nanoparticles
Into Macroscopic Materials.

Mirkin, C. A.; Letsinger, R. L.; Mucic, R. C.; Storhoff, J. J.

Nature **1996**, 382, 607-609.

A DNA-based method for rationally assembling nanoparticles into macroscopic materials

Chad A. Mirkin, Robert L. Letsinger, Robert C. Mucic & James J. Storhoff

Department of Chemistry, Northwestern University, Evanston, Illinois 60208, USA

COLLOIDAL particles of metals and semiconductors have potentially useful optical, optoelectronic and material properties¹⁻⁴ that derive from their small (nanoscopic) size. These properties might lead to applications including chemical sensors, spectroscopic enhancers, quantum dot and nanostructure fabrication, and micromachining methods⁵⁻⁷. A great deal of control can now be exercised over the chemical composition, size and polydispersity^{1,2} of colloidal particles, and many methods have been developed for assembling them into useful aggregates and materials. Here we describe a method for assembling colloidal gold nanoparticles rationally and reversibly into macroscopic aggregates. The method involves attaching to the surfaces of two batches of 13-nm gold particles non-complementary DNA oligonucleotides capped with thiol groups, which bind to gold. When we add to the solution an oligonucleotide duplex with 'sticky ends' that are complementary to the two grafted sequences, the nanoparticles self-assemble into aggregates. This assembly process can be reversed by thermal denaturation. This strategy should now make it possible to tailor the optical, electronic and structural properties of the colloidal aggregates by using the specificity of DNA interactions to direct the interactions between particles of different size and composition.

Previous assembly methods have focused on the use of covalent 'linker' molecules that possess functionalities at opposing ends with chemical affinities for the colloids of interest. One of the most successful approaches to date⁸ has involved the use of gold colloids and well established thiol adsorption chemistry^{9,10}. In this approach, linear alkanedithiols were used as the particle linker molecules. The thiol groups at each end of the linker molecule covalently attach themselves to the colloidal particles to form aggregate structures. The drawbacks of this method are that the process is difficult to control and the assemblies are formed irreversibly. Methods for systematically controlling the assembly process are needed if the materials properties of these unusual structures are to be exploited fully.

Our oligonucleotide-based method allows the controlled and reversible assembly of gold nanoparticles into supramolecular structures. Oligonucleotides offer several advantages over non-biological-based linker molecules. For example, discrete sequences of controlled length and with the appropriate surface binding functionality may be prepared in an automated fashion with a DNA synthesizer. In this way, the molecular recognition properties of the oligonucleotides may be used to trigger the colloidal self-assembly process. The interparticle distances and stabilities of the supramolecular structures generated by this method can be controlled through the choice of oligonucleotide sequence and length, solvent, temperature and supporting electrolyte concentration.

Others also have recognized the utility of DNA for the preparation of new biomaterials and nanofabrication methods. Previous researchers have focused on using the sequence-specific molecular-recognition properties of oligonucleotides to design impressive structures with well defined geometric shapes and sizes¹¹⁻¹⁴. The chemistry proposed here focuses on merging the chemistry of DNA with the chemistry of inorganic colloidal

materials. In addition to generating materials with properties that are hybrids of their DNA and colloidal precursors, the union of metal-colloid and DNA chemistry offers significant opportunities relative to the construction of pure DNA materials. As noted by Seeman¹⁵, 'the theory of producing DNA [structures] is well ahead of experimental confirmation. It is much easier to design a [structure] than it is to prove its synthesis.' An advantage of the DNA/colloid hybrid materials reported herein is that the assemblies can be characterized easily by transmission electron microscopy (TEM) and/or atomic force microscopy (AFM) as well as spectroscopic methods conventionally used with DNA.

Our approach to using oligonucleotides for the controlled assembly of gold nanoparticles into aggregate macroscopic structures is outlined in Fig. 1. First, 13-nm-diameter Au particles are prepared^{16,17}. These particles form a dark red suspension in water, and like thin-film Au substrates¹⁸, they are easily modified with oligonucleotides, which are functionalized with alkane thiols at their 3' termini. In a typical experiment, one solution of 17 nM (150 μ l) Au colloids is treated for 24 h with 3.75 μ M (46 μ l) 3'-thiol-TTTTGCTGA, and a second solution of colloids is treated with 3.75 μ M (46 μ l) 3'-thiol-TACCGTTG. Note that these oligonucleotides are non-complementary. After treatment with the thiol-capped oligonucleotides, the two colloidal Au solutions are combined, and because of the non-complementary nature of the oligonucleotides, no reaction takes place. A beneficial consequence of capping the colloids with these oligonucleotides is

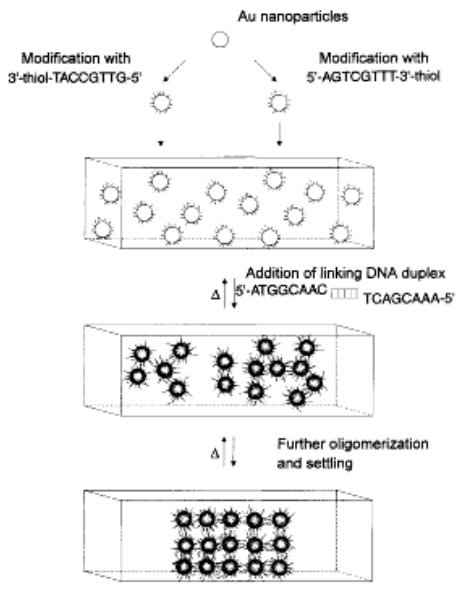


FIG. 1 Scheme showing the DNA-based colloidal nanoparticle assembly strategy (the hybridized 12-base-pair portion of the linking duplex is abbreviated as \square). If a duplex with a 12-base-pair overlap but with 'sticky ends' with four base mismatches (5'-AAGTCAGTATACCGCTAG and 3'-ATATGCCGATCAAAATCAC) is used in the second step, no reversible particle aggregation is observed. The scheme is not meant to imply the formation of a crystalline lattice but rather an aggregate structure that can be reversibly annealed. Δ is the heating above the dissociation temperature of the duplex.

LETTERS TO NATURE

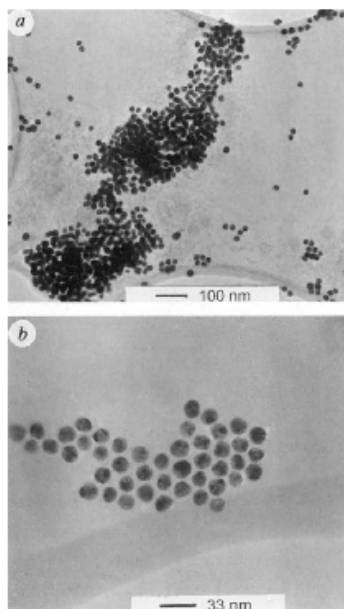


Fig. 4 TEM images of: a, an aggregated DNA/colloid hybrid material; b, a two-dimensional colloidal aggregate showing the ordering of the DNA-linked Au nanoparticles. Images were taken with a Hitachi 8100 Transmission Electron Microscope.

This work gives entry into a new class of DNA/nanoparticle hybrid materials and assemblies, which might have useful electrical, optical and structural properties that should be controllable through choice of nanoparticle size and chemical composition, and oligonucleotide sequence and length. We note that it should be possible to extend this strategy easily to other noble-metal (for example, Ag, Pt)²¹ and semiconductor (for example, CdSe and CdS)^{22,24} colloidal nanoparticles with well established surface coordination chemistry. Our initial results bode well for the utility of this strategy for developing new types of biosensing and sequencing schemes for DNA. The Au colloidal particles have large extinction coefficients for the bands that give rise to their colours (Fig. 2). These intense colours, which depend on particle size and concentration and interparticle distance, make these materials particularly attractive for new colorimetric sensing and sequencing strategies for DNA. \square

Received 19 April; accepted 24 June 1996.

- Schmid, G. (ed.) *Clusters and Colloids* (VCH, Weinheim, 1994).
- Hogg, M. A. (ed.) *Colloidal Gold: Principles, Methods, and Applications* (Academic, San Diego, 1992).
- Bassell, G. J., Powers, C. M., Tanaka, K. L. & Singer, R. H. *J. Colloid Interface Sci.* **126**, 863-876 (1994).
- Oreighan, J. A., Blatchford, C. G. & Abbot, M. G. *J. Chem. Soc. Faraday* **75**, 790-798 (1979).
- Burst, M., Bethel, D., Schiffrin, D. J. & Healy, C. J. *Adv. Mater.* **7**, 785-797 (1995).
- Daloz, L. H. & Sauer, R. G. *Adv. Phys. Chem.* **43**, 431-463 (1992).
- Barr, C. D. & Whitesides, G. M. *Angew. Chem., Int. Ed. Engl.* **28**, 506-512 (1989).
- Shokhtman, E. M., Wasserman, S. A., Cozzarelli, N. R. & Solomon, M. J. *New J. Chem.* **17**, 757-763 (1993).
- Show, S. Y. & Wang, J. C. *Science* **260**, 539-546 (1995).
- Hentzer, M. A., Nelson, J. S. & Letsinger, R. L. *J. Am. Chem. Soc.* **117**, 10151-10252 (1995).
- Chan, H. H. & Seeman, N. C. *Nature* **365**, 631-633 (1991).
- Smith, F. W. & Felsen, J. *Nature* **266**, 164-168 (1992).
- Wang, K. Y., McCarty, S., Shes, R. G., Swarnathan, S. & Bolton, P. H. *Biochemistry* **32**,

- 1869-1904 (1993).
- Chen, L. Q., Cai, L., Zhang, X. H. & Rich, A. *Biochemistry* **33**, 13540-13546 (1994).
- Horch, T. C., Josselyn, J. & Henderson, E. *Ruiz-Adels Res.* **22**, 696-700 (1995).
- Mirkin, S. M. & Frankamenetski, M. D. A. *Rev. Biophys. Biomed. Struct.* **22**, 541-576 (1994).
- Wells, R. D. *J. Biol. Chem.* **263**, 1085-1088 (1988).
- Wang, Y., Mueller, J. E., Remoer, B. & Seeman, N. C. *Biochemistry* **30**, 5667-5674 (1991).
- Sassan, N. C. et al. *New J. Chem.* **17**, 739-755 (1993).
- Grabar, K. C., Freeman, R. G., Hommer, M. B. & Natan, M. J. *Analyt. Chem.* **67**, 735-743 (1995).
- Mucic, R. C., Hentzer, M. A., Mirkin, C. A. & Letsinger, R. L. *J. Chem. Soc., Chem. Commun.* 555-557 (1996).
- Livshits, T., Mikhaleva, P. & Hendry, A. J. *Phys. Chem.* **97**, 679-682 (1993).
- Hinton, N., Wang, Y. & Eckert, H. *J. Am. Chem. Soc.* **112**, 1322-1326 (1990).
- Colvin, V. L., Goldstein, A. N. & Alivisatos, A. P. *J. Am. Chem. Soc.* **114**, 5221-5230 (1992).

ACKNOWLEDGEMENTS. We thank I. M. Ritz for discussions, and V. David for assistance with the TEM experiments. C.A.M. was supported by an ONR Young Investigator award, an A. P. Sloan Foundation Fellowship, a DuPont Young Professor award, an NSF Young Investigator award and a Camille Dreyfus Teacher-Scholar Award; C.A.M. thanks the Materials Research Center of Northwestern University for the use of a TEM, which was purchased by the MRSEC Program of the National Science Foundation; R.L.L. was supported by the NIGMS.

CORRESPONDENCE should be addressed to C.A.M. (e-mail: cmirkin@chem.nwu.edu).

Organization of 'nanocrystal molecules' using DNA

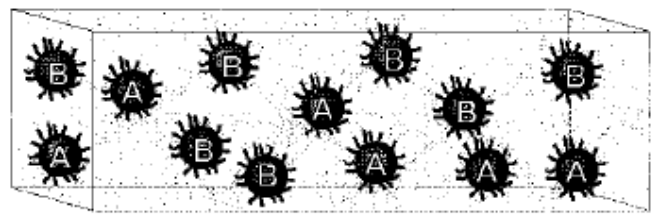
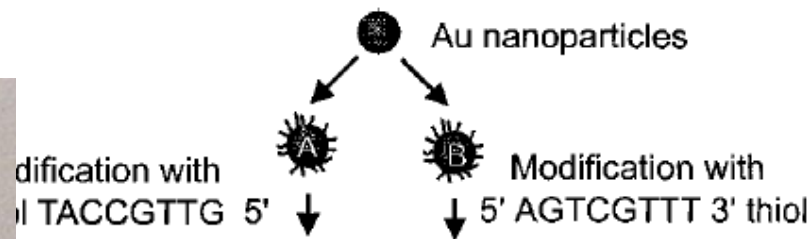
A. Paul Alivisatos*, Kai P. Johnson†, Xiaogang Peng*, Troy E. Wilson†, Colin J. Loweth†, Marcel P. Bruchez Jr* & Peter G. Schultz‡

* Department of Chemistry, University of California at Berkeley, Berkeley, California 94720, USA and Molecular Design Institute, Lawrence Berkeley National Laboratory, Berkeley, California 94701, USA
† Howard Hughes Medical Institute, Department of Chemistry, University of California at Berkeley, Berkeley, California 94720, USA

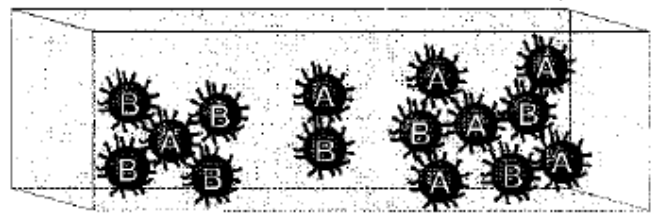
PATTERNING matter on the nanometre scale is an important objective of current materials chemistry and physics. It is driven by both the need to further miniaturize electronic components and the fact that at the nanometre scale, materials properties are strongly size-dependent and thus can be tuned sensitively¹. In nanoscale crystals, quantum size effects and the large number of surface atoms influence the chemical, electronic, magnetic and optical behaviour^{2,3}. 'Top-down' (for example, lithographic) methods for nanoscale manipulation reach only to the upper end of the nanometre regime⁴; but whereas 'bottom-up' wet chemical techniques allow for the preparation of monodisperse, defect-free crystallites just 1-10 nm in size⁵⁻¹⁰, ways to control the structure of nanocrystal assemblies are scarce. Here we describe a strategy for the synthesis of 'nanocrystal molecules', in which discrete numbers of gold nanocrystals are organized into spatially defined structures based on Watson-Crick base-pairing interactions. We attach single-stranded DNA oligonucleotides of defined length and sequence to individual nanocrystals, and these assemble into dimers and trimers on addition of a complementary single-stranded DNA template. We anticipate that this approach should allow the construction of more complex two- and three-dimensional assemblies.

Previous approaches towards the preparation of coupled quantum dots include co-colloids of cadmium selenide-zinc oxide (CdS-ZnO; ref. 11) and cadmium sulphide-silver iodide (CdS-AgI; ref. 12). In addition, small molecule crosslinking agents have been used to synthesize aggregates of Au (ref. 13) and cadmium sulphide linked to titanium oxide (CdS-TiO₂; ref. 14) as well as discrete dimers of cadmium selenide (CdSe; ref. 15). Finally, the collective properties of nanocrystals have been investigated using organic monolayers¹⁶⁻²² and crystallization²³⁻²⁸ to generate ordered arrays of inorganic quantum dots. It remains an open question whether self-assembly methods can be employed to generate complex sequences of nanocrystals.

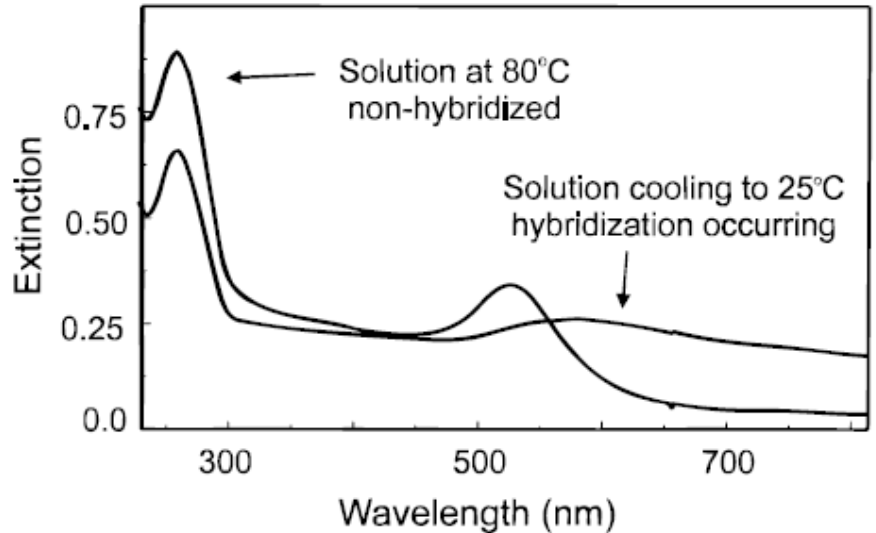
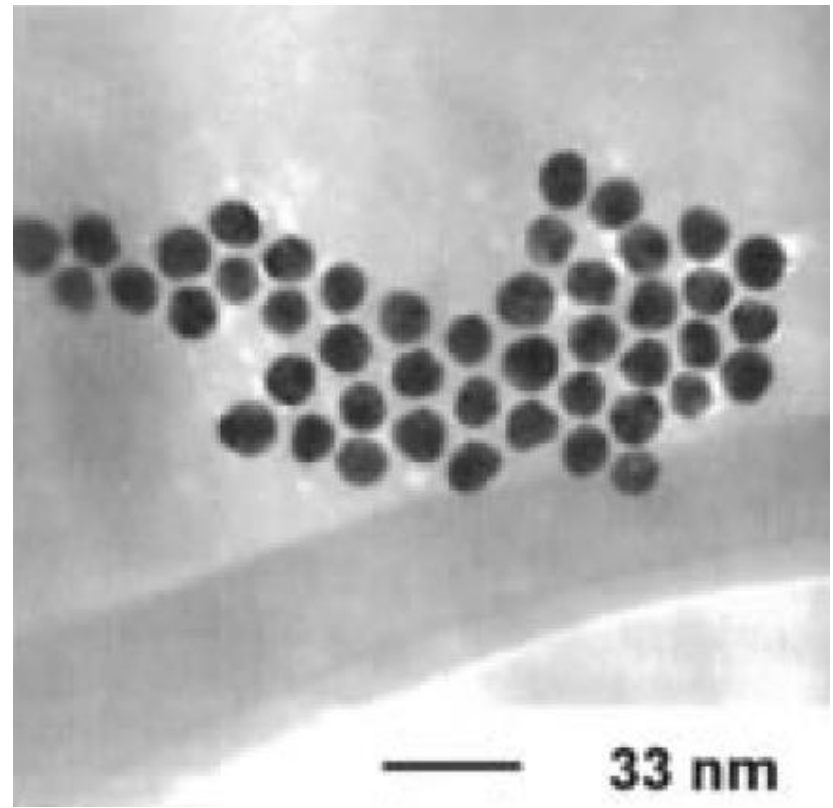
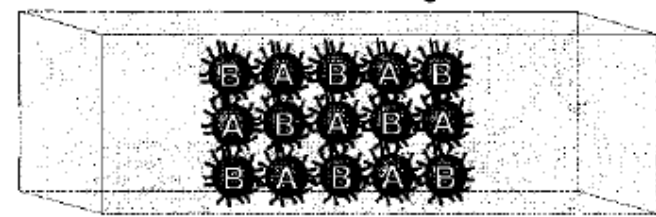
Biological systems are characterized by remarkably complex



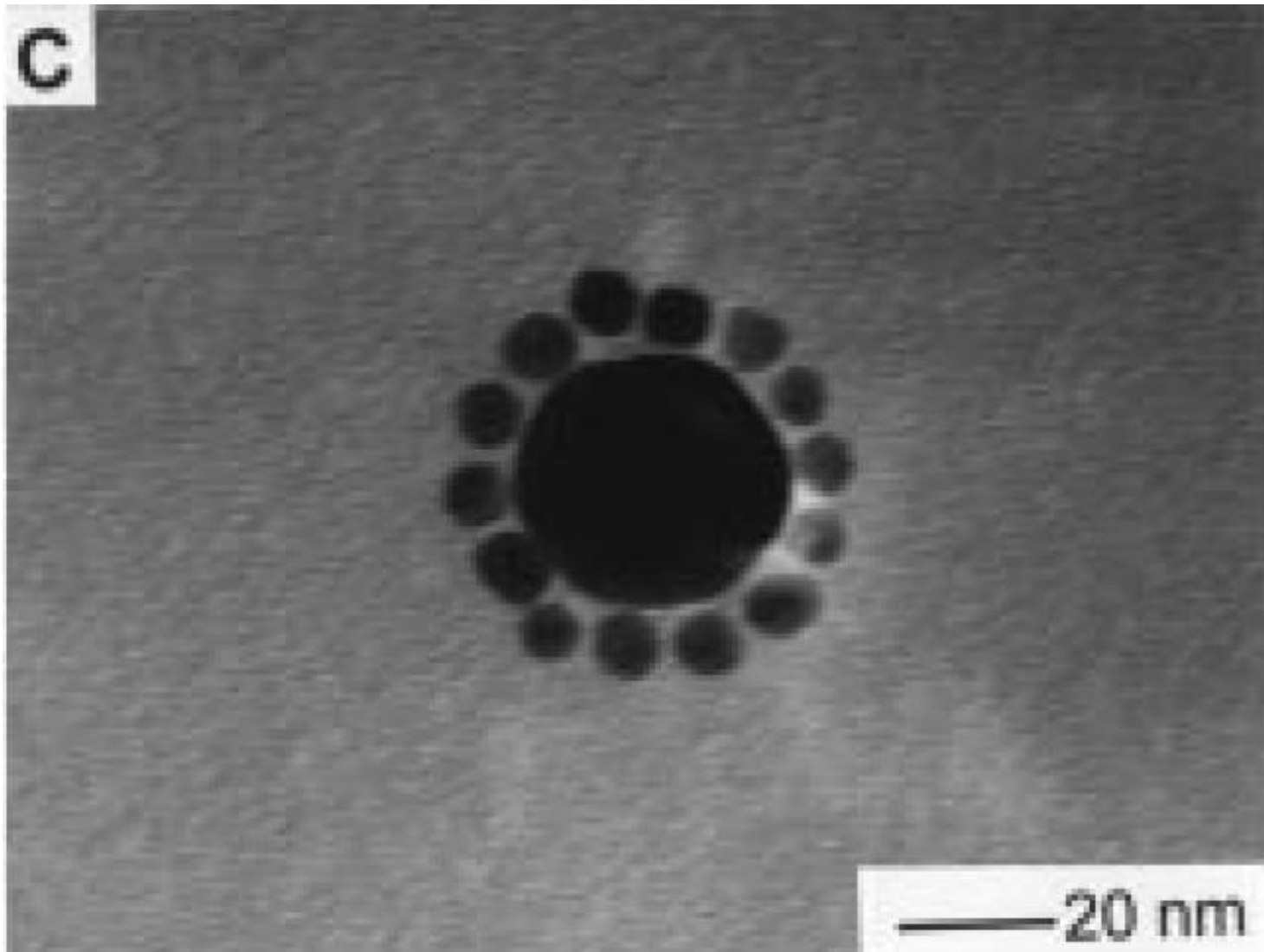
Δ↑↓ Addition of linking DNA duplex
5' ATGGCAAC  TCAGCAA 5'

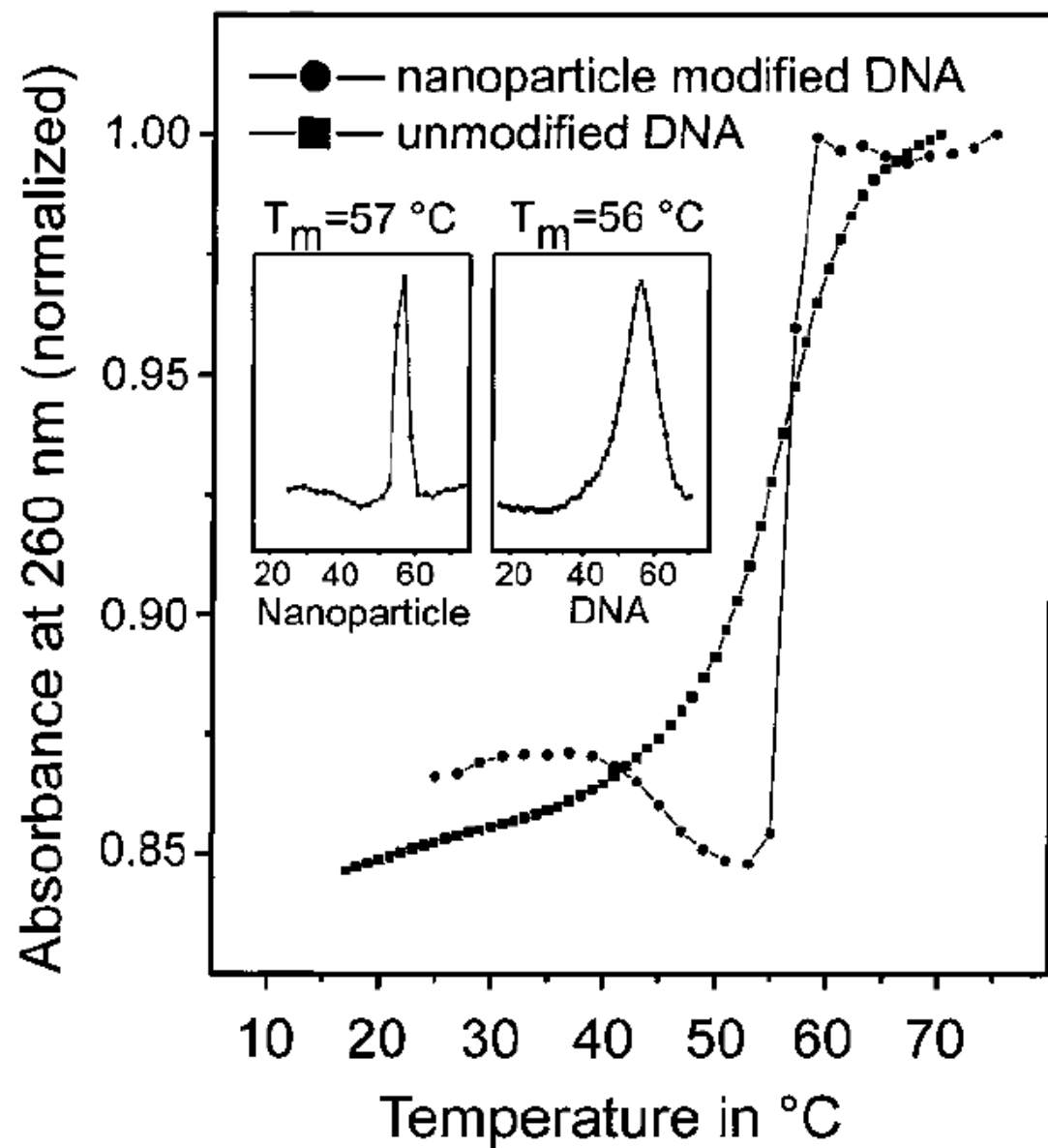
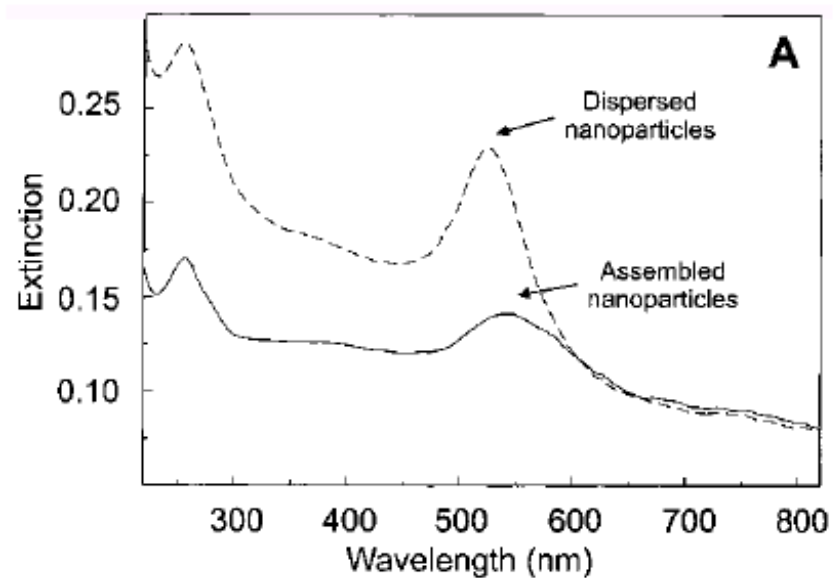
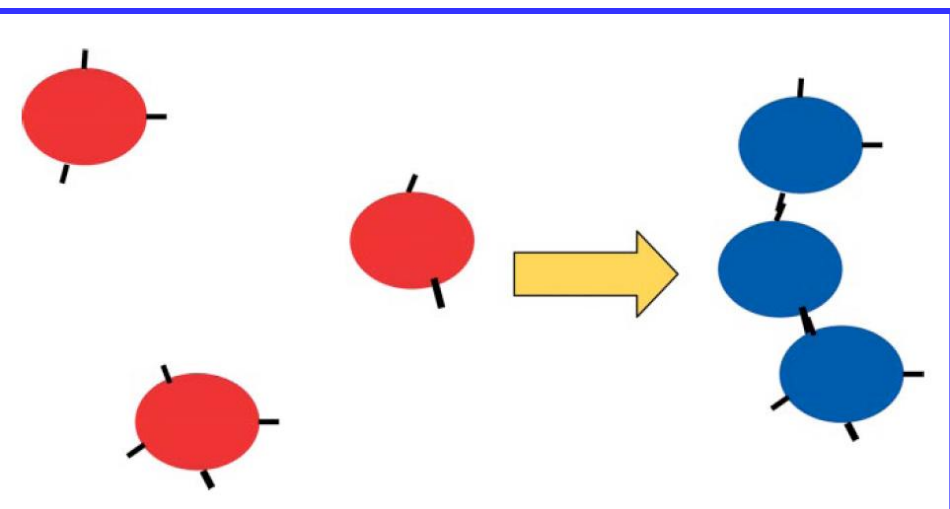


Δ↑↓ Further oligomerization and settling



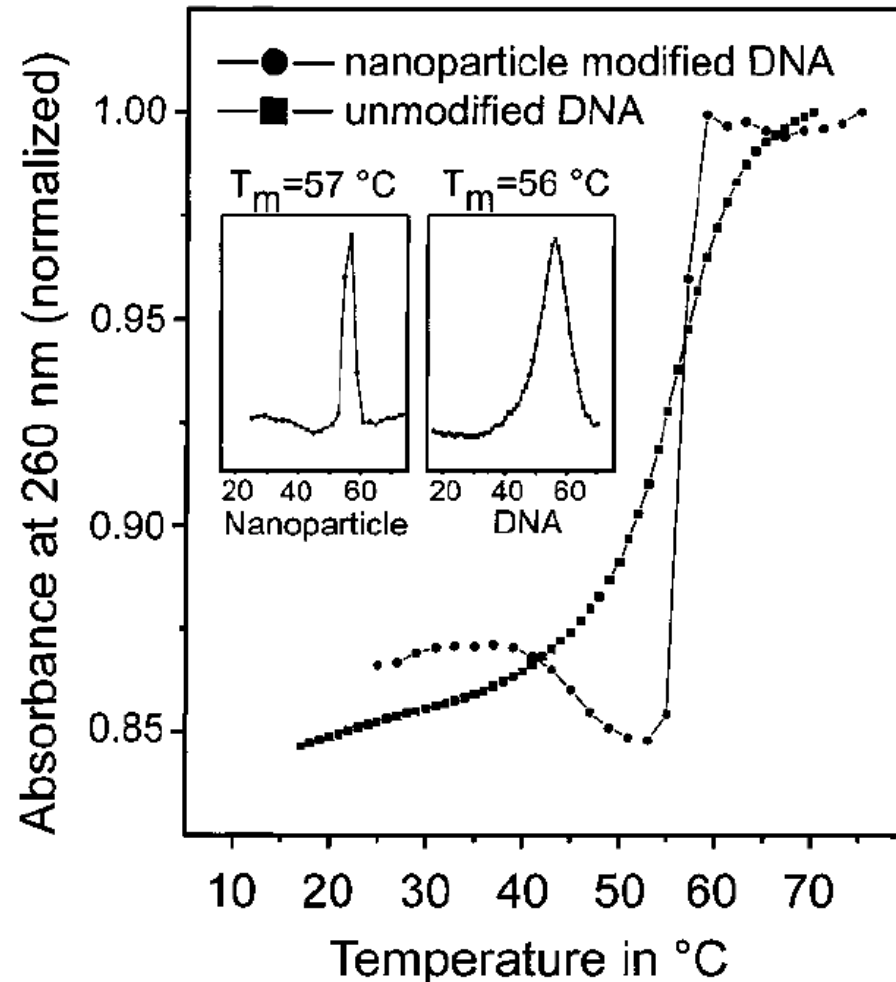
A nanoparticle “satellite structure” comprised of a 31 nm Au nanoparticle linked through DNA hybridization to several 8 nm Au nanoparticles,



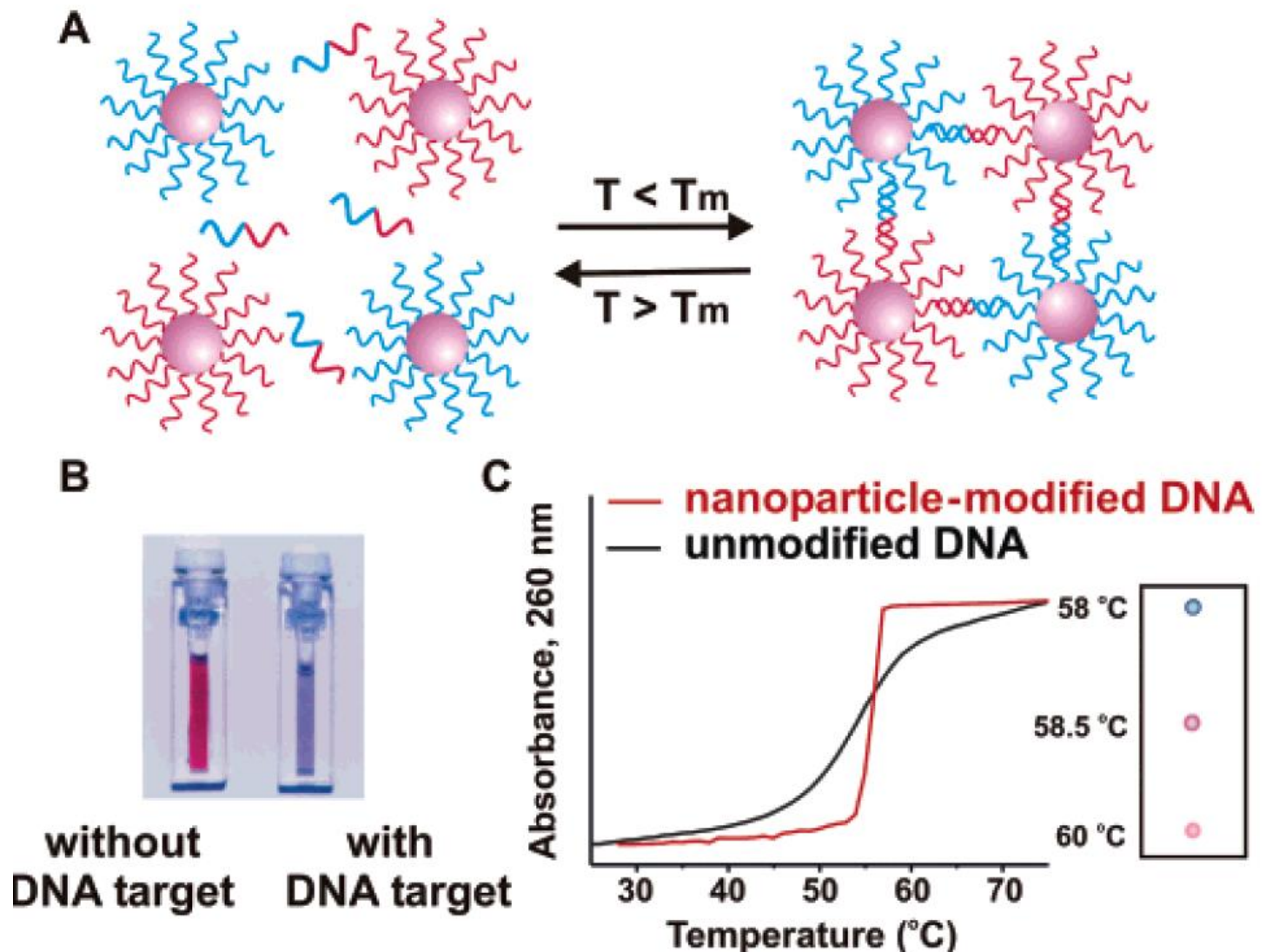


Sharp melting behavior of DNA-linked nanoparticles

- (1) the formation of an aggregate with many different DNA interconnects
- (2) the use of a nanoparticle optical signature rather than a DNA optical signature to map out the melting behavior of the aggregates.



In the presence of complementary target DNA, oligonucleotide-functionalized gold nanoparticles will aggregate.



Solution color changes from **red** to **blue** upon the analyte-directed **aggregation of gold nanoparticles**, a consequence of interacting particle surface plasmons and aggregate scattering properties.

Melting profiles of the nanoparticle-labeled DNA aggregates were **extraordinarily sharp**, occurring over a temperature range much more narrow than the transition for unlabeled or conventional fluorophore-labeled DNA.

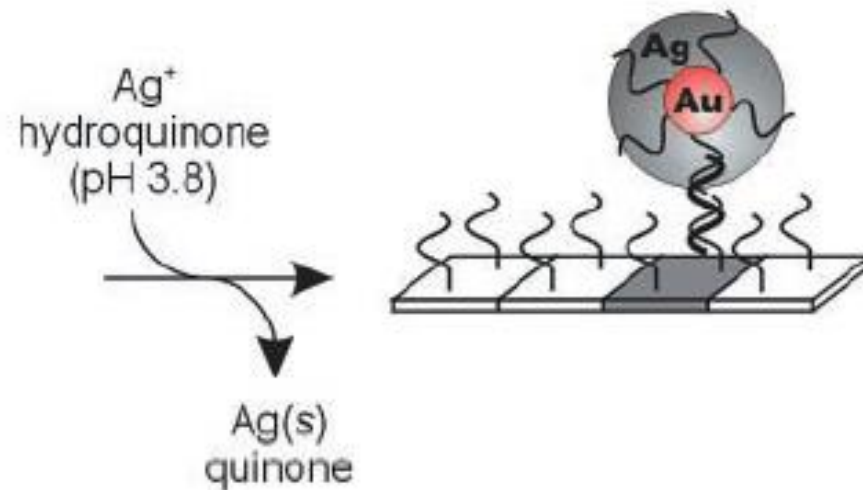
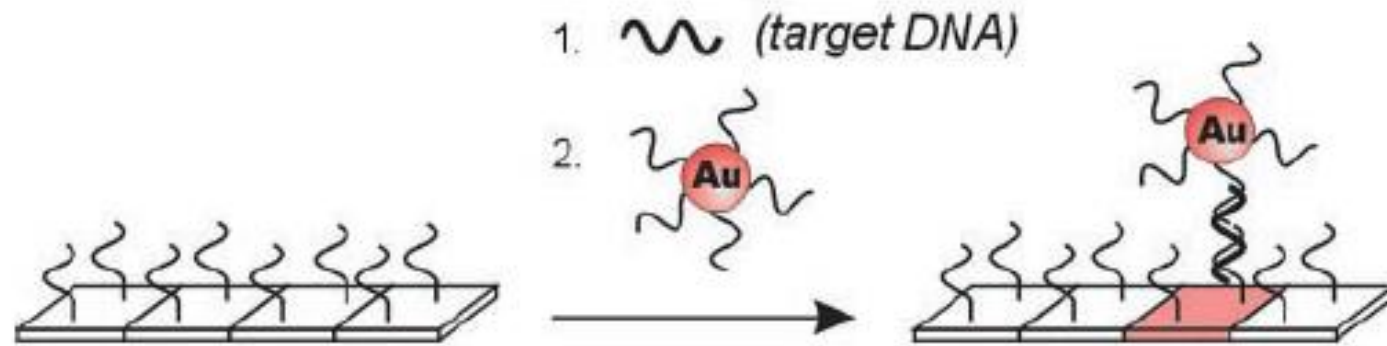
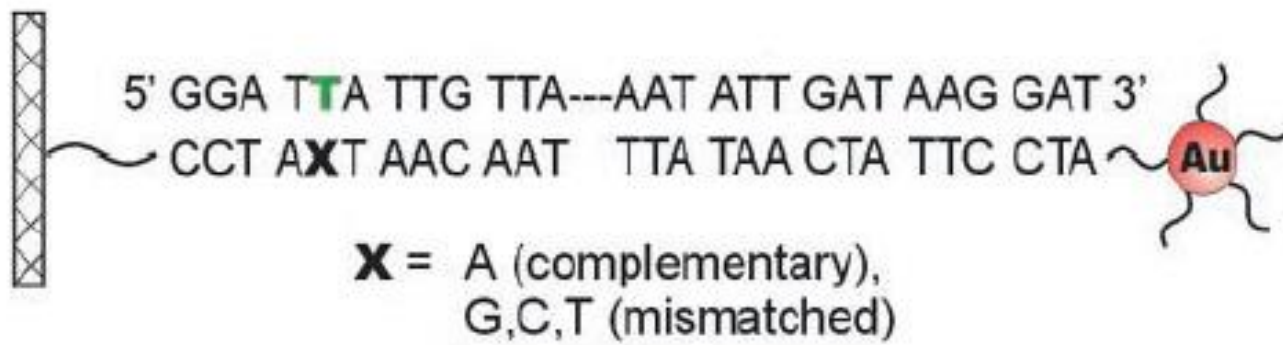
By virtue of sharp melting transitions target DNA could be differentiated from DNA with single base-pair mismatches simply by measuring absorbance (or looking at color) as a function of temperature.

Scanometric DNA Array Detection with Nanoparticle Probes

T. Andrew Taton,^{1,2} Chad A. Mirkin,^{1,2*} Robert L. Letsinger^{1*}
Science **2000**, 289, 1757.

- Specific hybridization of surface-bound, single strand capture oligonucleotides to complementary targets.
- Both the specificity and sensitivity of these assays are dependent on the dissociation properties of capture strands hybridized to perfect and to mismatched complements.
- These network structures exhibit exceptionally sharp melting profiles; FWHM as low as 2°C.
- Sharp melting transitions allow one to differentiate a perfectly complementary target strand from a strand with a single base mismatch

- Analyzing combinatorial DNA arrays using oligonucleotide-modified gold nanoparticle probes
- Melting profiles of the targets from an array substrate.
- Discrimination of an oligonucleotide sequence from targets with single nucleotide mismatches with a selectivity that is over three times that observed for fluorophore-labeled targets.
- When coupled with a signal amplification method based on nanoparticle-promoted reduction of silver(I), the sensitivity of this scanometric array detection system exceeds that of the analogous fluorophore system by two orders of magnitude.





A



B



C

(10 nM)



D

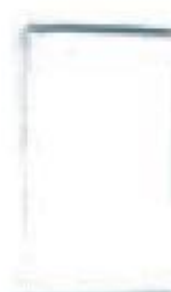


E



F

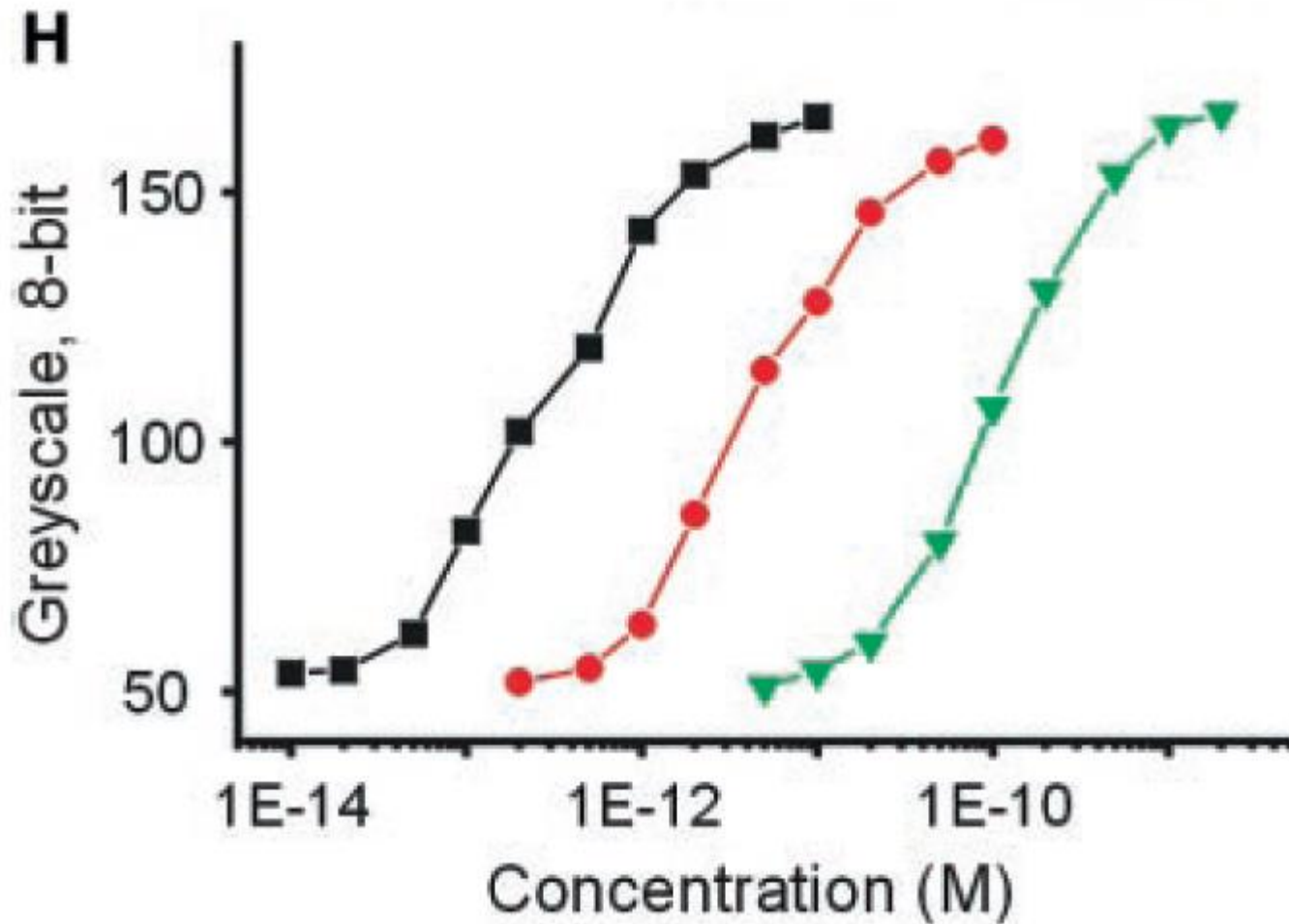
(100 pM)



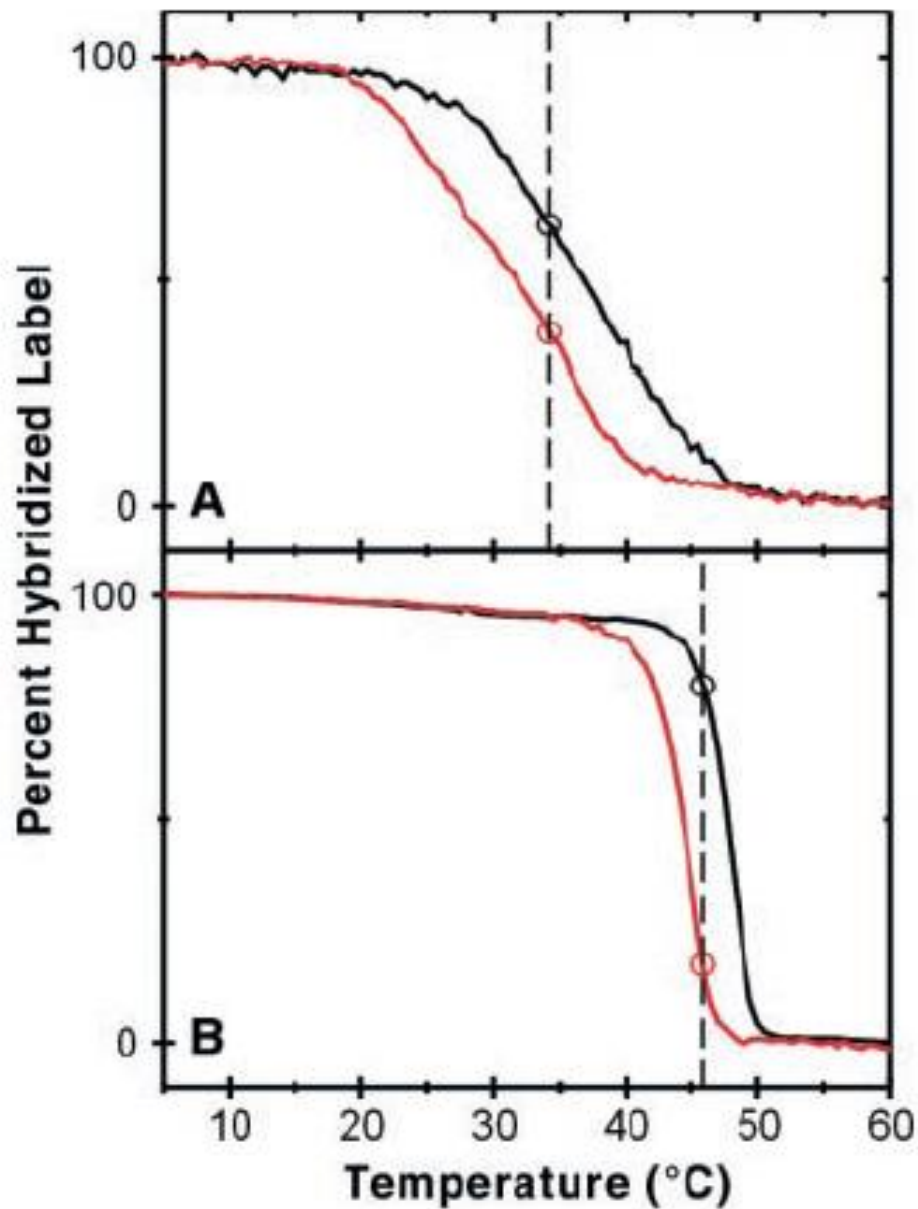
G

(control)

The lowest target concentration that can be effectively distinguished from the background baseline is 50 fM.

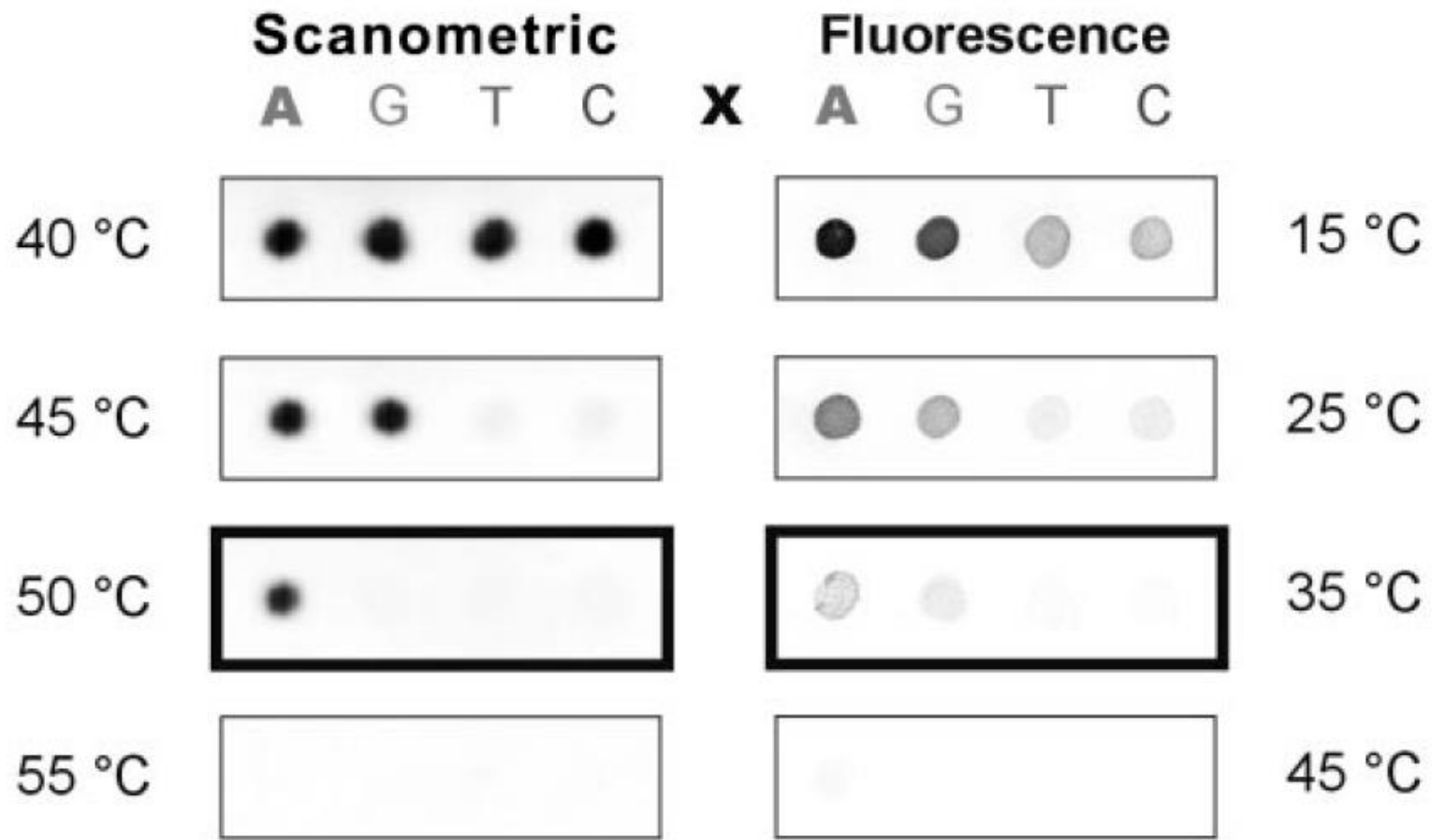


Melting curves for relative selectivity



FWHM of 18 C

3 C



Hybridization signal could be resolved at the X 5 A elements at target concentrations as low as 50 fM (5); this represents a 100-fold increase in sensitivity over that of Cy3-labeled arrays imaged by confocal fluorescence microscopy, for which target concentrations of > 5 pM required

“Northwestern Spot Test” for polynucleotide detection

